KEMIAN LAITOS
JYVÄSKYLÄN YLIOPISTO

Solvent effect on gel formation and properties of peptide-based gels

Master`s theses

University of Jyväskylä

Department of Chemistry

18.11.2023

Veera Nikkola

Abstract

This literature review goes through how different solvents affect the gelation process, morphology, and properties of peptide-based gels. The goal of the study was to find generalization about the effects of solvent properties, polarity, different solvent mixtures, and pH on the gelation process. By studying solvent conditions and control over self-assembly processes, new gel properties can be achieved, offering extensive prospects for developing novel peptide-based gel applications.

The focus of the thesis is mainly on low molecule weight gelators (LMWGs) and self-assembly, but a few interesting examples of polymer hydrogels and copolymerization were also included. The literature part introduces the gelation process and mechanical properties of gels, followed by a discussion of solvents used in gelation processes and ending it with a few interesting gel applications.

The experimental part aimed to form new gels with chemically active *tert*-butyl esters and ethers with a low molecular weight gelator, Fmoc-Leu-Phe-O*t*Bu. The gelation process, gel morphology, and time-dependent nature were studied and reported.

Tiivistelmä

Tämä opinnäytetyön kirjallisuuskatsaus käsittelee erilaisten liuottimien vaikutusta orgaanisten peptidipohjaisten geelien valmistukseen, morfologiaan ja ominaisuuksiin. Tutkielmassa perehdytään erityisesti liuottimien polaarisuuden, erilaisten liuotinseosten ja liuottimen pH:n vaikutuksiin geeliytymisprosessissa. Tutkielman lopuksi käsitellään erilaisia sovelluksia, joissa organogeelejä monipuolisine ominaisuuksineen on käytetty hyödyksi lääketieteellisten sovelluksien alustoina.

Opinnäytetyön kokeellisessa osuudessa syntetisoitiin aminohappopohjainen alhaisen molekyylipainon gelaattori Boc-Leu-Phe-O*t*Bu ja valmistettiin peptidipohjaisia geelejä käyttäen geeliytymisprosessissa liuottimina kemiallisesti aktiivisia *tert*-butyyliestereitä ja -eettereitä. Tutkimuksen hypoteesina oli aikaisempi tutkimus kemiallisesti aktiivisista liuottimista. Geeliytymisprosessissa muodostuneiden geelien aikasidonnaista, dynaamista reaktiotasapainon muutosta seurattiin infrapunaspektroskopialla (FT-IR), ydinmagneettisella resonanssispektroskopialla (NMR) ja pyyhkäisyelektronimikroskoopilla (SEM). Lisäksi geelien termodynaamista palautumista ja kykyä sitoa liuotinta seurattiin geeliytymislämpötilan $T_{gel\text{-}sol}$ avulla ja geelien turpoamistestillä (swelling-test).

Preface

The experimental part of this master's theses was completed during the summer of 2022. It was a part of a summer internship as a research assistant funded by the University of Jyväskylä. Special thanks to Dr Efstratios Sitsanidis for supervising the study. Thank you, M.Sc. Romain Chevigny, Dr Andreas Johansson and Dr Anniina Kiesilä, for helping us with measurements. The literature part of this theses was done from June 2022 to September 2023. Thank you, Professor Maija Nissilä, for your patient supervision.

Table of Contents

Abbreviations

ACN	Acetonitrile
ALP	Alkaline phosphate
AMF	Atomic force microscopy
BIS	*N*,*N*'-methylenebis(acrylamide)
BMA	Butyl methacrylate
Boc	*N*-*tert*-butoxycarbonyl
BP	Boiling point
CD	Circular dichroism
Da	Daltons
DCM	Dichloromethane
DMF	Dimethylformamide
DMSO	Dimethyl sulfoxide
EA	Ethyl acetate
ESI	Electrospray ionisation
E_T	Solvent polarity parameter
Fmoc	Fluorenylmethyloxycarbonyl
FT-IR	Fourier transform infrared
GdL	Glucono-δ-lactone
HEX	Hexane
HLC	Henry's law constant
HFIP	Hexafluoroisopropanol
HR-MS	High-resolution mass spectrometry
IKVAV	Ile-Lys-Val-Ala-Val
IMQTOF	Ion mobility quadrupole time-of-flight
In situ	Locally

In Vitro	Performed or taking place in a test tube
L-Asn-OH	N-Fluorenyl-9-methoxycarbonyl-*L*-asparagine
Leu-Leu	Leucine-Leucine
LMWG	Low molecular weight gel
MAA	Methacrylic acid
MeOH	Methanol
MGC	Minimum gelation concentration
Nap	Naphthalene
NPCs	Neural progenitor cells
NMR	Nuclear magnetic resonance
PBS	Phosphate buffer saline
PDA-N4	*N*-*N*-di(pyridin-4-yl)-pyridine-3,5-dicarboxamide
PG	Partial gel
Phe	Phenylalanine
R.T.	Room temperature
SD	The swelling degree
SEM	Scanning electron microscopy
SSG	Self-supporting gel
*t*BuOAc	*tert*-butyl acetate
TEM	Transmission electron microscopy
$T_{gel\text{-}sol}$	Gel-solution transition
TLC	Thin layer chromatography
YIGRS	Tyr-Ile-Gly-Ser-Arg

LITERATURE PART

1 Introduction

Organogels have gained interest due to varying mechanical and morphological properties and their potential ability to act as a platform for new materials for biomedical applications. However, although gelation processes are already quite widely studied, no general gelation procedures explaining certain gel morphology and properties are found due to the numerous, even complex, interactions between gelators and solvents used in gelation.[1] Gelation is also sensitive to external impacts, such as temperature; thus, adjusting the trial environment is important.[2]

Supramolecular gels, in general, are described as soft supramolecular materials with a continuous and permanent structure and solid-like rheological behaviour.[3] Gels can be classified into four categories based on their origins, constitutions, types of cross-links and the media they encompass. Here, the discussion is limited to physical, peptide-based gels, predominantly utilizing low molecular weight gelators (LMWGs). The gels are further classified after solvents that LMWGs immobilise: 1) organoges immobilizing organic solvents and 2) hydrogels immobilizing water. The gels type affects the formation, morphology, and properties of the gels.[4]

The solvent environment is one of the key regulators affecting gelation, gel morphology, and properties. The solvent is a gelling agent which the gelator immobilizes, but solvents can also be chemically active and participate in the gelation process.[5,6] To understand the gelation process, specific gel structures and properties, and why certain solvent leads to gelation and another does not, solvent properties, their role in the gelation process, and different gelation triggering methods have been studied.

By appropriately choosing the solvent for the gelation process, new effective soft materials with specific properties and better reproducibility can be achieved. Hydrogels, especially, have potential as synthetic biomaterials and in biomedical applications due to their ability to mimic living cells, such as their high water content and soft surface. Examples of potential applications are drug delivery and tissue engineering. However, the formation of gel with correct, safe, secondary structure is challenging.[7]

2 Gels and gel formation

The gel formation process, in general, can be divided into three steps: dissolving the gelator, self-assembly of gelators and formation of a 3D network (Figure 1). Supramolecular gels are formed when LMWGs self-assemble into one-dimensional aggregates, like fibers, ribbons, sheets or spheres.[3,4] These long anisotropic structures entangle and further organize into 3D networks via non-covalent interactions like hydrogen bonding, π-π stacking, van der Waals interactions, or solvophobic forces (hydrophobicity).[4] However, in most studies, only hydrogen bonding, π-π stacking and the ability to form hydrophobic interactions are described as the most predominant self-assembly and gel formation interactions.[8]

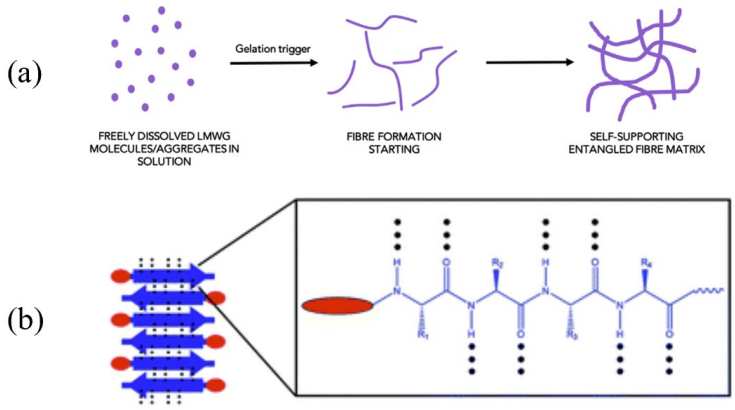

Figure 1. (a) Gelation process in three steps: low molecular weight gelators' (LMWGs) dissolution, LMWGs' self-assembly, and formation of the 3D network. (b) LMWGs' assembly in water forms hydrogels *via* non-covalent bonds, including hydrogen bonds, shown as black dots (·).[1,9] Used with permission of RSC, from Peptide conjugate hydrogelators, Adams, D., and Topham, P., 6, 2023; permission conveyed through Copyright Clearance Center, Inc.

Self-assembly and crystallization are two competitive reactions when gels are formed, which can be evaluated by thermodynamic free energy. It is commonly thought that crystallization and formation of nanotubes and wires occur in a minimum energy state under thermodynamic control, whereas gels are metastable (non-equilibrium) when the absolute energetic minimum state can be reached by kinetic control (Figure 2a).[8,10] The metastable state permits

polymorphism where various structures have close energy. This energy difference can be exceeded with external stimuli, and new structural phases with small differences can be found (Figure 2b). Thus, the ability to control the assembly process has a significant role in the future performance of the gels.[11]

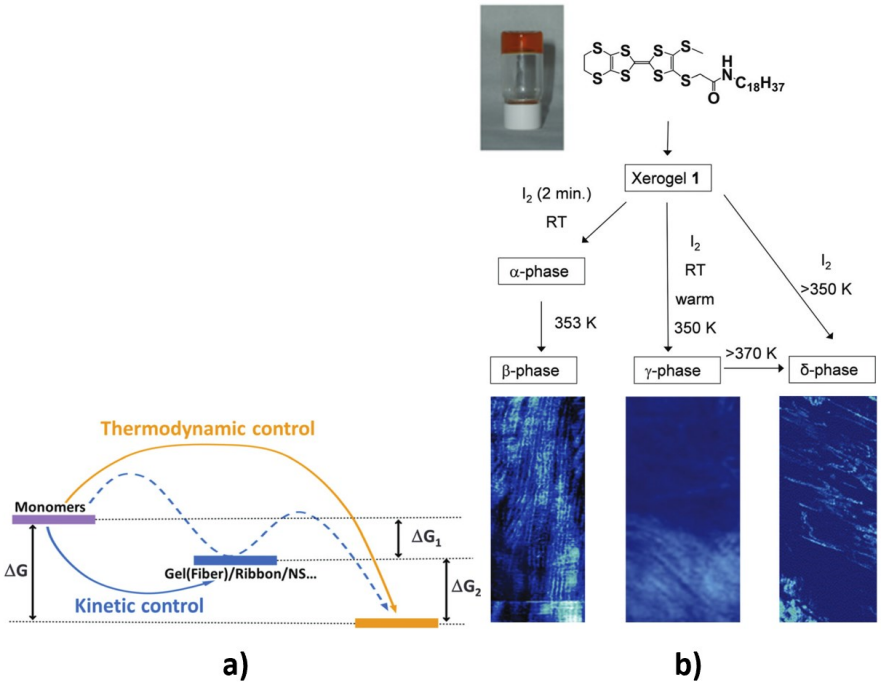

Figure 2. a) Crystallization is thermodynamically more favourable state (orange line). However, kinetic control (triggered by pH or chemical "fuel", for example) can lead to the formation of a metastable state in which self-assembly occurs (blue line). b) Polymorphism enables new gel phases.[8,11] Used with permission of RSC, from Supramolecular materials, Amabilino, D., Smith, D., Steed, J.,46, 2023, and from Peptide self-assembly: thermodynamics and kinetics, Wang, J., Liu, K., Xing, R., and Yan, X., 45, 2023; permission conveyed through Copyright Clearance Center, Inc.

Gels are prepared by solubilizing at least the minimum gelation concentration (MGC) of the gelator into a suitable solvent. Gel formation occurs above the MGC (Figure 3), which, without a general rule, must be found by empirical studies with different solvents. Gelator dissolution is also affected by the gelator's different polymorphs that can solubilize differently, affecting the gelation result.[12]

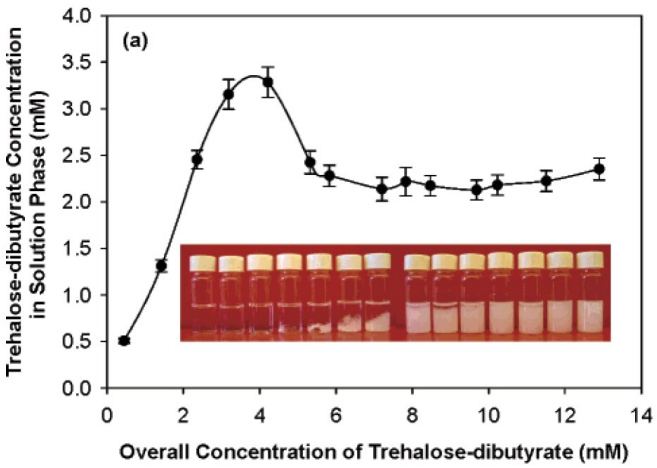

Figure 3. Gelation studies show that trehalose-dibutyrate concentration increases to the level where it exceeds the gelator's maximum solubility. After that, the concentration decreases as a result of self-assembly. MGC of trehalose-dibutyrate in ethyl acetate is 3.2 mM.[13] Reprinted (adapted) with permission from Solvent Effect on Organogel Formation by Low Molecular Weight Molecules, Zhu, G. and Dordick, J. S., *Chem. Mater.*, 2006, *18*, 5988–5995. Copyright 2023 American Chemical Society.

No gelation has been achieved without triggering the gelator self-assembly (excluding the two-component LMWG systems).[1,14] Self-assembly can be triggered by organic solvent, water or acid.[5,15–19] LMWG systems are rarely triggered by the heat-cool cycle, which is common for other organogels. When organic solvent-water mixtures are used, the order of mixing components is relevant. For example, DMSO reacts exothermically with water without a gelator which causes heating of the reaction mixture.[20]

The most frequently used methods for gel structure and properties characterizations are spectroscopic and microscopic techniques, x-ray techniques, thermal analyses, and rheology studies. Nuclear magnetic resonance spectroscopy (NMR) provides information on gel structures and components affecting the gelation and reveals, for example, the protonation of gelators. It can also be used to examine the time dependence of structural changes. Scanning electron microscopy (SEM), transmission electron microscopy (TEM), and atomic force microscopy (AFM) are used to produce high resolution and nanosized images to investigate gel morphology, individual fibre size, shape and properties and structure of the 3D network. Thermal analysis studies the energy needed to form non-covalent bonds and the rheology to measure the gel G modules (vector contributions). Rheological measurements provide

information about gel's elasticity and viscosity, whether gels are more liquid than solid and if gel deformation is permanent or transient.[4]

2.1 Peptide-based gels

Peptides are building blocks in peptide-based gels, which after the activation, lead to the assembly and formation of the gel. Depending on the molecular structure, peptides can adopt either α-helical or β-sheet structures.[21] When LMWGs are used, the required amount of gelator in the gelation process is less than 1.0 w-%, and relatively small gelators (200 Da) can form strong gels.[3] Peptide-based gelators typically consist of one or two amino acids connected to the C-terminus (e.g. COOH, OH), linker and N-terminus.[19] However, gels containing several amino acids have also been reported.[15] Most of the recent gelation studies have utilized 9-fluorenylmethoxycarbonyl (Fmoc) based peptide gelators (Figure 4).[19]

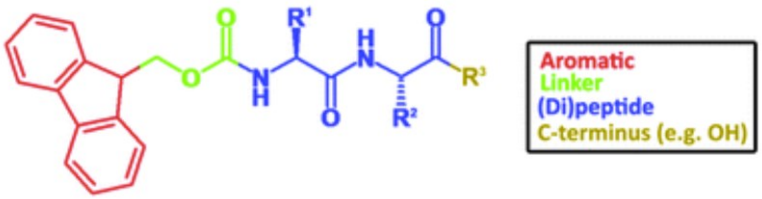

Figure 4. Fmoc-based peptide gelator. The aromatic N-terminus group, linker segment, peptide sequence, and C-terminus drive the gelator self-assembly and gel formation.[19] Used with permission of RSC, from Design of nanostructures based on aromatic peptide amphiphiles, Fleming, S., Ulijn, R. V., 43, 2023; permission conveyed through Copyright Clearance Center, Inc.

The N-terminus aromatic group has been found to be the most effective assistant to the self-assembly process and gelation. Besides of most widely used Fmoc terminus, many other aromatic moieties with the ability to drive gelation via π-π stacking and without being too hydrophobic to prevent dissolving have been studied (e.g. phenyl, naphthalene, pyrene derivates)[19,22] There is no general way to predict the best N-terminus group to a certain peptide sequence, although it is known that the hydrophobicity of aromatic group can be compensated

in N-terminus or peptide sequence and vice versa. The key to effective gel formation is to find an aggregate formation favouring balance between hydrophobic and hydrophilic interactions.[19,23]

C-terminus has a significant role in gel formation and 3D structure due to its ability to affect the gelator's solubility and charge. It can also have a functional role, for example, in the coupling of different conformers, the proteolysis resistance (protease cause the breakdown of proteins). In addition, it was observed to affect the minimum gelation concentration (MGC).[15,19] Via modification of the C-terminus, gelation triggering by pH adjustments can be controlled.[19]

Amino acids consist of a wide range of structures that affect the gelator properties: hydrophobicity, charge in physical pH, acidic or basic side chain, aromatic residues, aliphatic residues, and chirality. Thus, various intramolecular interactions are possible in hydrogel formation. Gelator dipoles and charges will be diminished through the hydrogen bond formation with water and interaction with other dissolving ions. Therefore, hydrogen bonding has been proposed to determine the self-assembly process. As the gel structure is based on weak non-covalent bonds, the gels generally are relatively easy to break down.[19]

In addition, the linker segment has an important role in the success of the gelation. The linker was observed to affect the final structure of the gel, and only linkers with a semilinear conformation (169 and 147 degrees)[24] were observed to lead to gelation. Linker segment can also be designed to form hydrogen bonds, thus improving the gelation.[19]

2.2 Properties of peptide gels

Due to the great potential of amino acid-based gelators to mimic natural structures, their gels have been studied as potential materials for biomedical applications. Amino acid-based gels have gained special interest due to their vast and easy modification possibilities (selection of the components and gelation process) and properties like stiffness, biodegradability and swelling. These properties enable compatibility with the cellular environment and a sufficiently porous platform where the cells can divide.[21,25]

The mechanical properties of the gels are determined by the gel structure, which in turn, is affected by the gelation mechanism. The mechanical properties can be classified into three categories according to length scale: (1) the average thickness and mechanical properties of fibres themselves, (2) the distance between branching cross-linking points, and (3) fibre distribution on a larger scale.[26] The properties of supramolecular gels are strongly related to their formation. Thus, triggering or controlling self-assembly with solvents is a huge possibility to modulate the free energy and gelation systems and create new gel applications.[8]

3 Solvent-triggered gelation

Certain gelators have selected sets of solvents leading to gel formation. Therefore, finding an individual solvent which leads to the gelation may not be meaningful.[27] Solvents parameters like partition coeffect (log P), Henry's law constant (HLC), solvatochromic parameters and Hansen solubility can be used to evaluate the solvent's ability to lead to gelator self-assembly and gel formation. However, there are no global solvent parameters to predict gelation for organogelators.[27]

Although this thesis concentrates on solvent properties, polarity, different solvent mixtures and water as a solvent, there is no doubt that gelation is a multifactorial phenomenon in which both the solvents' ability to dissolve (partially) the gelator and the gelator`s ability to self-assemble and many other external factors must be evaluated to visualize the whole gelation process.

3.1 Solvent polarity

Solvent polarity is one of the most studied properties affecting gel formation and gelation time. Zhu & Dordick[13] studied esters, ketones, and alcohols to compare how different solvents with different properties form intramolecular interactions with different kinds of gelators (different acyl group lengths) during gelation. In the study, they assumed that hydroxyl groups and

hydrogen bonds of trehaloses are the main key for gel formations. However, it was observed that also solvent polarity affects final gelation results, and hydrogen (and gelator-gelator interactions) do not define the gelation process by themselves.[13]

The effect of the solvent polarity can be studied by plotting the solvent polarity parameter E_T in the function of gelation number (Figure 5). The solvent polarity parameter E_T (30) represents solvent-gelator interactions by measuring the sum of nonspecific and specific (H-donor and acceptor interactions depending on solvent acidity or alkalinity) interactions. The gelation number represents the maximum number of solvent molecules gelled per gelator, and it is determined by measuring the MGC of the gelator. The results show that the gelation number of alcohols is the lowest, but they seem to settle in a smaller gelation number range than esters and ketones, which indicates minor differences in the gelation process when different alcohol solvents are used.[13] Thus, the gelation with alcohols is more predictable than with ketones and especially esters.

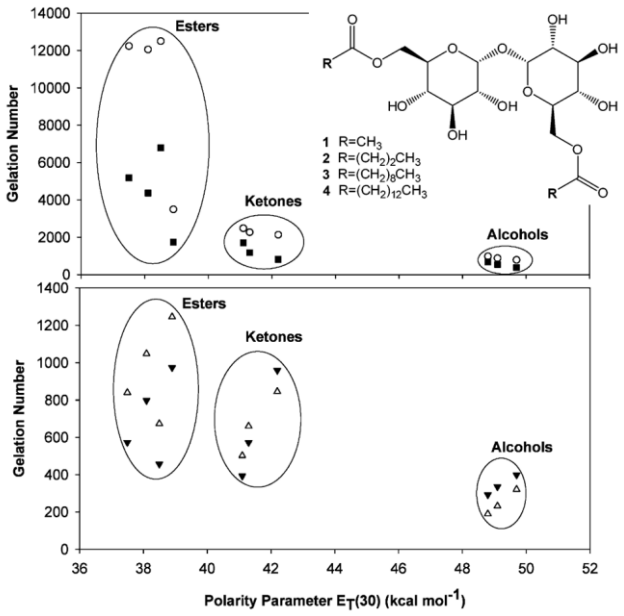

Figure 5. The gelation number decreaces in the order of esters > ketones > alcohols. The gels are more stable with gelators having a shorter acryl chain length. Trehalose gelators **1-4**. ∘ (trehalose diacetate), ■ (trehalose dibutyrate), △ (trehalose didecanoate) ▲ (trehalose dimyristate).[13] Reprinted with permission from Solvent Effect of organogel Formation by Low mlecular Weight Molecules, Zhu, G. & Dordick, J., *Chem Mater*., 2006, 18, 5988-5995. Copyright 2023 American Chemical Society.

The difference in gelation results with different lengths of the acyl group of trehalose also relates to solvent polarity. Unlike esters, ketones and alcohols show increasing potential for gelation when the chain length is increased. The best gelation results were observed when more polar gelators and solvents were used (Figure 6). However, better gelation results with less polar solvents were observed when trehalose's acyl chain was less than three carbons.[13]

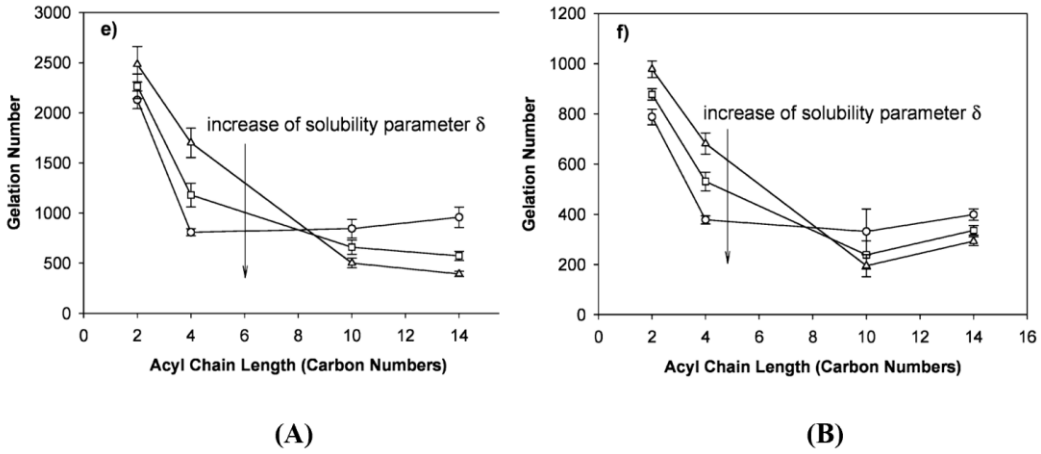

Figure 6. The acyl chain length affects the gelation differently when the polarity of the solvent changes. The best gelation results are observed in ketones (A) and alcohols (B) when the acyl chain length is < 3 carbons. (A) As the chain grows, the gelation in acetone gives a better gelation number than in less polar solvents, 2-butanone and 2-pentanone. (O) Acetone, (□) 2-butanone and (△) 2-pentanone. (B) As the chain grows, better gelation results were observed with a more polar solvent, 1-butanol. (O) 1-butanol, (□) 1-pentanol and (△) 1-hexanol.[13] Reprinted (adapted) with permission from Solvent Effect on Organogel Formation by Low Molecular Weight Molecules, Zhu, G. and Dordick, J. S., *Chem. Mater.*, 2006, *18*, 5988–5995. Copyright 2023 American Chemical Society.

Zhu & Dordick[13] noticed unexpected results when acetonitrile-solvent was studied with trehalose gelators. Even if acetonitrile's interactions are strongly comparable to ketones, gelators **3** and **4** (Figure 5) showed higher gelation numbers with acetonitrile than with any other solvents. This might refer to the existence of more complicated solvent-gelator interactions. Another point of view was that if the interactions between the solvent and the gelator are too strong, isotropic gelator molecular aggregation may occur, causing the gel structure to break down.[13]

Jain & Roy[15] studied the effect of the solvent polarity on self-assembly, final gel structure, and gel's mechanical properties with Ile-Lys-Val-Ala-Val (IKVAV; **5)** and Tyr-Ile-Gly-Ser-Arg (YIGRS; **6)**. In addition, N-terminal residues were varied between Fmoc, myristyl acid and acetyl anhydride. These two gelators (IKVAV and YIGRS) were chosen because of their different abilities to dissolve into water and water-organic solvent mixtures. IKVAV analogies represented more hydrophobic peptides, while YIGRS analogies represented more hydrophilic peptides.[15]

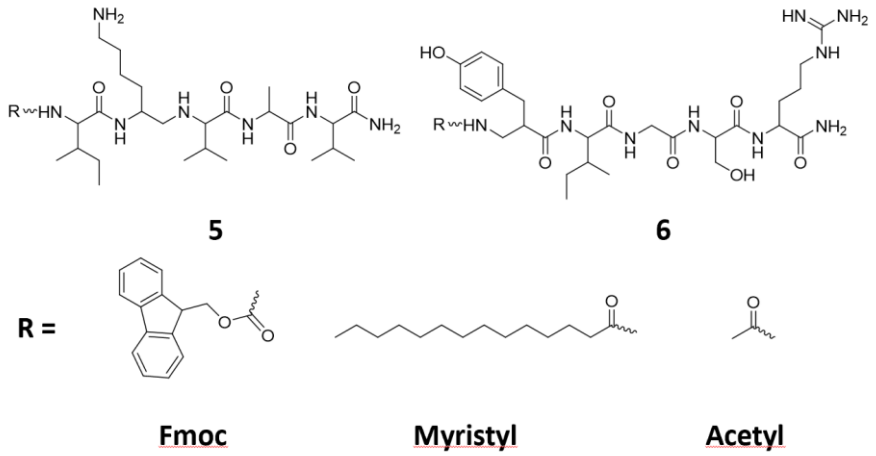

Figure 7. Structures of IKVAV (**5**), YIGRS (**6**), and N-terminal residues Fmoc, myristyl acid, and acetyl anhydride.

Solvents were observed to have a significant role in whether gelator-gelator or gelator-solvent interactions happened (Figure 8). The results show that water-organic solvent mixtures are better solvents to self-assemble hydrophobic peptides by promoting the strong hydrophobic and aromatic interactions between the gelators. Hydrophobic peptides' poor solubility to water leads to a less organized gel structure due to the gelator-gelator interactions, which reduces contact with the polar environment. The hydrophilic gelator, instead, forms dominantly gelator-solvent interactions in an organic solvent-water mixture, while gelator-gelator interactions were assumed to dominate in an aqueous solution due to the higher solubility.[15]

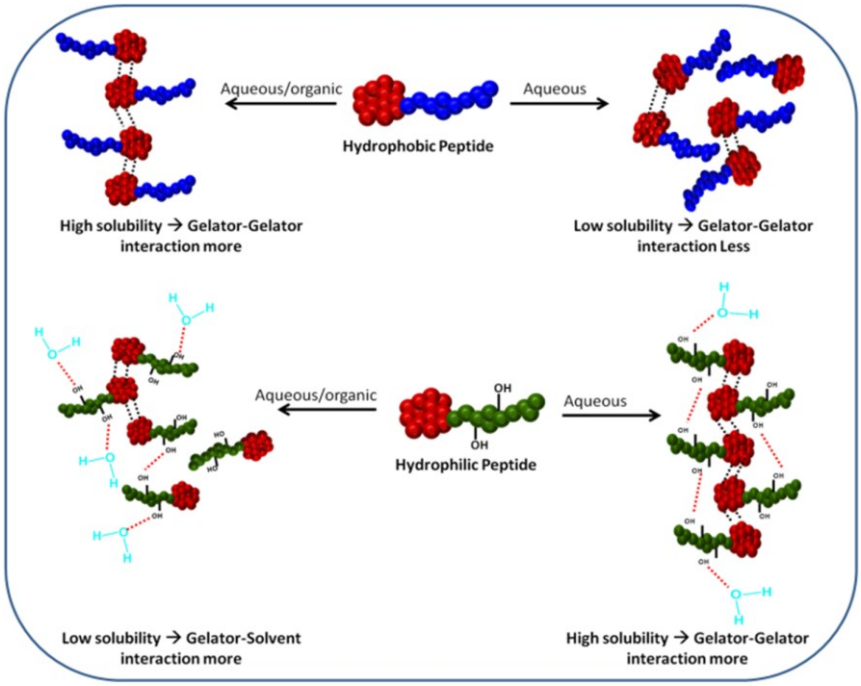

Figure 8. The gelation process results from the gelation-gelation and gelation-solvent interactions, which result from improper hydrophilic-hydrophobic balance. By varying the solvent polarity, the morphology of gels can be affected.[15] Reprinted from Materials Science and Engineering: C, 108, Jain, R., Roy, S., Tuning the gelation behavior of short laminin derived peptides via solvent mediated self-assembly, 110483, Copyright (2023), with permission from Elsevier.

As shown in Figure 8, solvent polarity affects the intramolecular interactions and thus the gel's self-assembly. Especially hydrophobic gelators were observed to be more sensitive to variations in solvent polarity (Table 1). This can also be noticed in Figure 5, where ester, as a more hydrophobic group, seems to settle in a larger gelation number range, indicating significant differences between different ester solvents. Hydrophilic peptides, instead, were observed to form weaker gels than hydrophobic ones. Atomic force microscopy (AFM) images of more hydrophobic Fmoc IKVAV analogies in an organic-solvent mixture showed homogeneous fibres with a 32 ± 10 nm diameter. In a more polar PBS solution, fibres were observed to be shorter with a larger diameter (82 ± 12 nm). However, depending on the protecting group, the AFM study showed many differences between different IKVAV analogies. Instead, YIGRS analogies were observed to be more homogeneous and dense. Fmoc-based YIGRS showed fibres with a diameter of 60 ± 12 nm in organic solvent and 20 ± 2 nm in PBS.[15]

Table 1. Dimensions and organization of IKVAV and YIGRS gels with different protecting groups and in different solvents.[15]

Solvent	IKVAV/YIGRS with different end-groups / diameter		
	Fmoc	Myristyl acid	Acetic anhydride
ACN/water (1:1; water containing 0.1 % trifluoroacetic acid)	32 ± 10 nm / 60 ± 11 nm	long fibres / 49 ± 11 nm	spherical aggregates and short fibres / 84 ± 11 nm /no results
DMSO / water (10 % *v/v* of DMSO and 90 % water)		short fibres/no results	
PBS (phosphate buffer solution, pH 6)	82 ± 12 nm/ 20 ± 2 nm	Sheet-like structure / 25 ± 5 nm	well-defined fibrillar network / 53 ± 11 nm /no results

Solvent polarity was also observed to affect the minimum gelation concentration (MGC). More hydrophobic IKVAV has lower MGC in less hydrophobic ACN/water solvent (5mM) than in phosphate buffer solution (PBS; Table 2). YIGRS has a much higher MGC (20 mM) with lower solubility in ACN/water solution.[13,15]

Table 2. Minimum gelation concentrations (MGC) for Fmoc-based Ile-Lys-Val-Ala-Val (IKVAV) and Tyr-Ile-Gly-Ser-Arg (YIGRS) in solvents with different polarities.[15]

Solvent	MGC of IKVAV/YIGRS with Fmoc C-terminus
ACN/water (1:1; water containing 0.1 % trifluoroacetic acid)	5 mM/20 mM
DMSO / water (10 % *v/v* of DMSO and 90 % water)	5 mM/20 mM
PBS (phosphate buffer solution, pH 6)	15 mM/10 mM

Solvent polarity is an interesting parameter to study due to its relatively clear effect on organogels' nanostructures and MGC. In addition, the study of the solvent effect on the gel's surface hydrophobicity could open new possibilities for gel appicatios, and with it, more

information about molecular packing could be achieved. IKVAV's surface studies in DMSO/water environment (40°) resulted in a hydrophilic gel surface, but in ACN (19.8°) and PBS environment (24.6°), the surface was even more hydrophilic (contact angle below 90 degrees, indicating the hydrophilic surface).[15]

Rheological studies indicate the viscoelastic nature of IKVAV and YIGRS gels. The mechanical strength was highly dependent on the solvent (Table 3). G` was relatively higher in ACN/water solutions when more hydrophobic IKVAV was studied. More hydrophilic YIGRS, instead, formed stiffer gel in a more polar PBS solution. As a generalization, it can be stated that less hydrophobic YIGRS formed weaker gels but was not as sensitive to the changes in the end group. Also, the solvent change effect to YIRGS was more stable (smaller variation).[15]

Table 3. Solvent environments affect the IKVAV/YIGRS-based gels' storage moduli (G`), which indicates gels' mechanical strength.[15]

Solvent	IKVAV/YIGRS with different end-groups / kPa		
	Fmoc	Myristyl acid	Acetic anhydride
ACN/water (1:1; water containing 0.1 % trifluoroacetic acid)	13.8 / 1.3	9.2 / 1.3	no results / 0.4
DMSO-water (10 % *v/v* of DMSO and 90 % H_2O)	14.7 / no results	no results / 0.5	no results / 0.2
PBS (phosphate buffer solution, pH 6)	2 / 0.5	0.06 / 0.5	no results / 5

Also, the recovery of gels was strongly related to the hydrophobicity of the solvent and gelators. Rheological studies showed that less hydrophobic YIGRS recovered better than IKVAV in water-containing solvents (Table 4), which could be considered a result of the ability of a less polar solvent to drive the formation of hydrophobic and $\pi - \pi$ interactions (gelator-gelator interactions). In addition, gel viscosity decreased with time in both cases.[15]

Table 4. The solvent environment affects the recovery from the solid state to the gel state of the IKVAV/YIGRS-based gels.[15]

Solvent	IKVAV/YIGSR with Fmoc end-group/ recovery % from an original gel state
ACN/water (1:1; water containing 0.1 % trifluoroacetic acid)	90 / 72 %
DMSO-water (10 % v/v of DMSO and 90 % H_2O)	45 / 87 %
PBS (phosphate buffer solution, pH 6)	3 / 99 %

3.2 Water in the gelation process

In addition to the use of organic solvents, the active role of water has been studied in the gelation processes. Safiullina *et al*.[28] studied the active role of the water in the gelation process of dipeptide *cyclo(*Leu-Leu) (**7**), where the solvent itself dissolves the gelator poorly. However, in solvent environments leading to the gelation by themselves as well, water was observed to induce the gelation and decrease the gelation time and minimum gelation concentration. At its best, gelation time even decreased from two days to six hours. However, improved gelation results were also observed when aromatic solvents (benzene, toluene, o-, p and m-xylene) were used, and volume was increased while the ratio between solvent and gelator was kept constant.[28]

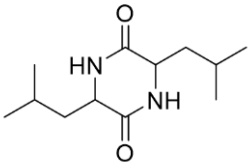

7

As previous studies by Jain and Roy stated,[15] different aromatic environments affected the gel's 3D structure. Differences also emerged between similar solvent-water mixtures, like H_2O/benzene (single, intertwined, and thick belts (580-770 nm)) and H_2O/toluene (belts (350 nm)). Surprisingly, water addition affected the fibre length only in H_2O/benzene mixture, while it did not affect in other aromatic solvents.[15,28]

The study proposes that gels form when a three-phase system of two poorly dissolving solvents and a gelator is formed, such as H_2O/alkane mixture with *cyclo*(Leu-Leu) (**7**; Figure 9). Three phase system forms because hydrocarbons have low density compared to the density of water, and *cyclo*(Leu-Leu) gelators have poor solubility to hydrocarbons and water. The solvent with higher density compared to water could not form gels. Therefore, it can be concluded that gel forms in the interfacial boundary when gelator molecules interact both with water and solvent.[28]

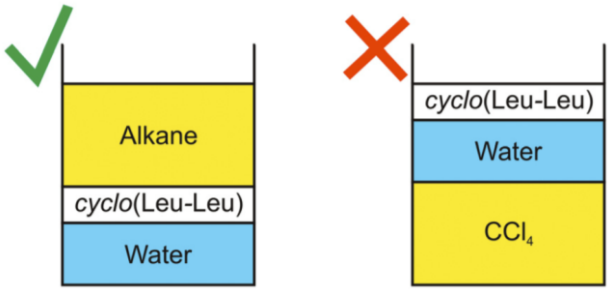

Figure 9. A three-phase water-gelator-solvent system in which gelation occurs when the gelator interacts with both water and solvent. The density of tetrachloride (CCl_4) is higher than water, preventing the interaction of gelators with both water and CCl_4 and, therefore, gel formation.[28] Used with permission of RSC, Role of water in the formation of unusual organogels with cyclo(leucyl-leucyl), Safiullina, A. S., Gorbatchuk, V., Klimovitskii, A., Lyadov, N., Ziganshin, M., Ziganshina, S., 15, 2023; permission conveyed through Copyright Clearance Center, Inc.

Safiullina *et al.*[28] presented that in solvents not dissolving gelators well, hydrogen bond formation between gelator-water-gelator significantly compensates for the energy loss of solid molecules when dissolving in the solvent environment. The significant role of water as an energy source was presented to occur via the surface tension of water due to the desolvation of the gelator to the solvent and arrangement according to the dipoles.[28]

The water content of organic solvents could also be the parameter to follow in the solvent's gelation ability. Gelation was known to occur with benzene (0.5 ml), while *n*-hexane (0.5 ml) was not forming a gel with Leu-Leu. Benzene consists of 44.3×10^{-1} ml water which means that when benzene is used as a solvent for Leu-Leu (1.5 mg/ml), there are ~ 7 molecules of water per dipeptide. In n-hexane, however, only 0.7 water molecules were calculated, which was insufficient to form a gel. In this case, water addition (70 µl) led to gel formation. The calculations did not consider moisture in the air or organic solvent's ability to absorb water from the air.[28]

Zhao *et al*.[5] studied the active role of water as a part of the gelation process of Fmoc-protected diphenylalanine (Fmoc-Phe-Phe) induced by solvent-triggering. Fmoc-Phe-Phe gelator was first activated with an organic solvent, DMF. DMF binding forms Fmoc-PhePhe-DMF dimer, which activates hydrogen bonding sites of the peptide. After activation, water addition immediately starts the formation of hydrogen bonds from terminal positions towards the middle parts of the gelator. Saturated gelator molecules then accumulate into anti-parallel stacking, which enables the formation of H_2O bridges and immobilizes the residual water molecules (Figure 10).[5] Water was observed to have a significant role in connecting the one-dimensional structures into a 3D network. Formed dimers accumulated to anti-parallel geometry where the opposite dimers are ~ 3.8 Å apart. Peptide amide bonds cannot form long hydrogen bonds between each other, but amides can be linked with the H_2O bridge.[5]

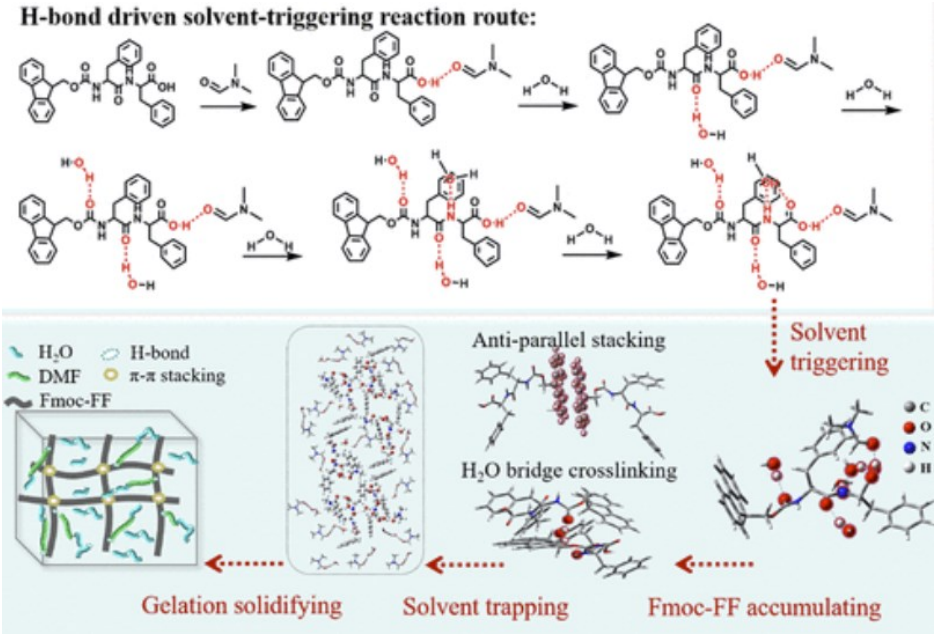

Figure 9. Proposed gelation mechanism for organic solvent-triggered gelation process of Fmoc-Phe-Phe in DMF.[5] Reprinted (adapted) with permission from Domination of H-Bond Interactions in the Solvent-Triggering Gelation Process, Zhao, C., Wang, Y., Shi, B., Li, M., Yan, W., and Yang, H., *Langmuir*, 2022, *38*, 7965–7975. Copyright 2023 American Chemical Society.

3.3.1 The effect of solvent-water ratio on gelation

The control and tunability of chirality is an important but challenging topic in supramolecular gels, as the biological functions are usually a consequence of these changes.[29] Zhang *et al.*[16] studied the solvent-trigging effect on gel morphology with Fmoc-based *N*-fluorenyl-9-methoxycarbonyl-*L*-asparagine (*L*-Asn-OH, **8**). The chirality of gels was controlled during the self-assembly process by controlling the solvent environment. Three different morphologies, nanofibers, nanosheets, and twisted fibers, were observed by varying the ratio between DMSO and water (Figure 10).[16]

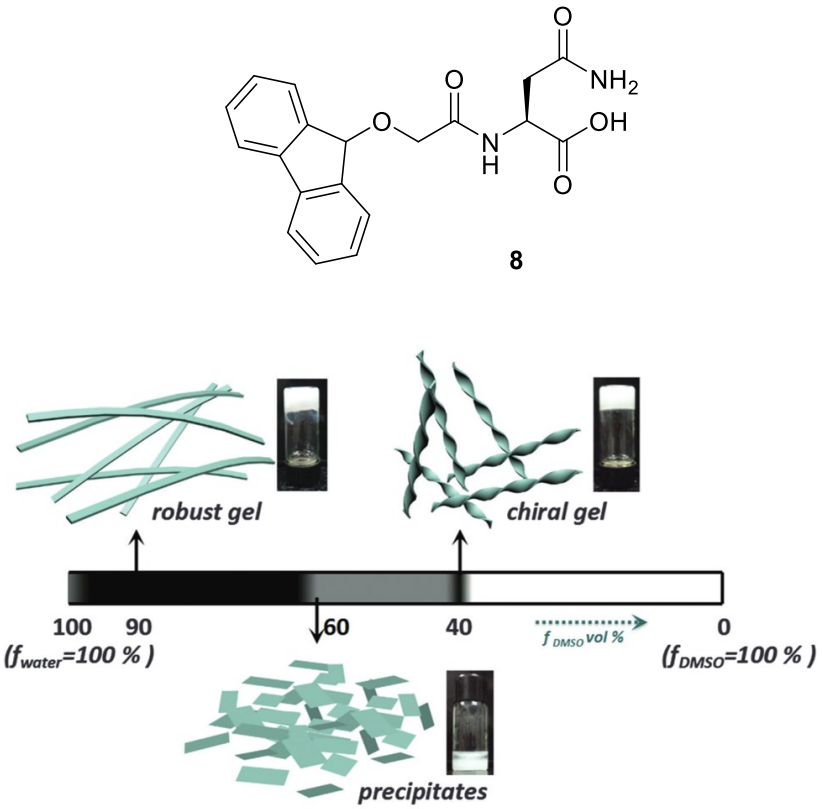

Figure 10. (A) Molecular structure of the Fmoc-*N*-fluorenyl-9-methoxycarbonyl-*L*-asparagine (Fmoc-*L*-Asn-OH). (B) The water ratio affects gel morphology. Gels were chiral when the water ratio decreased to 40 %. When the water ratio reached 40 %, the mixture of Fmoc-*L*-Asn-OH in solvent was changed from clear to turbid, which indicates the formation of a larger microstructure with the ability to scatter light.[16] Used with permission of RSC, Tuning of gel morphology with supramolecular chirality amplification using a solvent strategy based on an Fmoc-amino acid building block, Zhang, Y., Li, S., Ma, M., Yang, M., Wang, Y., Hao, A. ja Xing, P., 40,, 2023; permission conveyed through Copyright Clearance Center, Inc.

When the solvent mixture ratio of 1:9 DMSO/H_2O (gel I) was used, gel formation started immediately. This indicates kinetically controlled growth in which 1D nanofibres immobilize and entangle solvent and form a 3D network. The SEM results show a flat, fibrous structure with a width of 0.5 to 0.7 µm (Figure 11 a-b). When the amount of water was decreased to ratios 4:6 and 5:5 of DMSO/H_2O, gelation time increased, and precipitation was observed. The decrease in water content was considered to favor other dimensional growth weakening the capillary forces between aggregates. SEM results show interlaced nanosheets without the ability to capture all the solvent. Thus, precipitates are observed (Figure 1 c-d).[16]

Individual fibres were observed when the amount of water was reduced to 40% (gel II). The individual fibres were suggested to form by gel fibre digestion due to the lack of non-covalent bonds between the solvent and the gelator. These fibres had right-handed supramolecular chirality with a diameter of 2 mm and a helical pitch of 9 mm (Figure 11 e-f). Hydrogen bond interactions were suggested to favor chirality.[16]

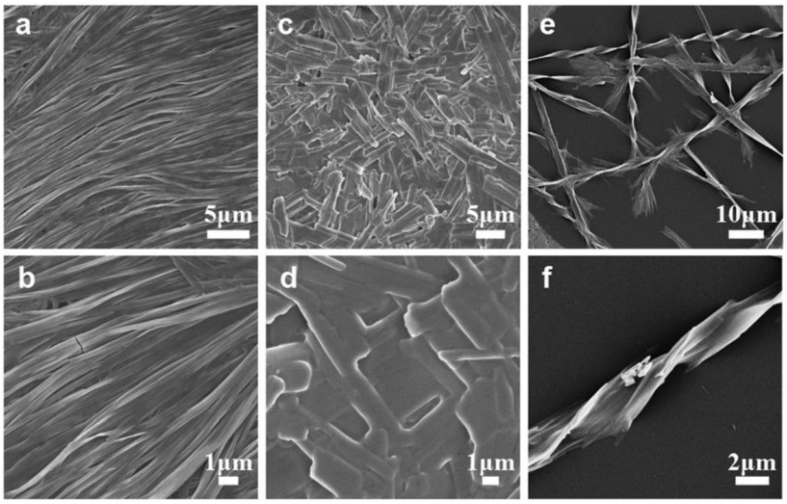

Figure 11. SEM images of Fmoc-based *L*-Asn-OH morphologies in water-DMSO mixtures. (a-b) v/v = 1/9 (gel I), (c-d) v/v = 4/6, and (e-f) v/v = 6/4 (gel II). SEM images show that chiral twists and widths of the gels can be affected by simply changing the water content.[16]

A study with FTIR shows that water amount affects the gel's morphology. Hydrogen bonds observed between ketones, amides, and asparagine acid moieties shifted to lower values, indicating a strong intermolecular hydrogen bond network in gels. With a 1:9 DMSO/H_2O (gel I) ratio, hydrogen bonds were weaker than with a solvent containing 40 % of water. Therefore, a twisted arrangement is formed to strengthen the hydrogen bonds. Unlike in the study of Zhu & Dordick[13], hydrogen bonds are the main factor for gel formation. Zhu & Dordick[13] also proposed the importance of other interactions due to the different gelation results in the same solvent varying the acyl chain lengths in the gelator [16]

The chirality of gels was studied with circular dichroism (CD) measurements, rotation as a function of wavelength (Gel I and II; Figure 12). Observed CD-silence indicates the absence of chiral aggregates in gel I. Gel II, instead, shows a cotton effect (rotation reaches a maximum value before changing the sign9, indicating twisted arrangements. Zhang *et al.*[16] consider that the twist likely results from the twist of fluorenyl groups. Based on the previous studies, the negative cotton effect indicates left-handed chirality.[30] The chirality was observed to follow the chirality of gelators.[31,32]

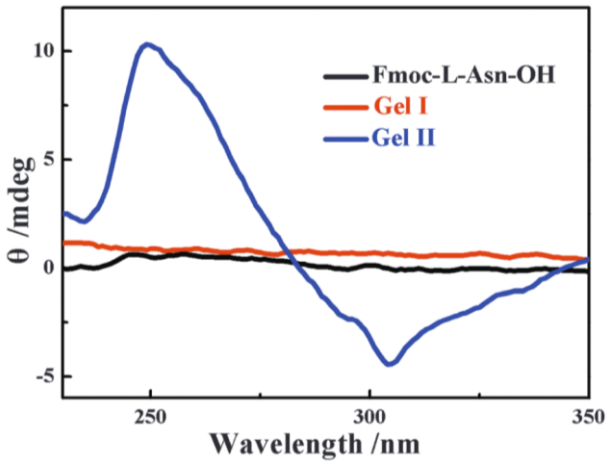

Figure 12. The chirality of gels can be affected by changing the solvent environment. Gel I (red) represents a solvent ratio of 1:9 of DMSO/H_2O, and gel II (blue) a water ratio of > 40 %. Observed negative cotton effect with gel II indicates left-handed chirality, while no chirality was observed with gel I.[16] Used with permission of RSC, Tuning of gel morphology with supramolecular chirality amplification using a solvent strategy based on an Fmoc-amino acid building block, Zhang, Y., Li, S., Ma, M., Yang, M., Wang, Y., Hao, A. ja Xing, P., 40,, 2023; permission conveyed through Copyright Clearance Center, Inc.

Fmoc-Phe-Phe (**9**) was studied in four different solvent environments.[20] Organic solvent-water mixtures (DMSO, ethanol, acetone and hexafluoroisopropanol (HFIP)) to which the peptide-based gelator is soluble were studied. The volume fraction of solvents (ϕ), i.e., the volume of the studied solvent divided by the volume of the water-solvent mixture leading to dissolution, was slightly different with each solvent. Higher ϕ is needed to dissolve into ethanol and methanol, likely due to the higher volatility.[20]

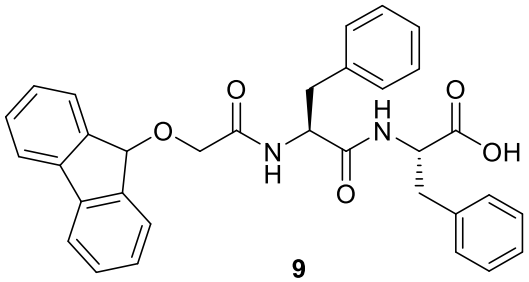

9

In ϕ_{volume} 0.3 of ethanol, the solution transition of spherulic structures into fibres was observed. Based on previous studies, these spherulic structures are considered nucleation points for fibril growth.[33] Confocal microscopy studies show that the transition between spherulic structures and fibres takes a few minutes (Figure 13). The solvent environment did not significantly affect the self-assembly processes, but the duration varied. The observed differences in turbidity of the gels are more likely due to the different sizes of spherulic or fibrous structures than the self-assembly process itself. However, interestingly, no spherulic structures are observed when gels are triggered with pH, which indicates that the self-assembly process can be affected by the gelation triggering method as well.[20]

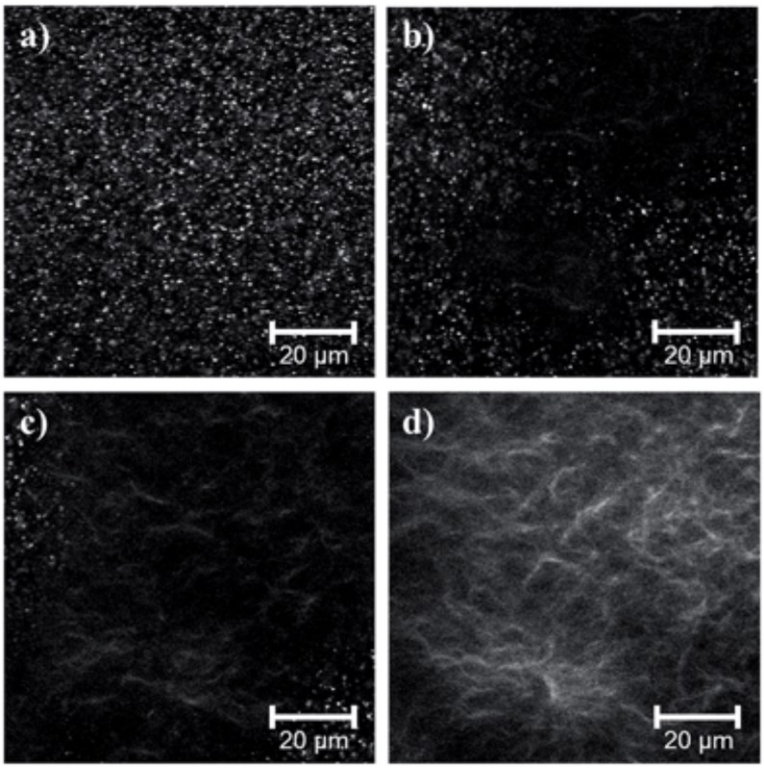

Figure 13. Confocal microscopy images of transitions between spherulic structure and fibres in the second timeline (a) 30 s, (b) 60 s, (c) 80 s, and (c) 120 s.[20] Reproduced from Ref. 20 with permission from the Royal Society of Chemistry.

However, differences in fibrous networks were observed when different solvent environments were compared with confocal microscopy. The DMSO-water mixture forms a homogeneous network of fibres, which seems to be packed into larger domains. These domains are surrounded by a less dense region of fibres with a length of 20 µm (Figure 14a). In the microstructures of gels formed in HFIP (Figure 14d) and acetone mixtures (Figure 14c), very similar domains were observed, but the fibres were the most easily noticeable in the HFIP mixture. Gels formed in the acetone mixture also included crystallized residual spherulites. Thus, crystallization occurred after gelation. As no crystallization was observed in trials with a water-ethanol mixture, the crystallization cannot be assumed to be unreacted Fmoc-Phe-Phe or caused by solvent volatility. The gels prepared using ethanol were the most homogenous and were observed to form fibres with equal length scale (Figure 14b).[20]

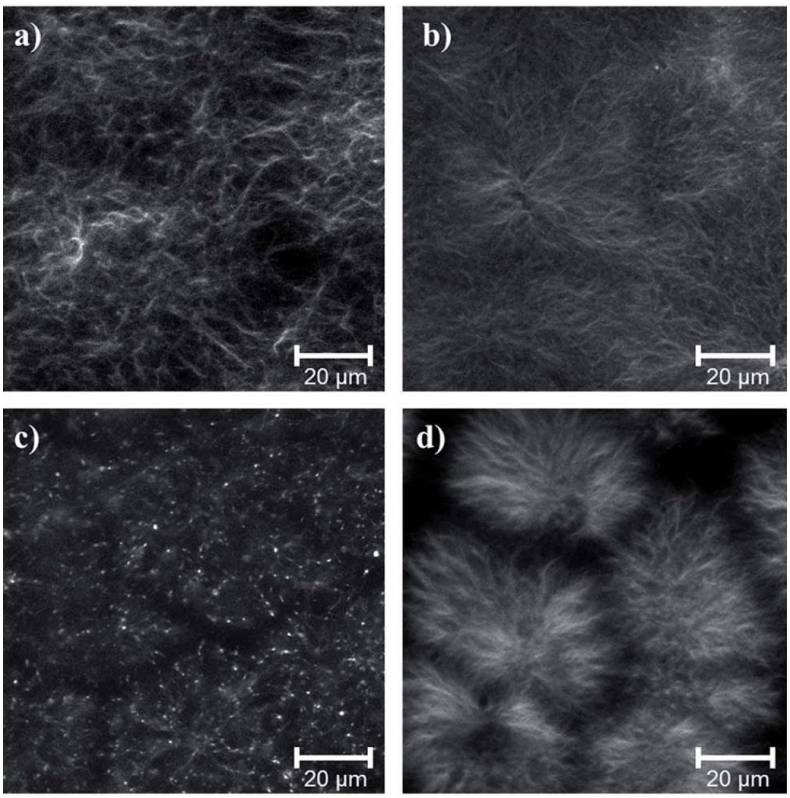

Figure 14. Confocal microscopy images of the structures of Fmoc-Phe-Phe gels formed in different organic solvent-water mixtures. The final $\phi_{solvent}$ of 0.3 resulted in different microstructures in different solvents (a) DMSO, (b) ethanol, (c) acetone, and (d) hexafluoroisopropanol (HFIP).[20] Reproduced from Ref. 20 with permission from the Royal Society of Chemistry.

3.3.2 Solvent environment affects gel properties

In addition to gel morphology and chirality, the solvent environment was observed to affect the thermal and mechanical properties. Fmoc-*L*-Ash-OH-based gel I (1:9 DMSO/H_2O ratio) resisted temperature changes better than gel II (water ratio of > 40 %). In the study of thermal residues and gel-to-sol trials ($T_{gel\text{-}sol}$), the amount of water in the total solution improved the heat resistance of the nanofibers (Table 5). Temperature affects the length and width of the supramolecular fibres, especially near $T_{gel\text{-}sol}$ temperature, due to the degradation of the carboxyl group, cleavage of amine and hydroxyl groups, and the separation of π-π- stacking. Less water in the solution improves the heat resistance of the nanofibers.[16]

Table 5. Solvent effects on gel-to-sol temperature.[16]

The ratio of water	$T_{gel\text{-}sol}$
Gel I (1:9 DMSO/H_2O)	81 °C
Gel II (water ratio of > 40 %)	62 °C

The solvent environment was also observed to improve thermo-reversibility. The less water-containing mixture was fully thermoreversible, while more water-containing gels had a network of non-reversible parts (Figure 15). Gel-to-sol transition was observed to be an exothermic reaction.[16]

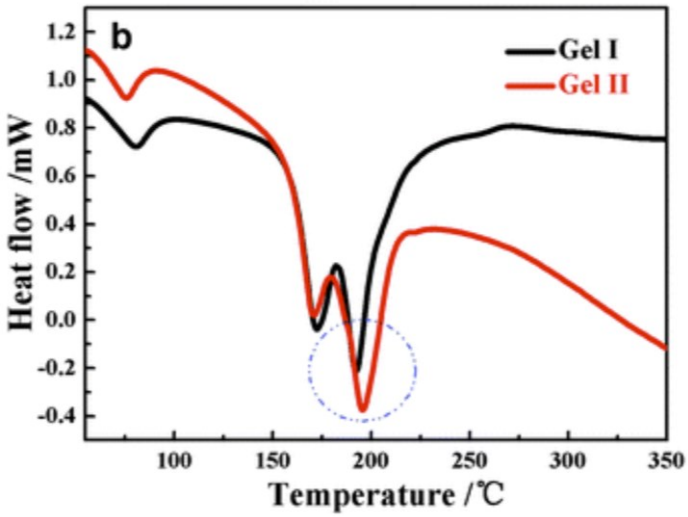

Figure 15. Differential scanning calorimetry plot shows that less water-containing gel I is more thermoreversible than more water-containing gel II. Intramolecular structures are assumed to break at 200 °C, but before that, heat flow decreases due to the evaporation of solvent residues.[16] Used with permission of RSC, Tuning of gel morphology with supramolecular chirality amplification using a solvent strategy based on an Fmoc-amino acid building block, Zhang, Y., Li, S., Ma, M., Yang, M., Wang, Y., Hao, A. ja Xing, P., 40,, 2023; permission conveyed through Copyright Clearance Center, Inc.

Fmoc-Phe-Phe-based gels (**9**) in different organic solvent (DMSO, acetone, ethanol and HFIP) - water mixtures had quite similar properties when $\phi_{solvent}$ was set between 0.2 and 0.4.

Outside this range, the mechanical properties were slightly weaker. Zhang *et al.*[16] observed that G` representing the elastic response for Fmoc-*L*-Ash-OH-based (**8**) gel I (1:9 ratio of DMSO/H_2O) was ten times higher (50 kPa) than for gel II (water ratio > 40 %) indicating that less water induces better elastic response for gels. Instead, Raeburn *et al.*[20] observed that Fmoc-Phe-Phe gel's (**9**) maximum G` with studied solvents (ϕ_{HFIP} of 0.05) was only 26 kPa.[16,20] Gel's ability to recover from shear is also an important feature to study. A dense fibre network and nucleation growth of fibres of Fmoc-Phe-Phe gels were proposed to indicate better recovery results (Figure 14). The recovery tests of G` show that the recovery of gels is strongly related to the solvent environment (Table 6).

Table 6. Mechanical properties of gels prepared in DMSO, HFIP, acetone and ethanol mixtures.[20]

Organic solvent-water mixture ($\phi_{solvent}$ of 0.3)	Recovery of their original G`	G` (after D_2O solvent change)
DMSO	100 %	70 %
Acetone	30 %	
HFIP	95 %	
Ethanol	26 %	

Solvent volume can affect the possibility of using gels in different applications by being harmful to cells, for example. Raeburn *et al.*[20] observed a promising possibility to remove the solvent after forming the self-assembled network by washing the gel with D_2O, which removed DMSO almost completely. However, the solvent washing decreased the gel's (**9**) mechanical strength by 13 %, and the recovery of the gel orginal G` decreased from 100 % to 70 % (Table 6).[20]

The study of Colquhoun *et al.*[34] with naphthalene-Phe-Phe (2Nap-Phe-Phe) (**10**) gels in DMSO/H_2O-mixture showed only 10 % recovery, which is much less than the reported values of Zhang *et al.*[16] for IKVAV (**5**) and YIGRS (**6**) based gels. Based on this, the strength of the gels is possibly affected by the gelator properties and the external environment. 2Nap-Phe-Phe gels were observed to break gradually.[2] Interestingly, the storage moduli (G`) value, indicating the gel's ability to store energy and resist degradation, never drops under the value of loss

moduli (G``), indicating lost energy. This was proposed to indicate that microstructures tend to recover at a higher frequency. However, more studies are needed to draw final conclusions.[34]

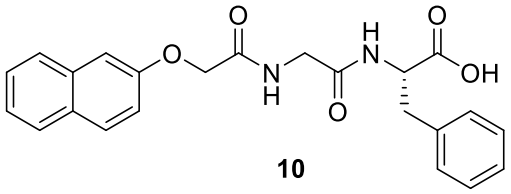

10

3.3.3 Switching H_2O to D_2O

A solvent environment changing from H_2O to D_2O was observed to affect the gel's density, viscosity and the strength of hydrogen bonds.[35] In the study of McAulay *et al.,*[36] LMWGs (**11-14**) were dispersed in high pH (10-11), after which pH was decreased with glucono-δ-lactone (GdL), leading to carboxylate protonation and gel formation. The isotopic change effect on the gel properties was studied assuming that differences between H_2O and D_2O environments are mainly accumulated between high pH and pH after decrease and thus difficult to perceive.[36]

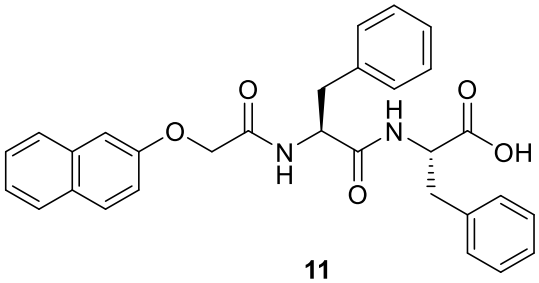

11

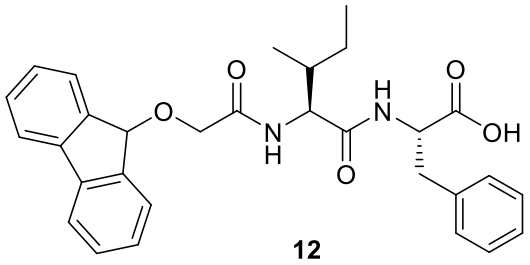

12

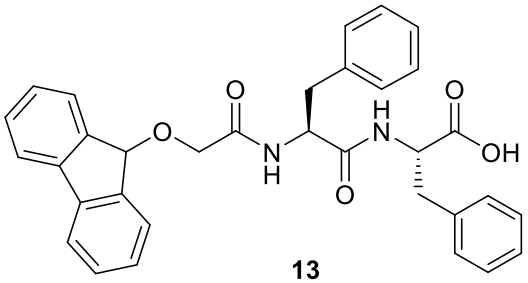

13

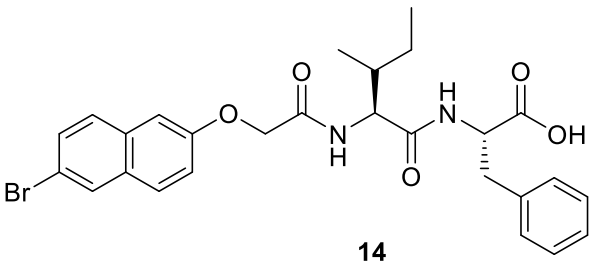

14

The study shows only a minor change in LMGW solutions of H_2O and D_2O at high pH, even when different LMWG were compared. Differences in radii (4.1/4.3 mm (**11**); 1.7/1.9 mm (**12**), H_2O/D_2O), indicating structural differences and explained by different solvation of gelators, and differences in viscosity were observed. However, after GdL addition, pH was observed to change differently, but gels were visually alike. In the D_2O solution, pH decreased more slowly over a 10 h period, whereas pH in the D_2O environment was approximately 5. In the H_2O environment, pH decreased approximately to 3 with the studied gelators. However, the H_2O environment leads to faster gelation, correlating with the pH drop at different times. In the gelation process, G` starts to differ from G`` (Figure 16). Differences in the process were only observed with gelators **13** and **14**. Alternatively, the observed similarity may indicate that the change in solvent does not significantly affect the primary structures and networks.[36]

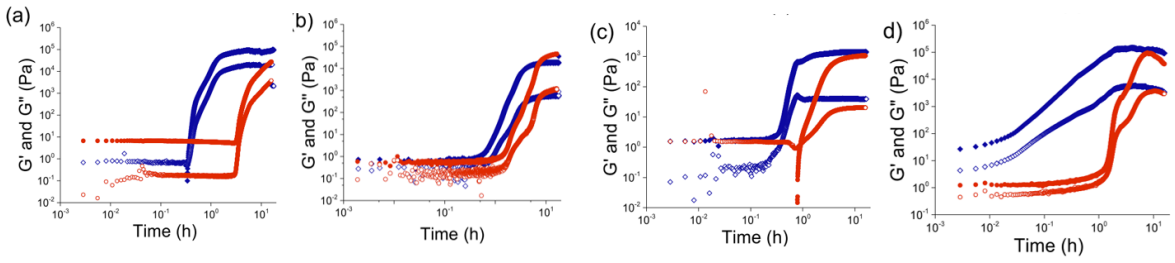

Figure 16. Rheological studies of a) **11**, b) **12**, c) **13**, and d) **14**. The blue line represents H_2O and the red line D_2O environment. The gelation process was very similar in both environments when gelators **11** and **12** were studied. However, a two-stage gelation process was observed when gelator **14** was studied.[36]

Final values of G` and G`` were similar both in H_2O and D_2O environments with gelators **11** and **12** (Figure 16a). This means that both gels could be considered equally rigid. Other gelators (**13** and **14**) showed potential differences between storage and loss moduli and their variation speed and gelation process (Figure 16). However, surprisingly, the early state cryo-TEM data show differences between the two studied environments (Figure 17). The results show that primary self-assembled structures do not impact the gel properties. In the absence of research on combined factors to the gel properties, it cannot be excluded that the sum of random factors

affecting the gel properties leads to the formation of similar gels at the end of the gelation process.[37,38] Despite the simplifications and the omission of temperature-related effects on hydrolysis, the findings of the study indicate that isotopic variations have the potential to influence the gel properties.[36]

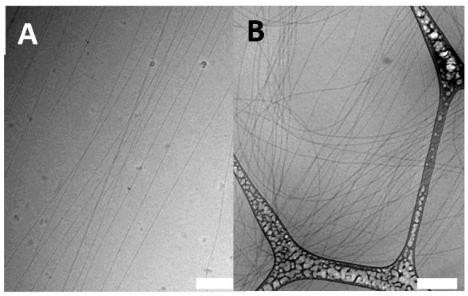

Figure 17. Cryo-TEM image of **11** in solution state A) in H_2O and B) in DMSO.[36] Reprinted with permission from ref. 36. Copyright © 2023 American Chemical Society.

Isotonic exchange from H_2O to D_2O was also reported to increase the gel's melting temperature by 30 degrees. The significant difference between the solvent environments was considered evidence that molecular interactions between gelators are more important to hydrogel formation than hydrophobic interactions.[39]

3.3.3 Solvent exchange

Chemical gels are formed via crosslinking strategy where covalent bonds are formed between polymer chains. Solvent response gels with excellent shape memory were formed as a result of the copolymerization of hydrophobic butyl methacrylate (BMA) and methacrylic acid (MAA) with *N*,*N*′-methylenebis(acrylamide) (BIS) crosslink. The solvent environment used in gelation was a mixture of H_2O and DMSO. Liao *et al.*[40] observed that gel properties could be changed by exchanging the solvent environment, which drives hydrophobic monomer to the association as a response to the unfavoured solvent environment (Figure 18).[40]

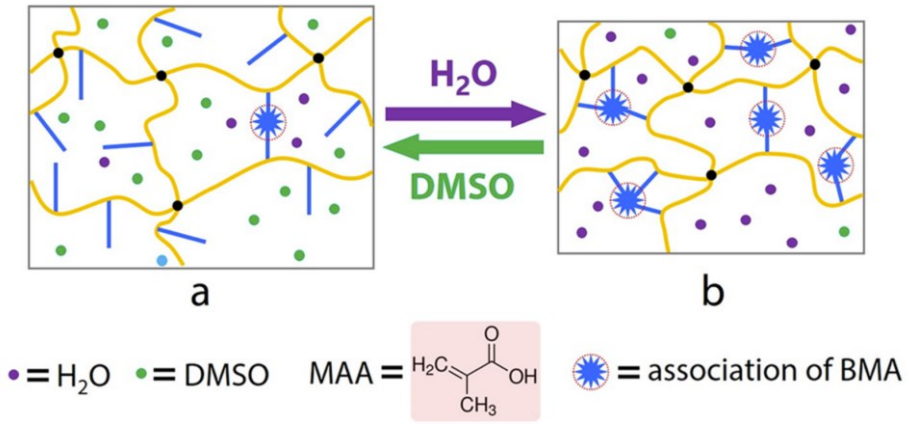

Figure 18. Solvent exchange from DMSO to H_2O leads to the association of hydrophobic butyl methacrylate while repelling water molecules. Hydrophobic monomer association and dissociation were reversible.[40] Reprinted (adapted) with permission from Ultra-Strong and Fast Response Gel by Solvent Exchange and Its Shape Memory Applications, Liao, J.; Huang, J.; Yang, S.; Wang, X.; Wang, T.; Sun, W. ja Tong, Z., *ACS Appl. Polym. Mater.*, **2019**, *1*, 2703–2712. Copyright 2023 American Chemical Society.

Solvent exchange to H_2O was observed to affect the strength of the gels. Exchange time increased Young's modulus, improving the possibility of affecting the gel's strength. A two-day dip formed (over 10^2 MPa) a hundred times stronger gels than a one-minute dip (10^0 MPa). In addition, these gels were observed to have a shape memory as a result of gel softening and hardening. The helix shape was reached after the H_2O exchange, but a reversible reaction towards the original shape was reached after the DMSO exchange (Figure 19). The gel colour was also observed to change from colourless to milky, which was considered a result of hydrophobic domain formation.[41–43]

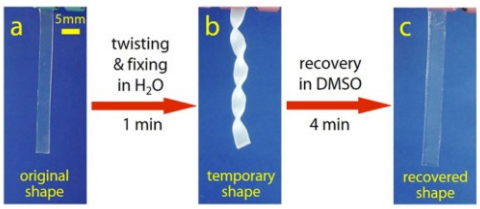

Figure 19. The gel shape was controlled by solvent exchange.[40] Reprinted (adapted) with permission from Ultra-Strong and Fast Response Gel by Solvent Exchange and Its Shape Memory Applications, Liao, J.; Huang, J.; Yang, S.; Wang, X.; Wang, T.; Sun, W. ja Tong, Z., *ACS Appl. Polym. Mater.*, **2019**, *1*, 2703–2712. Copyright 2023 American Chemical Society.

3.3 Chemically active solvent

Chevigny *et al*.[6] studied the triggering of a transient organo-gelation system in which a chemically active solvent controls the formation of the chemical equilibrium of LMWGs, driving the self-assembly of gels. This kind of solvent-induced kinetical control of gel's metastability (non-equilibrium) enables control of transient systems. The gelation process was based on the selective deprotection of the Boc-group from *N*-*tert*-butyloxycarbonyl (Boc)–*L*-phenylalanyl–*L*-phenylalanine *tert*-butyl ester (**15**) in the presence of *tert*-butyl ester group (*t*BuOAc).[44] In the presence of H_2SO_4 and *tert*-butyl acetate, the process enables the formation of *L*-phenylalanyl–*L*-phenylalanine *tert*-butyl (Phe-Phe-O*t*Bu) (**17**) ester. In these circumstances, the removal of the Boc-group is irreversible, forming CO_2 and amine product **17**, while the removal of the t*ert*-butyl ester group is reversible, forming reactive $t\text{Bu}^+$ cation and reforming the ester group (**15**) (Figure 20).[6]

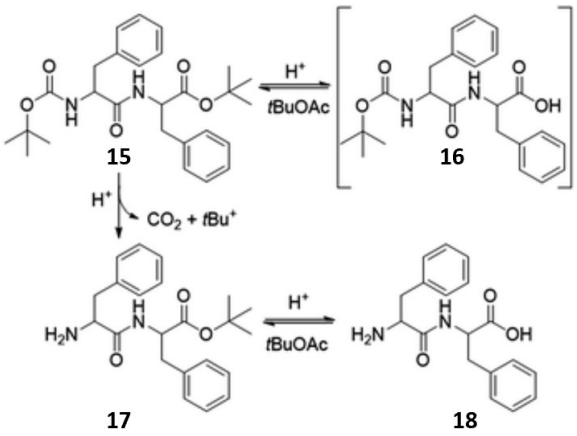

Figure 20. *Tert*-butyl acetate is a chemically active solvent driving the formation of LMWGs and gel collapse.[6] Reprinted with permission from ref. 6. Copyright © 2023 American Chemical Society.

The *tert*-butyl acetate has a significant role as a chemically active solvent by enabling the formation of LMWGs. The hypothesis of the study was that LMWG can be Phe-Phe-O*t*Bu (**17**), Phe-Phe (**18**) or both due to the dynamic equilibrium in which the formation of **18** from **15** can occur before the reformation of the ester group. However, gelation studies of individual

components **17** and **18** showed that, in this case, the gel is formed when the ratio between gelators is 0.9:1.0.[6]

Chemically active *tert*-butyl acetate also has a significant role in gel collapse by driving the chemical equilibrium between gelators towards **18**. The gels were observed to collapse in the presence of *tert*-butyl alcohol (*t*BuOH). The ratio between H_2SO_4 and tert-butyl acetate thus determines the gel's metastability. By regulation, this could enable, for example, controlled degradation of gels.[6]

4 Stimuli-responsive gels – triggering with pH

Non-covalent bonds are relatively weak, enabling the dynamic and reversible ability to respond to external stimuli, such as temperature, pH, solvent, light, and redox reactions.[8] pH sensitivity is based on the ionisable groups of the gelator, for example, carboxyl or pyridine group, which can interact with other molecules in the medium. pH has a role in gel formation, gel structure and applications. pH changes change the ratios between acid and base conjugates in C-terminus, thus affecting the LMWGs solubility to the solvent environment.[7,19,45] However, predicting the right pH for gelation is not easy. It is widely thought that gelation occurs when pH falls below the apparent pK_a of dipeptide-conjugates. However, this is not always the case, and multistep aggregation of Fmoc-Phe-Phe with two pK_a values (9.9 and 5.8) has been reported.[9] Gelator`s charge state depends strongly on their solvent environment pH. The charge can be experimentally evaluated by determining apparent pK_a. Apparent pK_a represents a state in which the protonated and deionized groups are equal in the system.[46]

Acid-based stimulation can cause heterogeneous particles or precipitates, which is the reason for the poor reproducibility of gelation (Figure 21). Due to rapid fibril formation at low pH, this problem leads to the formation of non-homogenous gels due to slower mixing kinetic than the initial gelation kinetics.[17] Adams *et al.*[17] introduced the use of hydrophilic glucono-*δ*-lactone (GdL) to stimulate Fmoc-Leu-Gly (**19**) gelation to improve gel homogeneity. GdL hydrolyses progressively in water and forms gluconic acid resulting in a steady pH decrease. Due to the homogeneity of the gels, reproducibility of gelation was achieved with controlled kinetics and gel properties.[17]

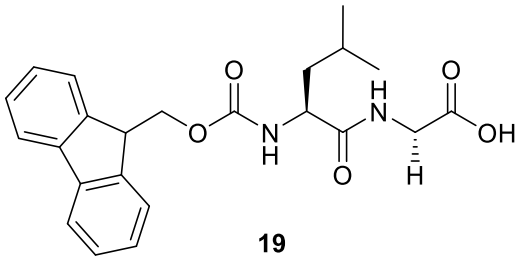

19

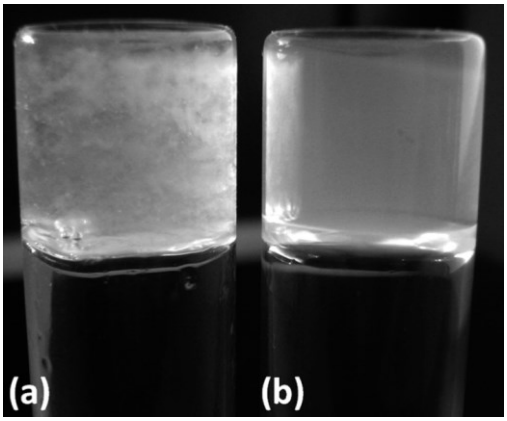

Figure 21. Gradual lowering of pH results in a homogeneous Fmoc-Leu-Gly gel. The pH (after 24 hours) is the same in both cases (a) acid activation with HCl and (b) acid activation with GdL.[17] Used with permission of RSC, A new method for maintaining homogeneity during liquid-hydrogel transitions using low molecular weight hydrogelators, Adams, D. J., Butler, M. F.; Frith,W., Kirkland, M, Mullen, L., Sanderson, P., 5, 2023; permission conveyed through Copyright Clearance Center, Inc.

The participation of GdL in the self-assembly process was studied with ^{1}H NMR. The results show that NMR shifts of GdL have remained the same in the gels. This indicates that GdLs mobility is not reduced when gels are formed, and they are not chemically incorporated into the gel. In addition to the possibility of regulating the gel's mechanical properties, the method allows following the gelation, such as fibre formation and broadening, over time, which opens possibilities for further studies with gels. When structural stability has been achieved, the effect of different gelators on the gel properties can be studied even better. The method is also suitable for studying different gelation conditions because pH can be controlled by varying the amount of added GdL. However, the pH change over time depends on the peptide used.[17]

4.2 The apparent pK_a value

Although the general understanding in the literature is to consider the pK_a of gelators as a good rule of thumb for gelation pH, it is not always valid. Adams *et al*.[18] studied pH-stimulated gelation with Fmoc dipeptides (Leu-Phe, Phe-Gly, Leu-Gly, and Ala-Gly) **(20-23)** using GdL acid-stimuli and observed higher pK_a values than expected, noticed to effect especially to more hydrophobic gelators. The study shows that the kinetics of pH change is highly dependent on the hydrophobicity of the gelator used in the gel formation. More hydrophobic ones (Phe-Gly, Figure 22) tend to show a faster decrease in pH in a shorter time than more hydrophilic ones (Leu-Gly and Ala-Gly). Additionally, after this initial pH drop, there is a subsequent rise in pH before it decreases permanently again. Described phenomenon is not observed with hydrophobic Fmoc-Leu-Phe due to the even more rapid change in pH. However, the final pH values are very similar. To compare acid stimuli with HCl and GdL, titration of HCl was also studied. pH drops more dramatically even though the final pH seems to set a bit lower than with GdL stimuli (Figure 22).[18]

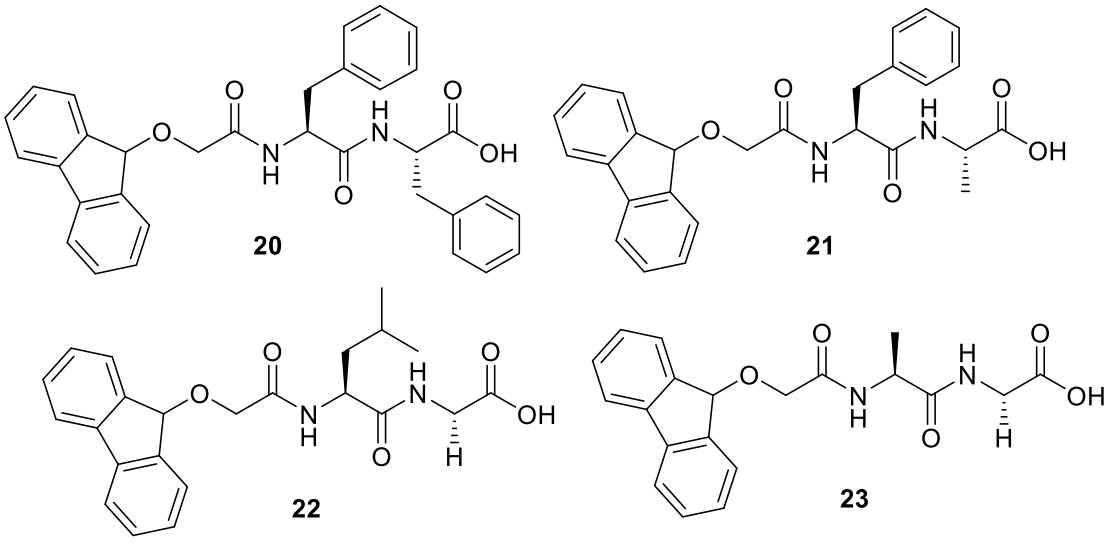

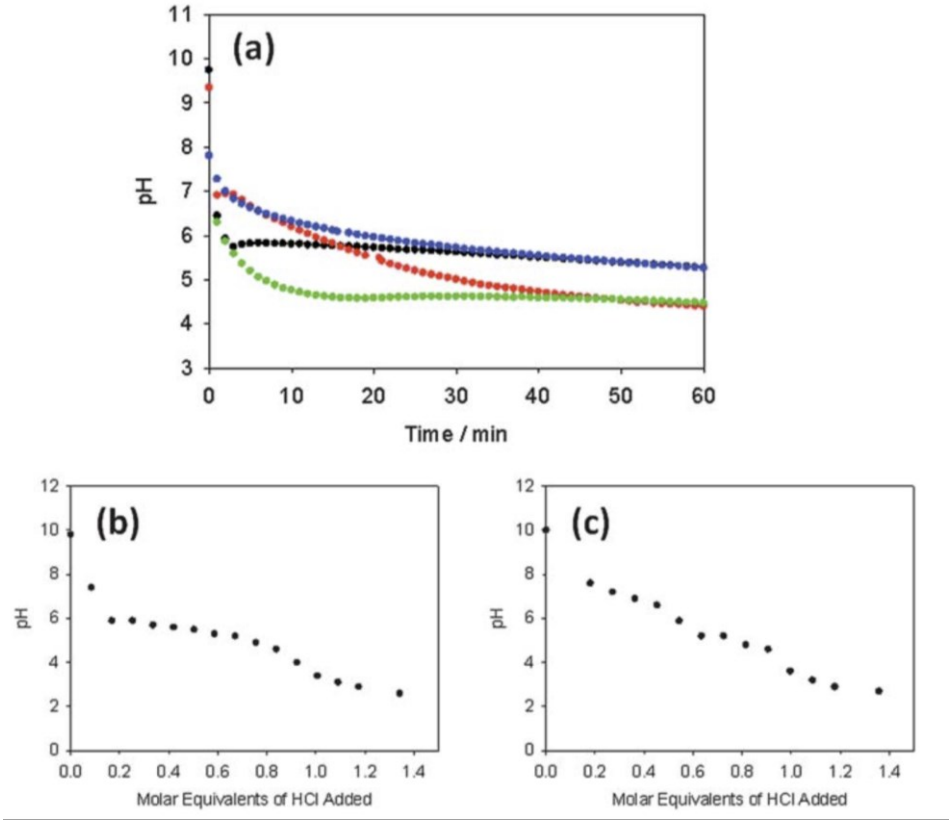

Figure 22. (a) The pH change with GdL was studied with Fmoc-based gels: Fmoc-Leu-Phe (blue line), Fmoc-Phe-Gly (red line), Fmoc-Leu-Gly (black line), and Fmoc-Ala-Gly (green line). After 24 h, the final gel pH was set to 3.9 ± 0.1. However, more and less hydrophobic gelators react differently to GdL addition. (b) HCl titration with Fmoc-Leu-Gly and (c) with Fmoc-Phe-Gly.[18] Used with permission of RSC, Relationship between molecular structure, gelation behaviour and gel properties of Fmoc-dipeptides, Adams, D., Mullen, L., Berta, M., Chen, L., Frith, W., 6, 2023; permission conveyed through Copyright Clearance Center, Inc.

Two possible explanations for higher-than-expected apparent pK_a were presented: (1) Self-assembly begins when the pK_a of the gelator's C-terminus is reached. However, assembled structures have higher pK_a than free peptides. Thus, due to higher pK_a, hydrolysis of GdL slows down and pH increases. (2) Dipeptide forms a saturated solution of non-assembled molecules when pH decreases. Due to the assembly, the concentration of free dipeptides drops, leading to an increase in pH.[18]

In addition to the fact that gelation pH does not have a comprehensive explanation and self-assembly is strongly dependent on both acid-stimuli and gelators, predicting the assembly of multicomponent gelators (two or more peptides) is even more complicated. Gelators with two

different pK_a values varying by 0.9 units were observed to co-self-assemble via pH stimuli in order of pK_a values.[34] Advantage of this type of gel is the possibility to form anionic, zwitterionic, or cationic forms. Thus, the gelation pH can vary in a broad range.[47] However, the opportunity and challenge of multicomponent gels are that LMGWs can self-assemble alone, act as inhibitors for each other's self-assembly or co-assemble.[34]

Colquhoun *et al*.[2] studied the gelation mechanism of naphthalene-Phe-Phe (2Nap-Phe-Phe) (**10**) gelators in two different ways: (1) dissolution at high pH followed by the addition of salt, (2) pH decrease with GdL followed by the gradual increase of pH. Study shows that, like previous examples, the microstructure and mechanical properties of gels depend on their formation route.[34]

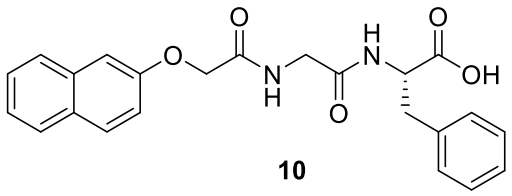

10

Rheological studies of 2Nap-Phe-Phe gels show that acid-triggered gels broke down more easily than NaOH triggered ones. However, both broke down sharply when the strain is applied, and storage moduli (G`) drops under loss moduli (G``). The total G` and G`` were observed to be alike, which indicates that gel strength alone cannot account for all the differences observed in how gels behave. Under five cycles of shear deformation, both gels recovered approximately 50 % of their original G` values (Table 7). Shear parameters: Constant frequency of 10 rad s^{-1} and a strain of 0.5% for 200 seconds followed by a higher strain of 500% for 60 seconds.

Table 7. The triggering method affects gels recovery from their original storage moduli.[2]

2Nap-Phe-Phe gels	Gels recovery after first high shear deformation	Average recovery after five cycles
NaOH triggered assembly	32 %	50 %
GdL triggered assembly	100 %	58 %

4.2 pH effects on the secondary structure

The secondary structure plays a significant role in forming three-dimensional structures of peptides, and it contributes to many vital cellular functions. On the other hand, incorrect folding can lead to the onset of various diseases. Thus, the ability to control the gels' secondary structure is interesting to study.[48,49] Structures including β-sheets can entangle into lateral assemblies or aggregates, leading to different twists, bends and topologies of β-sheets due to the influence of the environment on gels triggering. The problem is not only applied to the gel formation but also to its further processing. The 3D structure also impacts the possibility of predicting receptor-ligand binding between gels and cells in the biological environment.[7,45]

Yang *et al*.[45] observed that the secondary structure could be controlled by controlling the surface charge of the peptides' C-terminus. The study of peptide-based gel (**24**) shows that alkaline phosphate (ALP) treatment (pH 7.4) drives hydrophobicity, and the formation of COO^- leads to electron repulsion between negative charges. Negative repulsion was also assumed to form between the gelator's lysine residues. ALP-treated gels seemed to adapt α-helix conformation. pH treatment (pH 5) instead protonates the COO^- group, and charge repulsion is lost due to the formation of COOH. This, in turn, leads to the formation of electrostatic interactions and drives the formation of β-sheet (Figure 23).[45]

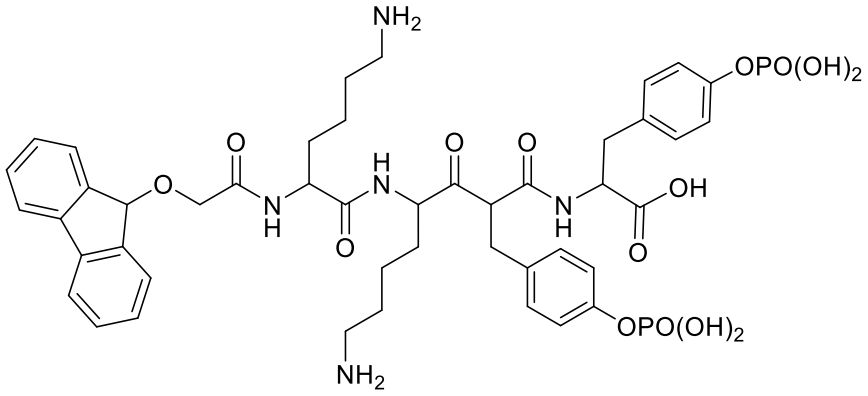

24

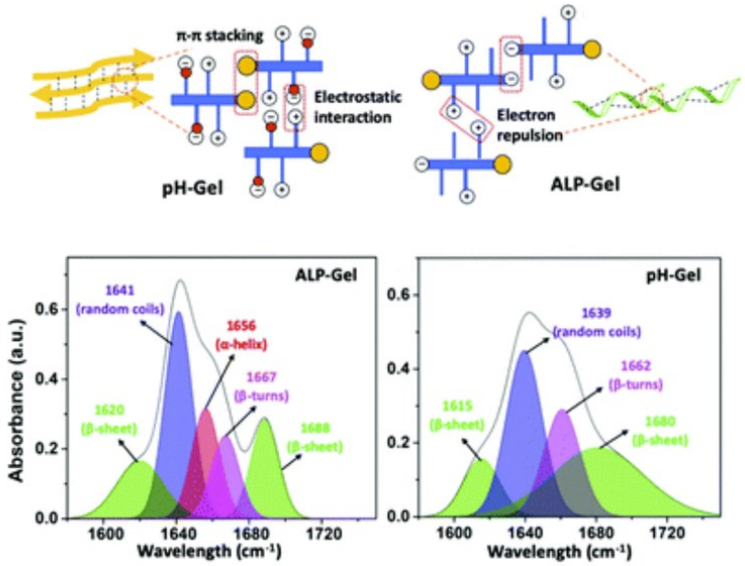

Figure 23. FTIR spectra show that ALP-treated gel's amide vibration refers to the formation of α-helix while acid treatment leads to the formation of β-sheets.[45] Used with permission of RSC, Stimuli-controlled peptide self-assembly with secondary structure transitions and its application in drug release, Yang, L., Gan, S.,; Guo, Q., Zhang, H., Chen, Q., Li, H., Shi, J., Sun, H., 5, 2023; permission conveyed through Copyright Clearance Center, Inc.

5 Applications

Supramolecular hydrogels have gained a lot of attention in gel applications due to their good biocompatibility, high-water content and soft matrix. Hydrogels also have minimal ability to absorb proteins due to interfacial tension. In addition to the biocompatibility, gelation kinetics, matrix resorption rate, possible toxicity and elimination routes should be considered, when considering potential applications.[7,50]

However, the stiffness of the hydrogels varies approximately between 4-7 pK_a, which can be modified by varying the peptide concentration or pH, but the softness of the material is still limiting their use.[7,25]

5.1 Drug delivery

The conventional drug delivery systems are limited due to their divergent drug release time compared to the required time for therapeutical effects. Hydrogels could be used as a platform for drug release at desired time and site when gels are explored for structural changes via stimuli action.[7] The drug release by hydrogels conformational changes or solubility changes can occur via 1) swelling, 2) dissociation, or 3) alteration of the drug partition coefficient.[51,52]

pH varies in different body parts like the gastrointestinal tract[53] and blood vessels[54]. Thus, pH can be utilized as a potential method for drug release from polymer-based hydrogels with ionic groups. Ionization of ionic groups in appropriate pH leads to the formation of charged ions and electrostatic forces in the polymer network. This causes the swelling of the polymeric network and the release of the drug.[55] Anionic groups were observed to ionise above polymer pK_a while cationic ionized below the pK_a of polymer amine groups (Figure 24).[7]

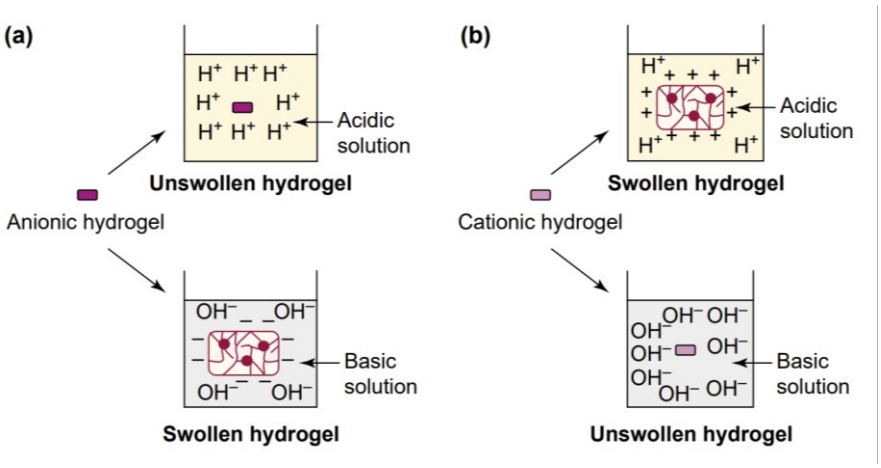

Figure 24. Swelling of the gel at appropriate pH leads to drug release.[7] Reprinted from Hydrogels: from controlled release to pH-responsive drug delivery, 7, Gupta, P., Vermani, K., Garg S., 11, 2023, with permission from Elsevier.

The idea represented in Figure 24 is used in hydrogel applications for cancer treatment. pH differences between the acidic extracellular matrix and the alkaline intracellular matrix characterize cancer cells. Anionic hydrogels are therefore used for controlled drug release inside the tumor cell while cationic are used for controlled release to the extracellular matrix.[56]

Although the study presents the simplified rule for predicting proper pH for swelling, the drug release is dependent on the polymer properties and properties of the swelling material as well. Therefore, different buffers affecting pH in the physiological environment make it more difficult to predict the suitable pH for drug release. Luckily, changes in the polymeric network are observed even with small changes in pH (for example, from 5.7 to 5.3).[7]

Liao *et al.*[50] studied *N*-*N*-di(pyridin-4-yl)-pyridine-3,5-dicarboxamide (PDA-N4) as a potential platform for controlled drug release. Gelation of PDA-N4 was implemented via solvent-mediate strategy in which self-assembly of LMWGs was observed with water ratio ≤ 50 % (DMSO/H_2O).[50] PDA-N4 was observed to have good cytocompatibility *in vitro*. The cytocompatibility was studied with human umbilical venous endothelial cells, which could divide in the platform. Studying PDA-N4 showed a high potential as a B12 releaser in 1/9 DMSO/H_2O solvent mixture. The release of B12 as a water-soluble and UV-active molecule was observed to follow a first-order kinetic drug release mechanism. The concentration of released B12 increased gradually over time, and no difference was noticed when different amounts of B12 were trapped in the PDA-N4 platform (Figure 25).[50]

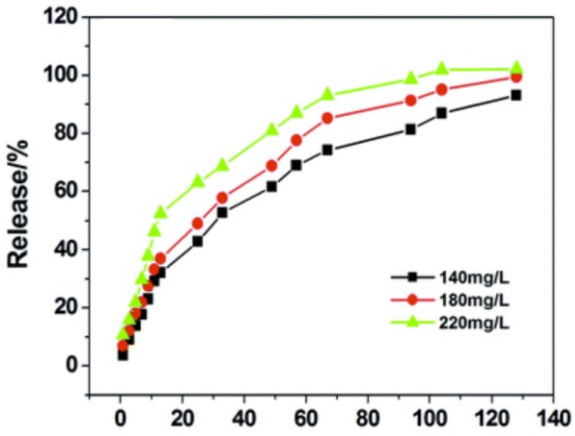

Figure 25. Release profile of PDA-N4 can release vitamin B12.[50] Reprinted with permission from ref. 50. Copyright © 2023 American Chemical Society.

5.2 Tissue engineering

Silva *et al.* succeeded in encapsulating *in vitro* neural progenitor cells (NPCs) found in laminin and known to induce neurite growth to IKVAV (**5**) hydrogels. However, the epitope of the NPCs was modified via glutamic acid-glutamine-serine to control bioactivity and induce cationic electrostatic repulsion in the cell matrix to promote self-assembly.[57–65] These scaffolds could be used to control cell differentiation. The gel self-assembly was induced in an aqueous solution, which allowed injecting gels into the tissue as a liquid and used, for example, to replace lost nerve cells after trauma.[57,57,66–68]

Fast gel formation was observed when an aqueous gelator media (1 w-%) was mixed with a suspension of NPCs with a 1:1 ratio. The gels were observed to stay alive during the self-assembly of the gelator, which indicates sufficient oxygen diffusion. Based on the results, the external matrix of the gels is not only a supporting factor for the scaffold but provides a media through which the diffusion can occur. Gel's water content was observed to be critical to keeping NPCs alive. Thus, rigid networks containing less than 99,5 % of water were unable to keep cells alive.[57]

6 Conclusion

Even though LMGWs peptide gels are quite widely known, a general sum of factors affecting the gel formation, structure, and properties have not been identifiedSolvent polarity, pH, different solvent mixtures, and water as a solvent have been studied as influencing factors in gel formation, morphology, and properties.

The most divergent opinions were discovered about the role of hydrogen bonding in gelation. Safiullina and Zhang *et al.*[5,28] present that hydrogen bonding has a significant role in gel formation, but Zhu and Dordick[13] present that hydrogen bonds do not define gelation themselves. Canrinus *et al*.[39] also show that hydrogen bonds impact the gel properties. Solvent polarity was observed to have a considerable role by affecting the intramolecular interactions between gelator molecules or gelator and solvent molecules. Surprisingly, hydrophobic gels were observed to be more sensitive to solvent polarity even though the hydrophilic gels were reported to form weaker gels.[13,15]

Different solvents affect the gel's fiber length and network homogeneity. However, the effect on fiber length was different for each studied solvent and even similar groups of solvents, like benzene and other aromatic solvents, did not show similar behaviour.[28] Different solvents were not observed to directly affect the gel's self-assembly, but they were was strongly connected to the variation of gelation time. However, the gelation triggering method has been proposed to exert a more significant influence on the process of self-assembly than the solvent environment in which it occurs.[20]

In addition to the structural changes, the solvent environment affects the gel's properties, like gelation time, MGC, stiffness and gel's ability to recover.[13,15] Also, the triggering method of the gelation affects the gelation, gel's homogeneity, and ability to recover.[17,18,34] pH-stimuli was found to be an effective way to stimulate the self-assembly of LMWG. The pK_a of the gelator C-terminus is a good gelation pH indicator, but it does not cover all the cases since apparent pK_a values were observed to be higher than expected. pH-stimulation could be used to form more homogeneous gels and to modify gel structure and properties, and it has an undisputed role when different gel applications are studied.[7,18]

Solvent environment and gel triggering undoubtedly have a role in gel self-assembly, morphology and properties. No gels, excluding multiple LMWG systems, are observed to form

without triggering process.[1,9] LMWG gels are generally considered good application platforms, for example, due to their biocompatibility. However, cell ability, for example, to survive only in 99,5 % of water containing matrix[57] might set limitations to gelation and solvents used in gelation. Although the preceding literature extensively addresses the influence of the solvent environment on gelation outcomes, it is important to acknowledge that the selection of the gelator itself also plays a crucial role in the gelation process, including aspects such as solubilization. The gelation process is influenced by multiple factors, making it challenging to isolate the individual effects of each factor without disregarding the potential influence of other factors, such as the trial temperature, which can impact gelator solubility or protonation.

EXPERIMENTAL PART

7 Motivation

Supramolecular gels have several uses in pharmaceutics, the food industry, and cosmetics. Amino acid-based gels have gained great momentum especially in biomedical applications, for example, drug delivery, cell culture, hygiene products, tissue engineering scaffolds, and wound dressings. Gels are generally classified as semi solid, soft materials (no gravitational flow is observed upon inversion). The structure of supramolecular or physical gels is based on low molecular weight gelators (LMWGs), which can self-assemble into ribbons, fibres, sheets, or spheres. The resulting assemblies then interact with each other by non-covalent interactions to forming a 3D network[1,4] which encapsulates the solvent (water or organic solvent).

This work is based on the previous studies of Lin *et al.*[44] referring to the selective deprotection of the *N*-*tert*-butoxycarbonyl (Boc) group of a precursor gelator in the presence of a *tert*-butyl ester group, using a *tert*-butyl based solvent under acid conditions. The previous studies of Chevigny *et al.*[6] report the *in situ* transient gelation of the dipeptide precursor gelator Boc-Phe-Phe-O*t*Bu in a chemically active solvent (*tert*-butyl acetate, *t*BuOAc). During the selective deprotection of the Boc group, two compounds form, Phe-Phe-O*t*Bu and Phe-Phe, which are active LMWGs and which ratio varied over time. Boc-Phe-Phe-O*t*Bu based gels had a lifespan of four days, affected by the formation of a secondary solvent (*t*BuOH), which acts antagonistically against the primary *t*BuOAc solvent. The gelation process was influenced by varying the concentration of the precursor gelator and acid.

In this work, Boc-Leu-Phe-O*t*Bu and Leu-Phe-O*t*Bu were synthesized and characterized. The organogel formation of precursor gelator Boc-Leu-Phe-O*t*Bu (Scheme 1) was studied using five different solvents, namely *tert*-Butyl esters and ethers (*tert*-butyl acetate, *tert*-butyl chloroacetate, *tert*-butyl acetoacetate, *tert*-butyl methyl ether and *tert*-butyl formate), which produce a tertiary carbocation under acidic conditions.

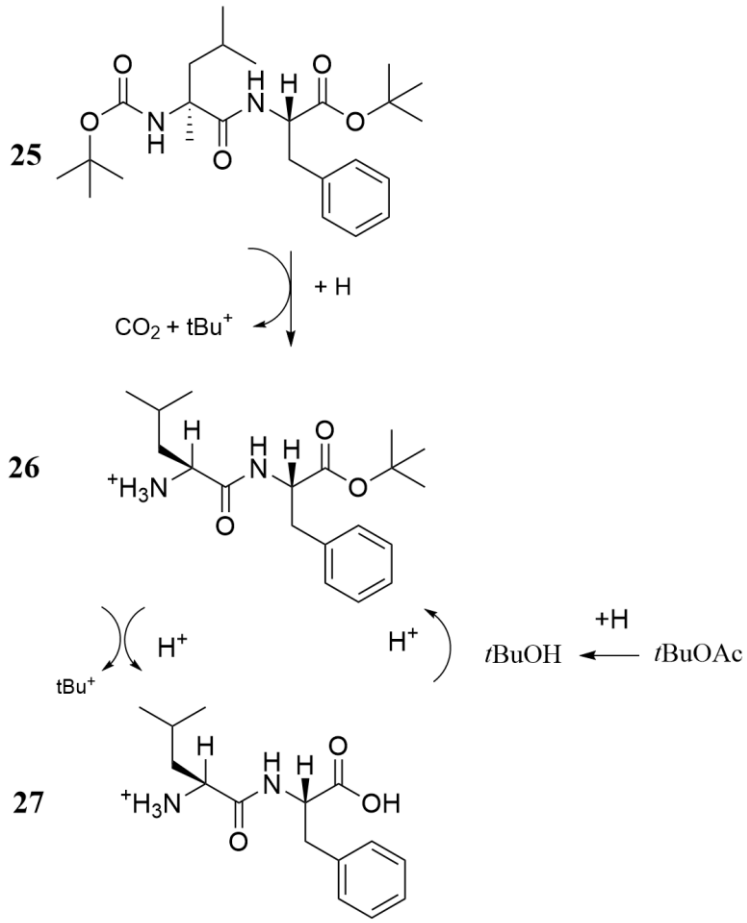

Scheme 1. Proposed mechanism of *in situ* gelation.[6] Boc-Leu-Phe-O*t*Bu **(25)** is activated by sulfuric acid and the Boc group is removed irreversibly. Leu-Phe-O*t*Bu **(26)** and Leu-Phe **(27)** are the active gelators (LMWGs) forming a self-supporting gel. *tert*-butyl acetate is a chemically active solvent and thus can reverse the deprotection of the *tert*-butyl group by donating *tert*-butyl cations. The *tert*-butyl alcohol formed from the hydrolysis of *t*BuOAc converts the gel to a solution.

The aim of the work was to study if the gelation behaviour is similar to previous studies when using different active solvents and acid concentrations.[6] Additionally, we wanted to explore the dynamic nature of the reaction equilibrium with respect to time and the effect of different solvents on the gelation process and gel composition. In this study the precursor gelator Boc-Leu-Phe-O*t*Bu was selected as a model. Based on literature, it is difficult to predict the structure of the supramolecular gel and foresee which solvents may be suitable in the process of dynamic systems.[1]

Dipeptide organogels were characterized by ^{1}H NMR, high-resolution mass spectrometry (HR-MS), Fourier transform infrared spectroscopy (FT-IR) and scanning electron microscopy imaging (SEM). In addition, swelling tests and gelation studies were performed, while the gel-to-sol transition temperature was measured.

8 Materials and methods

A Mettler Toledo XP205 DeltaRange (d = 0.01mg/ 0.1 mg) scale was used to measure raw materials. A Denver instrument APX-200 scale was used to measure the final yield of Boc-Leu-Phe-O*t*Bu and Leu-Phe-O*t*Bu. Stuart SMP30 was used to measure raw materials' melting points. The temperature was raised by 5°C at one minute intervals. Hielscher UP50H ultrasonic processor was used to sonicate raw materials and solvents to fine solution. Hanessian`s stain was used for TLC. The reagents used in work are presented in Table 8.

Table 8. Reagents used for synthesis and gelation.

Materials	**Molecular weight (g/mol)**	**Manufacturer**	**Purity (%)**
Boc-Leu-OH	231.29	Sigma-Alrich	> 99
Leu-Phe	248.28	Sigma-Alrich	95
(S)-3-Phenylalanine-*tert*-butyl ester	257.76	BioSynth	
TBTU (2-(1H-Bentrotriazole-lyl))	321.09	FluoroChem	
DMF	73.09	Arcon Organics	99.8
$NaHCO_3$	84.01	FluoroChem	98.5
$MgSO_4$	120.37	Sigma-Alrich	
HCl	36.6		
DCM	84.93	VWR Chemicals	99.5
Hexane	86.18		
Ethyl acetate	88.11	VWR Chemicals	99.9
Methanol	32.04	Honeywell	> 99.8
Toluene	92.14	VWR Chemicals	
tert-butyl acetate	116.16	TCI	> 99
tert-butyl methyl ether	88.15	TCI	> 99
tert-butyl acetoacetate	158.2	TCI	> 95
tert-butyl formate	102.13	Sigma-Alrich	99
tert-butyl chloroacetate	150.61	Thermo scientific	98
H_2SO_4	98.08	Fluka	95-97
DMSO	84.17	Merk	99.8

NMR spectra were measured by a Bruker Avance III HD 300 MHz NMR spectrometer. ppm scale was assigned to the residual signal of deuterated d_6-DMSO, which was used as a solvent (δ (DMSO) = 2.50 ppm). The samples of self-supporting gels and partial gels were dried under vacuum overnight prior the preparation of NMR samples. Liquid samples (sol state) that had not gelled and powder samples (raw starting materials) of Boc-Leu-Phe-O*t*Bu and Leu-Phe were directly dissolved in d_6-DMSO.

Fourier transform infrared (FT-IR) spectrophotometer Bruker Tensor 27 was used to analyse the supramolecular interactions in gels based on the spectra of raw materials Boc-Leu-Phe-O*t*Bu and Leu-Phe-O*t*Bu. The FT-IR spectra were recorded in the wavelength range 400-4000 cm^{-1} with 24 scans. For the measurement of Leu-Phe raw material 124 scans was used.

Mettler Toledo FiveEasy pH meter was used to measure the pH of gels. Agilent 6560 was used to measure the mass (High resolution mass spectrometry) of raw materials Boc-Leu-Phe-O*t*Bu and Leu-Phe-O*t*Bu and of vacuum dried gel samples (xerogels). A 10 μM of HR-MS samples was diluted in MeOH and measured with ESI-IMGTOF. The capillary voltage was set to 4000 V, and the flow rate was set to 5 μl/min. Chemcalc was used to determine the theoretical m/z values. The transition temperature of organogels was measured with a Thermo Fisher Scientific Block heater.

SEM images were analysed with ImageJ software. Boc-Leu-Phe-O*t*Bu gels were left to dry for 72 h on a petri dish and transferred thereafter on copper grids. Electron high tension was set to 10,0 kV and an aperture was set to 30 μm.

9 Synthesis and characterization of dipeptides

9.1 Synthesis of Boc-Leu-Phe-O*t*Bu

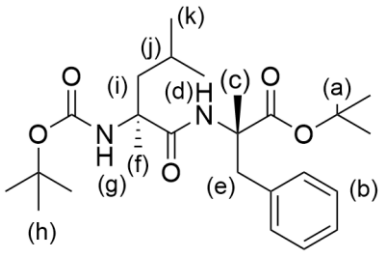

25

Figure 26. The chemical structure of Boc-Leu-Phe-O*t*Bu with proton assignment (**25**).

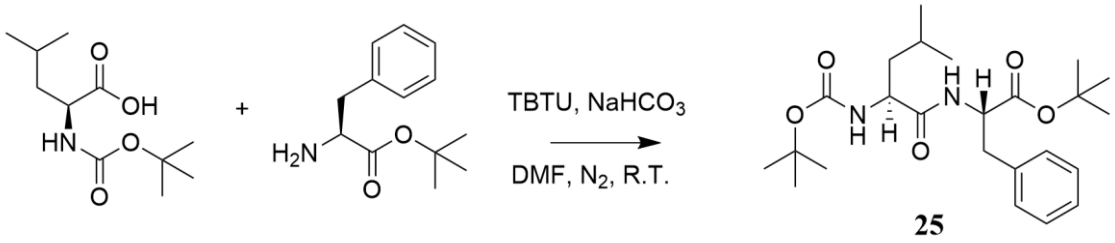

25

Scheme 2. Reaction synthesis of Boc-Leu-Phe-O*t*Bu.

Boc-Leucine (400.37 mg, 1.0 eq), TBTU (555.63 mg, 1.0 eq), $NaHCO_3$ (305.36 mg, 1.1 eq) and phenylalanine-*tert*-butyl ester (490.30 mg, 1.1 eq) were added to anhydrous DMF (10 ml) under N_2 atmosphere. The solution was left to stir overnight at R.T. under an N_2 atmosphere. The next day, the starting materials had been consumed, and the TLC indicated the formation of the product (hexane (Hex): ethyl acetate (EA) 1:1 Hanssians`s stain, $R_f = 0.54$). The solvent was evaporated under vacuum (co-evaporation with toluene x3) and left under vacuum overnight. The next day, the residue was dissolved in DCM. The organic phase was extracted with water (x2) and subsequently washed with HCl (0.1M), water (x2), and a saturated $NaHCO_3$ solution. The organic phase was then dried with $MgSO_4$ and evaporated under vacuum, yielding a yellow powder (752.3 mg, 69 %). Melting point: 123-125 °C.

^{1}H NMR (300 MHz, d_6-DMSO) δ 7.98 (d, *J* = 7.6 Hz, 1H, **NH**), 7.23 (q, *J* = 6.4 Hz, 5H, **Ar**), 6.79 (d, *J* = 8.6 Hz, 1H, **NH**), 4.44 – 4.25 (m, 1H, **CH**), 3.96 (d, *J* = 7.3 Hz, 1H, **CH**), 3.03 – 2.86 (m, 2H, **CH_2**), 1.61 – 1.48 (m, 1H, **CH**), 1.37 (s, 9H, **CH_3**), 1.31 (s, 9H, **CH_3**), 0.84 (dd, *J* = 8.4, 6.5 Hz, 6H, **CH_3**) (Figure 27). Protons responded to Chevigny et al. [6] observations.

^{13}C NMR[6] (126 MHz, DMSO) δ 172.36, 170.32, 155.11, 137.11, 129.18, 128.05, 126.38, 80.58, 77.90, 53.83, 52.57, 40.84, 36.78, 28.14, 27.45, 24.14, 22.87, 21.51.

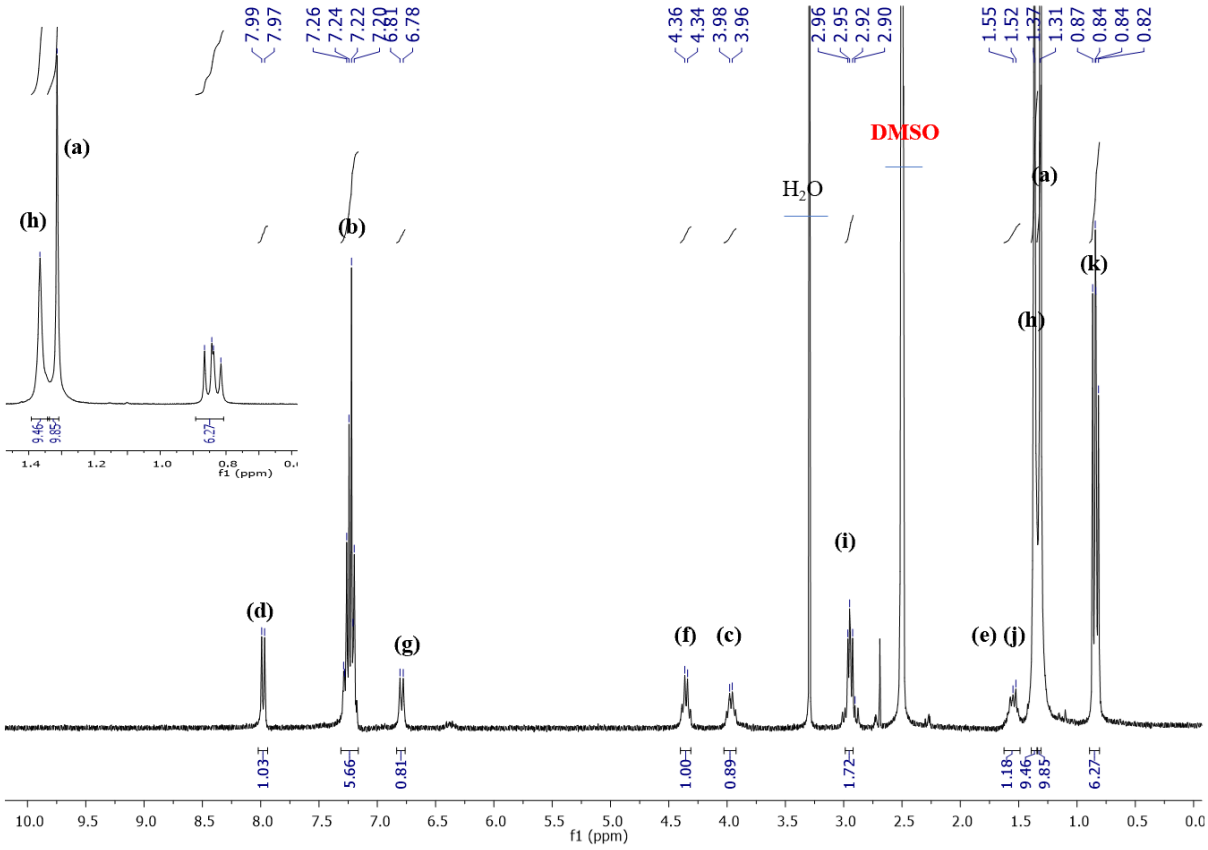

Figure 27.[1]H NMR (300 MHz, d6-DMSO) of Boc-Leu-Phe-O*t*Bu (**25**).

9.2 Synthesis of Leu-Phe-O*t*Bu

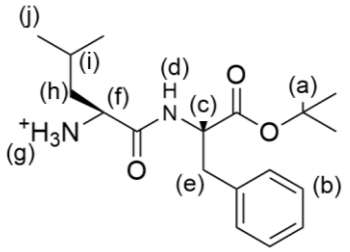

26

Figure. 28. The chemical structure of Leu-Phe-O*t*Bu with proton assignment (**26**).

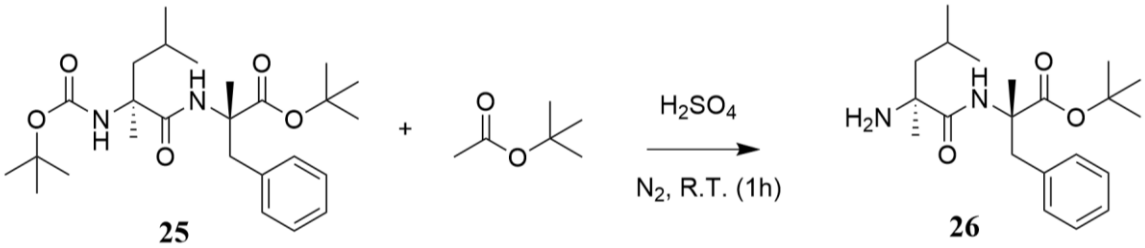

Scheme 3. Reaction synthesis of Leu-Phe-O*t*Bu.

Boc-Leu-Phe-O*t*Bu (500.00 mg) was suspended in *t*BuOAc (5.75 ml). Concentrated H_2SO_4 (0.31 ml, 5.0 eq) was then added dropwise at R.T. After 1 h, the formation of the product was confirmed by TLC (Hex: EA 3:1 and with EA: MeOH: H_2O 7:2:1, Hanessian`s stain, R_f = 0.37). The reaction mixture was neutralized by adding saturated $NaHCO_3$ solution and extracted with ethyl acetate. The organic phase was dried with $MgSO_4$ and evaporated under vacuum, yielding a yellow oil (299.7 mg, 78 %).

^{1}H NMR (300 MHz, d_6-DMSO) δ 8.17 (d, J = 8.1 Hz, 1H, **NH**), 7.20 (m, 5H, **Ar**), 4.37 (dd, J = 14.3, 7.4 Hz, 1H, **CH**), 3.18 (s, 1H, **CH**), 3.00 – 2.84 (m, 2H, **CH_2**), 1.62 (dd, J = 14.2, 6.6 Hz, 1H, **CH**), 1.30 (s, 9H, **CH_3**), 0.82 (m, 6H, **CH_3**) (Figure 29). Protons responded to Chevigny *et al.*[6] observations.

^{13}C NMR (126 MHz, DMSO) δ 172.36, 170.32, 155.11, 137.11, 129.18, 128.05, 126.38, 80.58, 77.90, 53.83, 52.57, 40.84, 36.78, 28.14, 27.45, 24.14, 22.87, 21.5.

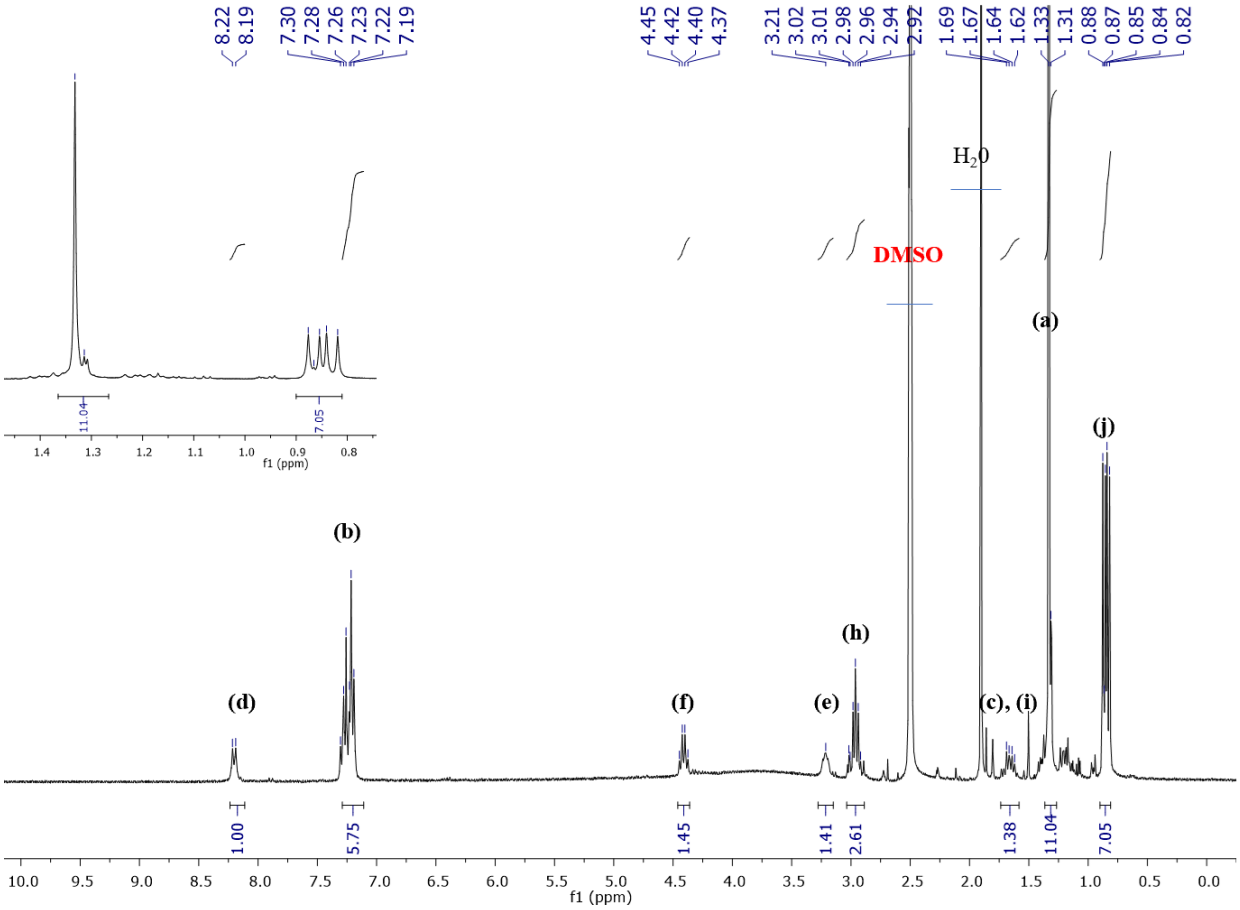

Figure 29.[1]H NMR (300 MHz, d6-DMSO) of Leu-Phe-O*t*Bu.

10 Gelation trials and results

The gelation behaviour of Boc-Leu-Phe-O*t*Bu was studied in five different solvents (*tert*-butyl acetate, *tert*-butyl chloroacetate, *tert*-butyl acetoacetate, *tert*-butyl methyl ether and *tert*-butyl formate (Figure 29)) using three different acid concentrations. The concentration of Boc-Leu-Phe-O*t*Bu (0.05M) was kept constant. The reaction deprotection mechanism of esters and ethers is very different, but both produce a carbocation, which was assumed to react with deprotected Boc-Leu-Phe-O*t*Bu after adding the acid (Figure 30).

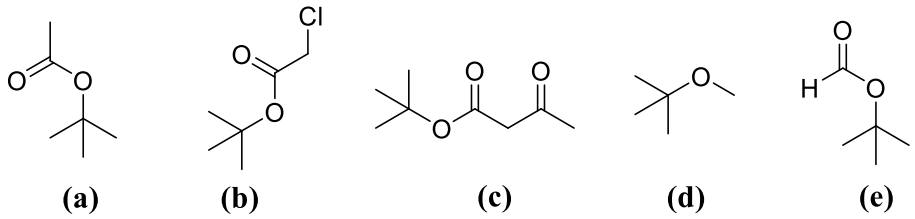

Figure 30. Solvents used in gelation tests (a) *tert*-butyl acetate, (b) *tert*-butyl chloroacetate, (c) *tert*-butyl acetoacetate, (d) *tert*-butyl methyl ether and (e) *tert*-butyl formate.

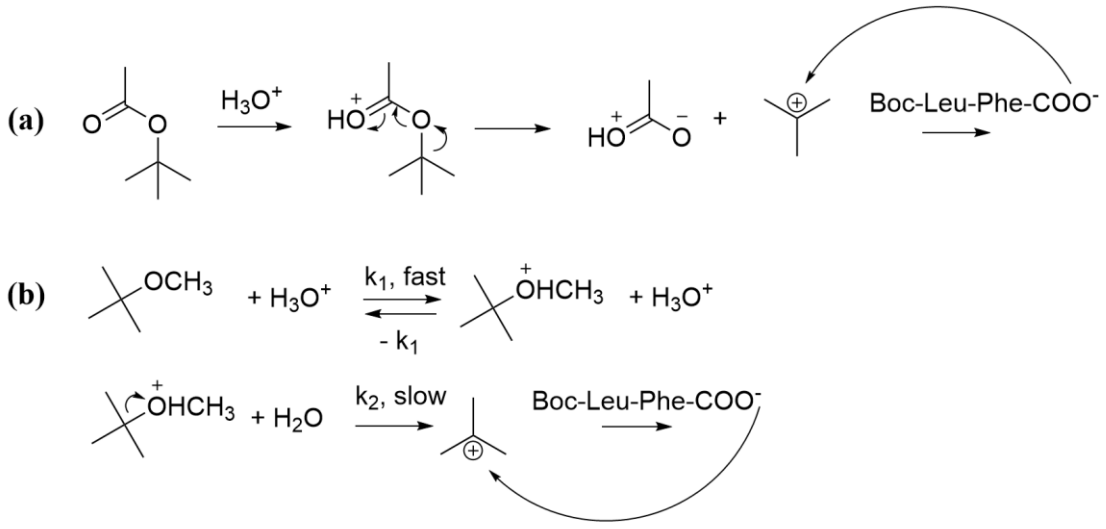

Figure 31. (a) Ester group forming a *tert*-butyl carbocation and (b) ether group forming *tert*-butyl carbocation[69] in the presence of acid.

General procedure: Boc-Leu-Phe-O*t*Bu was suspended in the chosen solvent and sonicated with until a fine suspension formed. H_2SO_4 was then added, the mixture was gently swirled and left to stay at room temperature for at least 12 h. The gelation process was confirmed by the vial inversion method. Gelation results are shown in Table 9. The pH value was measured at the initial suspensions since the addition of acid dropped the pH under zero, which was not possible to be measured due to the given measuring range of the pH meter.

Table 9. Gelation trials at different solvents. The amount of Boc-Leu-Phe-O*t*Bu was 21.7 mg suspended in 1 mL of solvent (200 µl were used for the *tert*-butyl formate trials). SSG = self-supporting gel and PG = partial gel.

	Conc. H_2SO_4 (eq)/ (µl)	**Gelation outcome**	**Gel formation**	**Gel decompose**
tert-butyl acetate	1/2.7	SSG	Day 1	-
tert-butyl chloroacetate	1/2.7	SSG	Day 1	-
tert-butyl acetoacetate	1/2.7	-	-	-
tert-butyl methyl ether	1/2.7	SSG	Day 12	-
tert-butyl formate	1/0.54	-	-	-

	Conc. H_2SO_4 (eq)/ (µl)	**Gelation outcome**	**Gel formation**	**Gel decompose**
tert-butyl acetate	0.5/1.35	SSG	Day 1	-
tert-butyl chloroacetate	0.5/1.35	SSG	Day 1	-
tert-butyl acetoacetate	0.5/1.35	PG	Day 1	Day 5
tert-butyl methyl ether	0.5/1.35	SSG	Day 12	-

	Conc. H_2SO_4 (eq)/ (µl)	**Gelation outcome**	**Gel formation**	**Gel decompose**	**pH (3 vials)**
tert-butyl acetate	0.18/0.5	SSG	Day 2		5.53; 5.01; 4.83
tert-butyl chloroacetate	0.18/0.5	SSG	Day 1	-	2.30; 2.52; 2.58
tert-butyl acetoacetate	0.18/0.5	-	-	-	4.75; 4.81; 4.70
tert-butyl methyl ether	0.18/0.5	PG	Day 5	-	4.25; 4.72; 4.16

Based on the gelation trials, three solvents at specific acid concentrations were selected for a more detailed review (Table 9). The solvents (*tert*-butyl acetate (0.18 eq), *tert*-butyl chloroacetate (0.18 eq) and *tert*-butyl methyl ether (1.0 eq)) form self-supporting gels at room

temperature (Figure 32). Studies with *tert*-butyl formate were abandoned after the first set of experiments because the solvent showed no signs of gelation and was expensive to use.

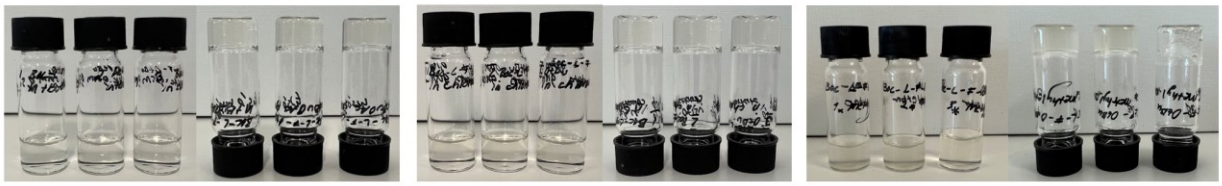

A B C

Figure 32. Self-supporting organogels of Boc-Leu-Phe-O*t*Bu in A) *tert*-butyl acetate (0.18 eq of acid), B) *tert*-butyl chloroacetate (0.18 eq of acid) and C) *tert*-butyl methyl ether (1.0 eq of acid).

Trials also indicate that the gelation results and gelation time are affected by changing the concentration of the acid in different solvents (Figure 33). By decreasing the concentration, gelation results improved in *tert*-butyl acetate and t*ert*-butyl chloroacetate solvents, whereas increasing the concentration yielded better gelation results in *tert*-butyl methyl ether solvent. pH tests combined with visual observations of the gels indicate that gels form under acid conditions and as previously observed,[6] acid is the driving force of the deprotection reaction, acting as the "gelation initiator".

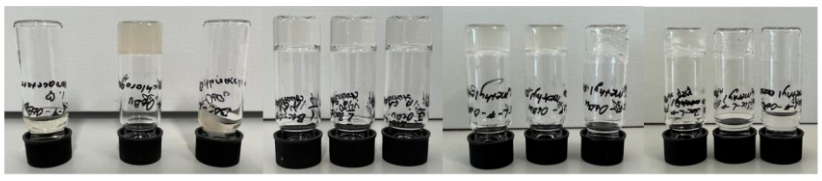

A B C D

Figure 33**.** The presence of acid drives the gelation process, which can be affected by varying its concentration. Boc-Leu-Phe-O*t*Bu in A) *tert*-butyl chloroacetate at day one (1.0 eq of acid), B) in *tert*-butyl chloroacetate at day one (0.18 eq of acid), C) in *tert*-butyl methyl ether at day 13 (1.0 eq of acid) and D) in *tert*-butyl methyl ether at day 12 (0.5 eq of acid).

pH measurements shows that *tert*-butyl chloroacetate suspensions of Boc-Leu-Phe-O*t*Bu are more acidic than those in other solvents and thus the lower amount of acid added (0.18 eq.) was sufficient for gelation. However, based on the results it is not clear why *tert*-butyl methyl ether suspensions need more acid to induce gelation than *tert*-butyl acetate (a SSG forms at Day 12). Since after the addition of acid the pH is negative in all trials, it is suggested that the formed gelators and their solubility should determine the formation of partial gels, self-supporting gels or solutions.

Unlike in previous studies,[6] Boc-Leu-Phe-O*t*Bu based gels did not decompose within 30 days, which means that the formed gels are not transient but rather static. Only in *tert*-butyl acetoacetate (Table 2) the partial gel turns to solution on day 5. Further to this, the temporal nature of the self-assembly event is apparent since the gels can form at different time periods after the addition of acid, while the self-assembly per se is affected by the acid concentration.

Based on previous studies,[6] dipeptide organogels should show potential changes in the ratio of the in-situ formed components (gelators). Gelation tests with Boc-Leu-Phe-O*t*Bu also indicate that the chemical equilibrium or the secondary structure of the materials may change after several days (Figure 34). For example, the gels in *tert*-butyl chloroacetate changed from transparent to opaque, meaning that the assemblies increased their size and absorb more visible light.

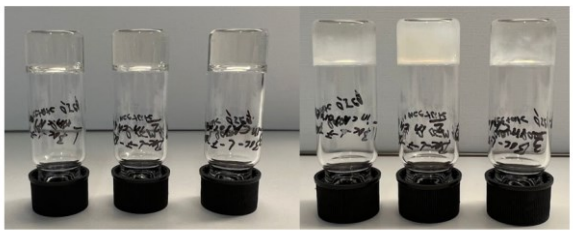

A B

Figure 34. Colour change after 4 days indicates changes in chemical equilibrium and/or the secondary structure of the gel materials. Three replicates of Boc-Leu-Phe-O*t*Bu in chloroacetate (0.05 eq of acid) at A) day one and B) day four.

11 Gelation test of Leu-Phe-O*t*Bu and Leu-Phe

Gelation trials were performed for Leu-Phe-O*t*Bu and Leu-Phe. The purpose of the study was to identify the active gelator molecule in different solvents. The gelation process was studied in *tert*-butyl acetate (0.18 eq), *tert*-butyl chloroacetate (0.5 eq) and *tert*-butyl methyl ether (1.0 eq) solvents.

As can be seen from Table 10, only Leu-Phe-O*t*Bu formed a self-supporting gel in *tert*-butyl methyl ether after 12 h (Figure 35). However, an interesting observation was made. In the case of *tert*-butyl methyl ether and *tert*-butyl chloroacetate, gelation started almost immediately after the acid addition. In the case of *tert*-butyl chloroacetate, however, sonication after the solvent addition possibly broke the gel network structure, and therefore, self-supporting gels were not formed. Additional trials would be necessary to confirm the observation. It would be also meaningful to study other dissolution methods to protect the structure of the gel. No gels were formed also when using Leu-Phe.

Table 10. Gelation test of Leu-Phe-O*t*Bu and Leu-Phe in three different solvents.

	***tert*-butyl acetate**	***tert*-butyl chloroacetate**	***tert*-butyl methyl ether**
Leu-Phe-O*t*Bu	no gel (0.18 eq)	gel formation (0.18 eq)	SSG (1.0 eq)
Leu-Phe	no gel (0.5 eq)	no gel (0.5 eq)	no gel (0.5 eq)

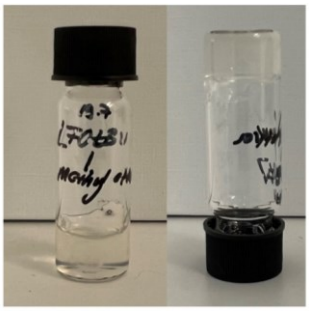

Figure 35. Vial inversion test of Leu-Phe-O*t*Bu gel in *tert*-butyl methyl ether at day one.

Based on the gelation studies, Leu-Phe-O*t*Bu forms a gel in *tert*-butyl methyl ether and *tert*-butyl chloroacetate, but no gel was formed in *tert*-butyl acetate. However, due to the small number of trials the possibility of Leu-Phe-O*t*Bu being a gelator in *tert*-butyl acetate cannot be ruled out. According to the aforementioned results, Leu-Phe cannot be considered a gelator per se.

During the pH measurements of the pre gel solutions, the *tert*-butyl methyl ether sample showed potential gel formation right after Boc-Leu-Phe-O*t*Bu was dissolved. This may indicate that the solvent can also participate actively in the gelation process by chemically modifying the structure of Leu-Phe-OtBu towards Leu-Phe-OMe.

12 Transition temperature $T_{gel\text{-}sol}$ measurements

For the transition temperature ($T_{gel\text{-}sol}$) measurements, three vials of Boc-Leu-Phe-O*t*Bu in *tert*-butyl acetate (0.18 eq), *tert*-butyl chloroacetate (0.18 eq) and *tert*-butyl methyl ether (1.0 eq) were prepared. The vials were heated at 10-minute intervals by 5 °C increments. Heating started at 30 °C and continued until the free flow of the gels was observed. All gels reformed after cooling at R.T. The $T_{gel\text{-}sol}$ results are given in Table 11. According to the results, the observed gel-to-sol-to-gel transition of Boc-Leu-Phe-O*t*Bu gels verifies the thermoreversible nature of the materials, while we suspect that the gels' lifetime may be potentially affected by triggering gelation by heat.

Table 11. The Phase transition temperature of Boc-Leu-Phe-O*t*Bu organogels.

	conc. H_2SO_4 (eq)	**$T_{gel\text{-}sol}$ (°C)**
tert-butyl acetate	0.18	55-60
tert-butyl chloroacetate	0.18	55-60
tert-butyl methyl ether	1.0	55-60

13 Analysis of the gels

13.1 FT-IR Analysis

FT-IR was used to observe the structural differences between the raw materials and dried gels (xerogels prepared after 12 h of drying in open air). The conformational changes of the xerogels' gel network (secondary structure) were assessed by comparing the amide A, I and II spectral regions. In this study, the amide III region was not observed.

According to literature, the amide region A is around 3270–3310 cm^{-1} and is caused by the vibration of the NH-group.[70] The amide I region is seen around 1650 cm^{-1} and it is mainly associated with the C=O stretching vibration and not so much the out-of-phase NH stretching. The amide II is seen around 1510–1580 cm^{-1} and is caused by a combination of NH and CN stretching vibrations.[70] The amide I region is correlated to the α-helix region between wavelengths 1648-1657 cm^{-1}, and to β-sheets between wavelengths 1623-1641 cm^{-1} and 1674-1695 cm^{-1}.[71]

13.1.1 IR spectra of Boc-Leu-Phe-O*t*Bu, Leu-Phe-O*t*Bu and Leu-Phe

The IR spectra of neat powder samples Boc-Leu-Phe-O*t*Bu (**25**), Leu-Phe-O*t*Bu (**26**) and Leu-Phe (**27**) were compared at two different spectral regions (Figure 36). In the Boc-Leu-Phe-O*t*Bu spectra (purple line in Fig. 11), two NH stretching vibrations are seen at 3334 cm^{-1} and 3275 cm^{-1}. The corresponding broad peaks are also observed in the spectra of Leu-Phe-O*t*Bu (yellow line, 3313 cm^{-1}) and Leu-Phe (grey line, 3291 cm^{-1}). These peaks refer to the amide region A. In the case of Leu-Phe spectrum, the broadness of the peak is due to the O-H stretching originating from the COOH group and in the case of Leu-Phe-O*t*Bu it is due to the protonated amine group. The CH vibrations of the aromatic ring can be seen around 2960 cm^{-1}.

In the Boc-Leu-Phe-O*t*Bu and Leu-Phe-O*t*Bu spectra, the peak around 1730 cm^{-1} is due to the C=O stretching vibration of the ester group, whereas in the Leu-Phe spectrum, C=O absorbs much lower at 1674 cm^{-1} due to the COOH group. The peak at 1681 cm^{-1} is seen only in the Boc-Leu-Phe-O*t*Bu spectra, indicating the presence of the Boc protective group. The Amide region I has been assessed for the Boc-Leu-Phe-O*t*Bu (1655 cm^{-1}) and Leu-Phe-O*t*Bu spectra

(1657 cm^{-1}). According to Goormaghtigh *et al.*[71] this region provides information relative to a β-sheet secondary structure. The peaks at wavelengths 1556 cm^{-1} in the Boc-Leu-Phe-O*t*Bu spectra and at 1560 cm^{-1} in the Leu-Phe spectra refer to the amide II region.

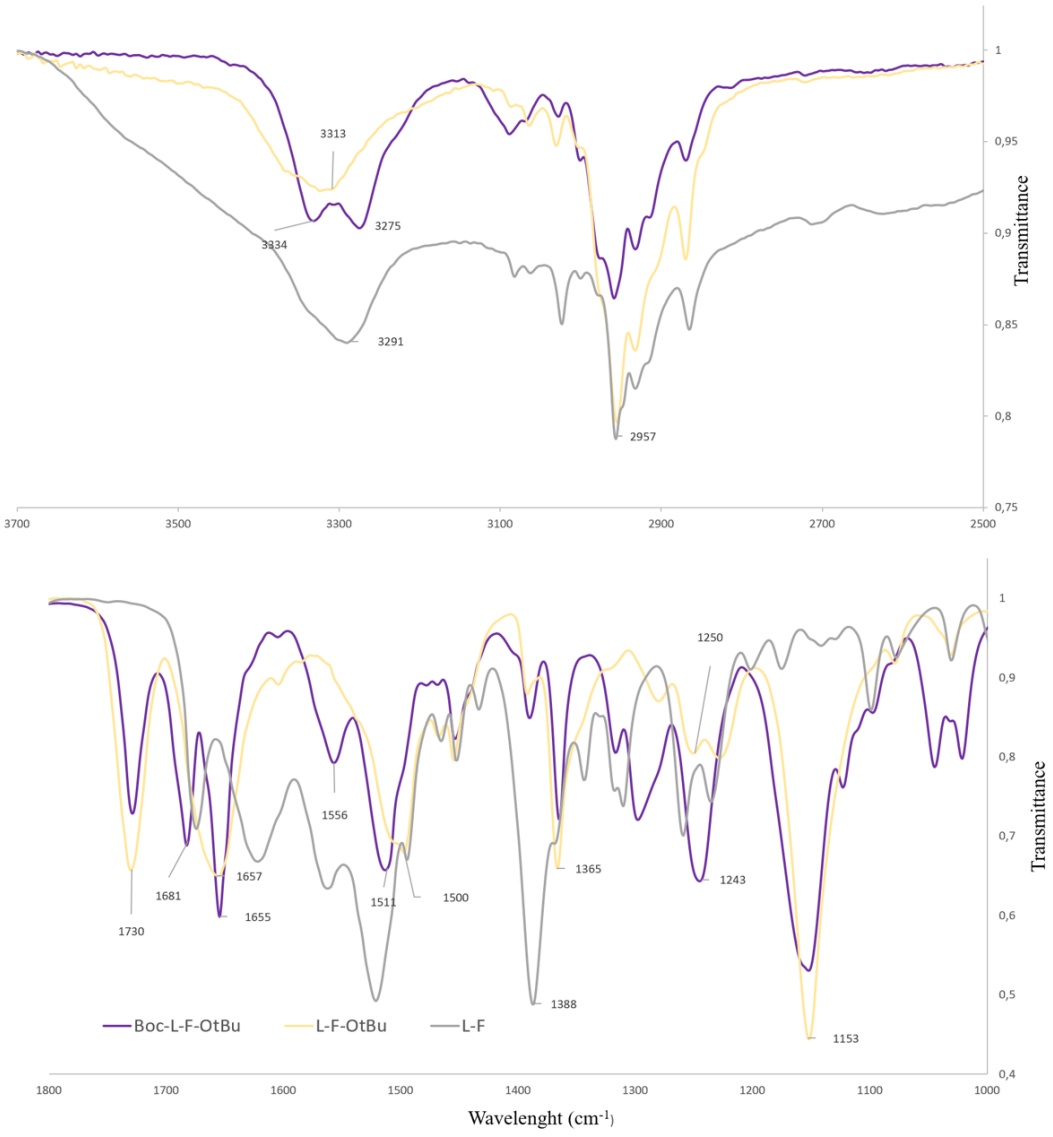

Figure 36. IR spectra of Boc-Leu-Phe-O*t*Bu (**25**), Leu-Phe-O*t*Bu (**26**) and Leu-Phe (**27**).

The C=C peak of the aromatic ring is slightly shifted to a lower frequency in Leu-Phe-O*t*Bu (1500 cm^{-1}) compared to the Boc-Leu-Phe-O*t*Bu and Leu-Phe spectra. In addition, the C-H bonds are observed in the Boc-Leu-Phe-O*t*Bu and Leu-Phe-O*t*Bu spectra around 1365 cm^{-1}, but in the Leu-Phe spectrum the peak is shifted to a higher frequency (1388 cm^{-1}).

The C-N bonds are observed around 1250 cm^{-1} and the peak at 1153 cm^{-1} shows the C-O vibrations in the ester group. The C-N peak gives two bands in the Leu-Phe-O*t*Bu spectrum, while in the Boc-Leu-Phe-O*t*Bu spectrum, the peak is sharp. In contrast, the N-H bond is sharp and slightly shifted to a higher frequency in the Leu-Phe spectrum.

13.1.2 IR spectra of Boc-Leu-Phe-OtBu xerogels with different acid concentrations

The effect of different equivalents of acid (spectrum (a) with 1.0 eq and spectrum (b) with 0.18 eq) was studied by comparing two Boc-Leu-Phe-O*t*Bu xerogels obtained in *tert*-butyl acetate solvent (Figure 37). Two NH stretching vibrations are seen in both spectra, in spectrum (a) at 3384/3323 cm^{-1} and in spectrum (b) at 3327/3276 cm^{-1}. Thus, at a lower acid concentration the vibrational bands are slightly shifted to a lower frequency.

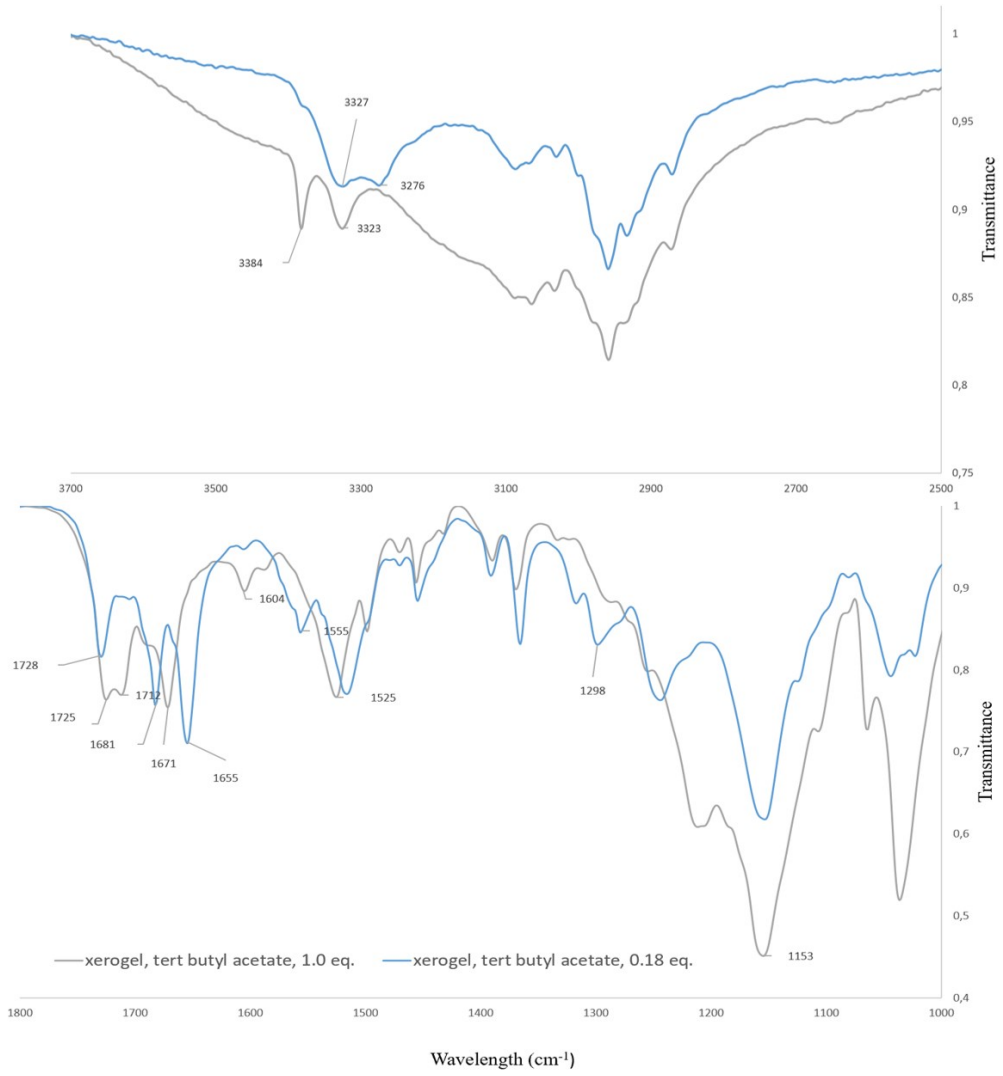

Figure 37. The effect of acid concentration on the Boc-Leu-Phe-O*t*Bu based xerogels in *tert*-butyl acetate solvent, using (a) 1.0 eq and (b) 0.18 eq of acid.

The ester group C=O in spectrum (b) is seen as a single sharp edge (1725 cm^{-1}) but in spectrum (a) the vibration gives two bands (1725 cm^{-1} and 1712 cm^{-1}). The peak at wavelength 1681 cm^{-1} is likely due to the Boc group (C=O), and it is only seen at lower acid concentration, meaning that there is still present Boc-Leu-Phe-O*t*Bu in the xerogel sample. The amide I region in both spectra shows peaks at 1671 cm^{-1} in spectrum (a) and at 1655 cm^{-1} in spectrum (b). According to Bath,[70] the amide II region findings refer most likely to a β-sheet configuration in the spectrum (a) and to an α-helix in spectrum (b). The peak at 1604 cm^{-1} in spectrum (a) and that at 1555 cm^{-1} in spectrum (b) are located at the amide II region. The NH stretching is clearly shifted to a lower frequency at a lower acid concentration.

The peaks around 1520 cm^{-1} are due to the phenyl rings, which is slightly shifted to higher wavenumbers in spectrum (a). The acid addition seems to have an impact on the C-O band around 1153 cm^{-1} as it appears sharp in spectrum (b) but as a shoulder in spectrum (a).

According to Chevigny *et al.,*[6] the sulfuric acid is an accelerator of the gelation process. Also in this case, the sulfuric acid concentration affects the supramolecular structure (gel network) of the organogels and its gelator components. The IR spectra indicate that xerogels at a lower acid concentration (spectrum b) contain both unreacted diprotected Boc-Leu-Phe-O*t*Bu and mono-protected Leu-Phe-O*t*Bu, but at a higher acid concentration, the diprotected Boc-Leu-Phe-O*t*Bu is missing.

13.1.3 IR spectra of Boc-Leu-Phe-O*t*Bu xerogels in different solvents

Boc-Leu-Phe-O*t*Bu xerogels were prepared using the same acid concentration (0.18 eq) but in different solvents (*tert*-butyl chloroacetate and *tert*-butyl acetate) and compared (Figure 38). The spectra are quantitatively similar, and it seems that the type of solvent does not play an intimate role in the organogels' composition or secondary structure. Based on the spectra, both xerogels consist of the diprotected Boc-Leu-Phe-O*t*Bu and the monoprotected Leu-Phe-O*t*Bu, while no Leu-Phe was observed.

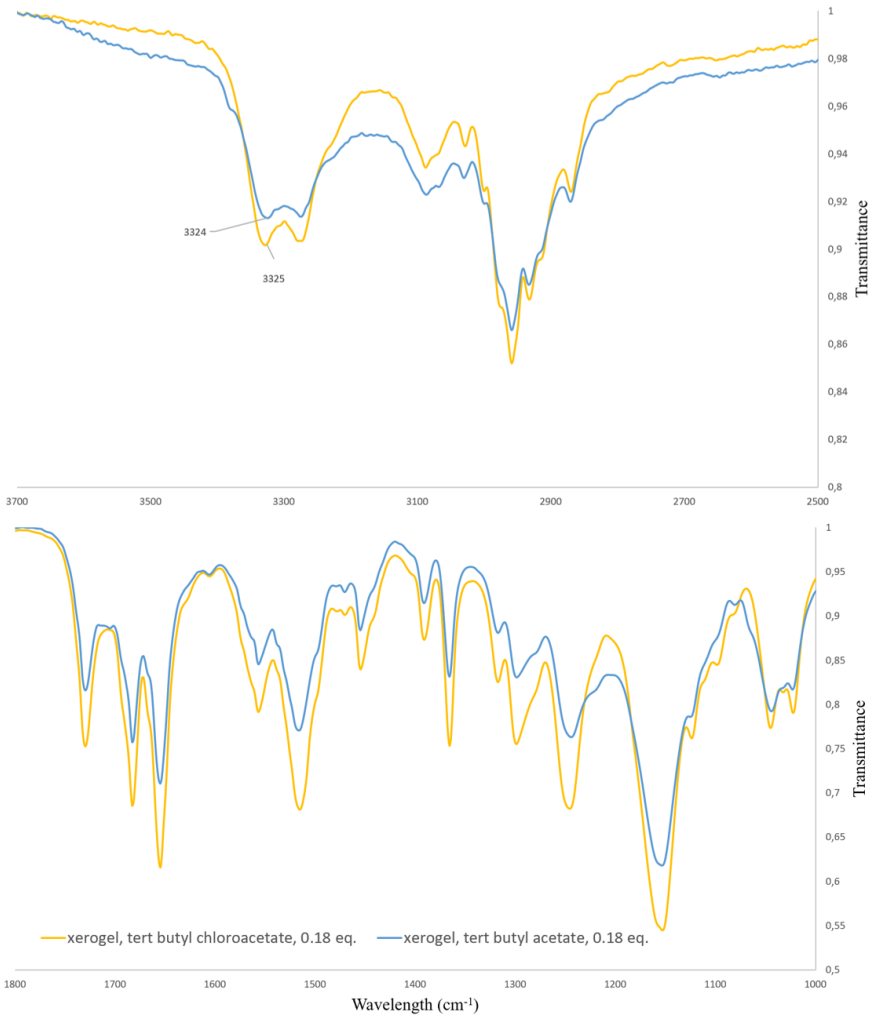

Figure 38. FT-IR spectra of Boc-Leu-Phe-O*t*Bu xerogels in different solvents (*tert*-butyl chloroacetate and *tert*-butyl acetate). No considerable solvent effects are observed. The acid concentration is constant (0.18 eq.)

13.2 NMR Spectroscopy

^{1}H NMR spectra were measured from gel samples to confirm the identity of compounds in different solvent containing samples and to study the compounds' ratio at different stages of gelation. Gel samples of dipeptide Boc-Leu-Phe-O*t*Bu in *tert*-butyl methyl ether (1.0 eq of acid) were chosen to study dynamic gelation at three different stages (time points). The samples were assessed at day one when no gel was formed (sol), at day eight when a partial gel was formed and at day thirteen when a self-supporting gel was formed. Self-supporting gels samples in *tert*-butyl chloroacetate (0.18 eq of acid) and *tert*-butyl acetate (0.18 eq of acid)

were chosen to study the effect of different solvents on self-assembly. The changes in component (gelator) ratios and ^{1}H NMR chemical shifts were compared. The corresponding ^{13}C NMR spectra of these gels were also measured and are given in Appendix 3-4.

13.2.1 Dynamic gelation

At day one, no gelation was observed. The solution sample for ^{1}H NMR analysis was prepared from Boc-Leu-Phe-O*t*Bu in *tert*-butyl methyl ether (1.0 eq; Figure 39). A doublet peak at δ = 8.83 ppm is attributed to the NH group. According to Chevigny *et al.*[6] this indicates that the deprotected Leu-Phe is not present in the solution. The peak at δ = 8.81 ppm is due to the NH_3^+ group of Leu-Phe-O*t*Bu. However, the NH_3^+ integral (6) is slightly inconsistent suggesting the absence of Leu-Phe. In addition, based on the integral of the aromatic region, there could be three different phenyl rings in the Boc-Leu-Phe-O*t*Bu solution in *tert*-butyl methyl ether. The peak at 6.80 ppm relates to the NH group from the diprotected starting material Boc-Leu-Phe-O*t*Bu.

The *t*BuOH solvent, causing the gel to break as reported previously,[6] is observed around at δ = 5,5 ppm (-OH). The signal at δ = 1.31 ppm is attributed to the *tert*-butyl group and at δ = 1.36 ppm to the Boc group, which confirm that the sample contains both Boc-Leu-Phe-O*t*Bu and Leu-Phe-O*t*Bu. The ratio of the starting material Boc-Leu-Phe-O*t*Bu and the mono-protected Leu-Phe-O*t*Bu is approximately 1:2.

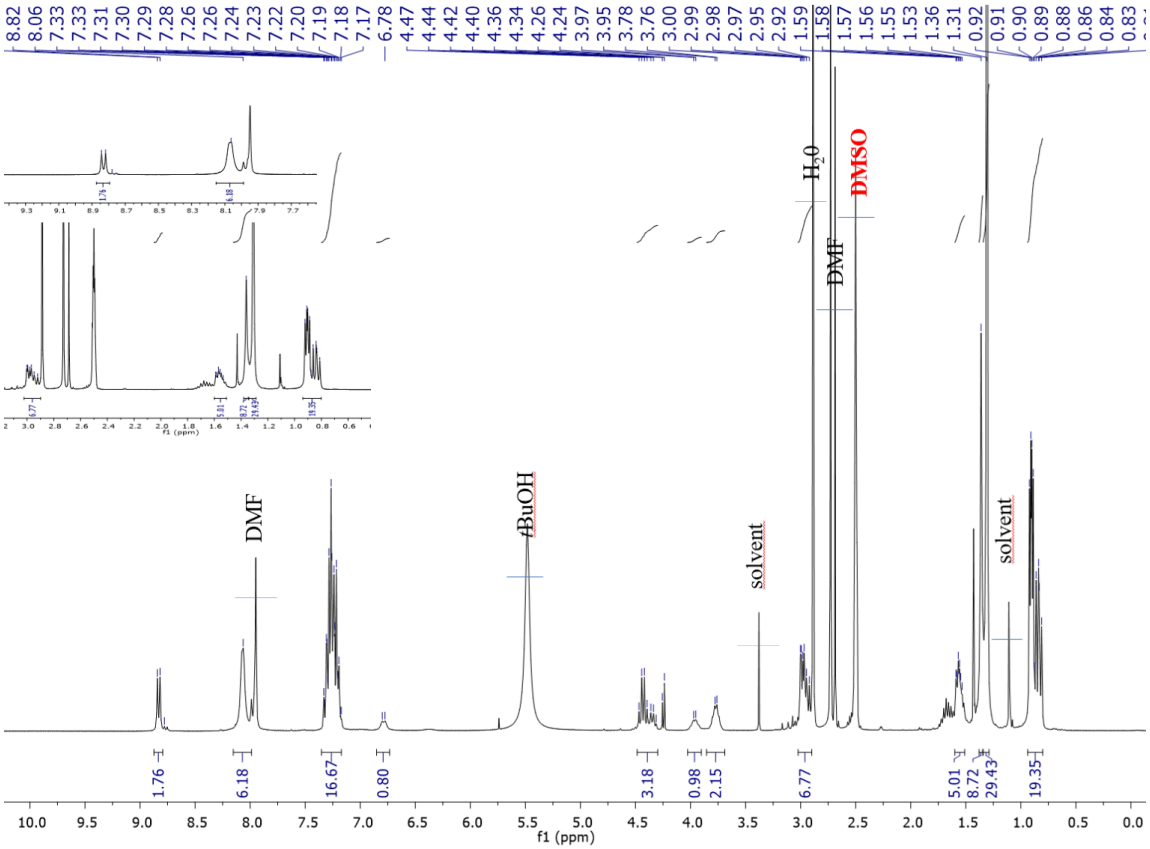

Figure 39. ^{1}H NMR (300 MHz, d_6-DMSO) spectrum of the Boc-Leu-Phe-O*t*Bu solution in *tert*-butyl methyl ether (1.0 eq of acid) at day one.

At day 8, partial gelation in *tert*-butyl methyl ether (1.0 eq) was observed, and therefore we measured ^{1}H NMR spectrum of the corresponding sample. When the solution and partial gel (Figures 30 and 40) were compared, it was noticed that the downfield doublet showing the NH group (peak δ = 8,83 ppm) did not change, which indicates that no Leu-Phe had formed after eight days. Also, the integral of the NH_3^+group (δ = 8.06 ppm) was reduced from 6 to 3. Lack of the peak δ = 6.80 ppm corresponding to the NH group next to the Boc group, indicates the complete deprotection of Boc-Leu-Phe-O*t*Bu. In the partial gel, the signal of *tert*-butyl alcohol is shifted upfield compared to the solution sample. It almost overlaps with the CH group peak at δ = 4.40 ppm. Otherwise, the CH groups' chemical shift was identical compared to the solution (day one).

As seen from the given enlarged spectrum area, only one *tert*-butyl signal δ = 1.31 ppm is observed. The absence of the Boc group indicates that the chemical equilibrium of the

components has changed, and the partial gel contains now only the monoprotected Leu-Phe-O*t*Bu.

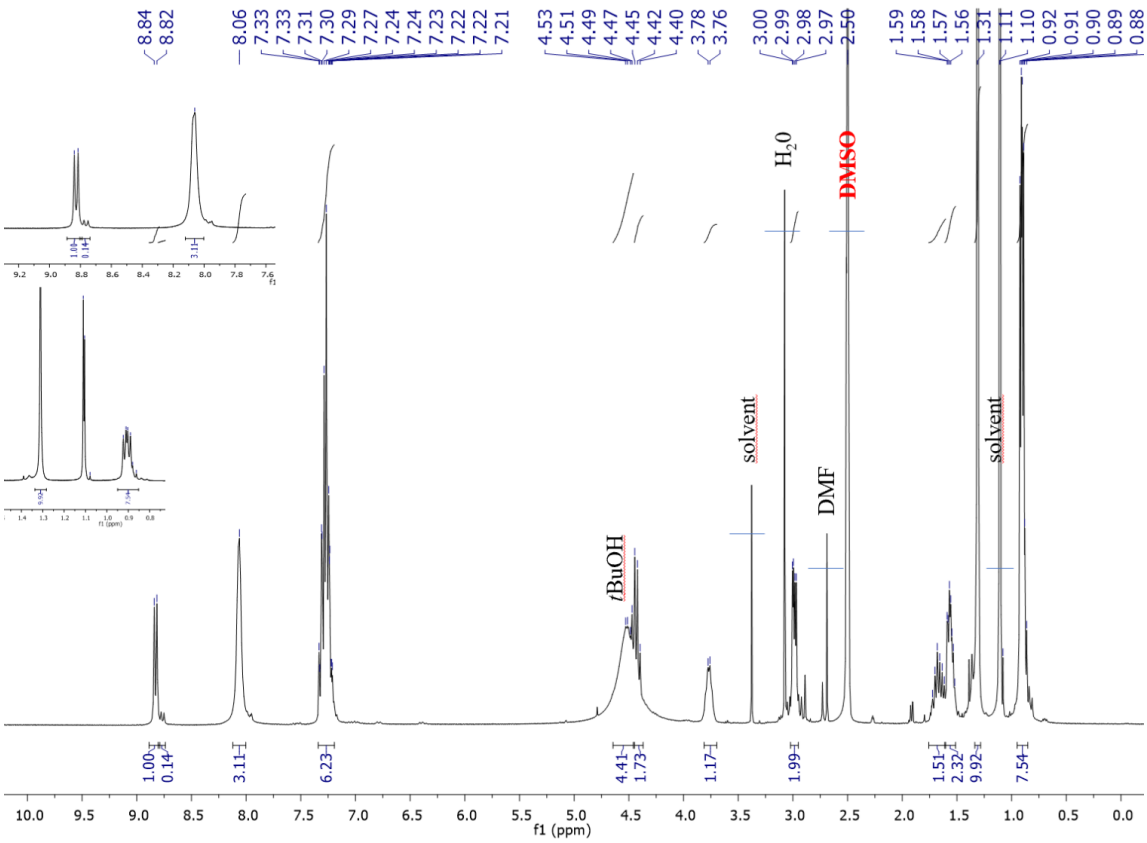

Figure 40. ^{1}H NMR (300 MHz, d_6-DMSO) spectra of the Boc-Leu-Phe-O*t*Bu partial xerogel in *tert*-butyl methyl ether (1.0 eq of acid) at day 8.

At day 13, a self-supporting gel in *tert*-butyl methyl ether (1.0 eq; Figure 41) formed, and the corresponding ^{1}H NMR spectrum of the sample was prepared. We therefore compared the spectra of the sample at day one (not gelled sample-solution phase), day 8 (partial gel) and day 13 (self-supporting gel; Fig. 39, 40, and 41). The two NH doublets at a ratio of 1:1 are observed at δ = 8.80 ppm. This indicates the presence of Leu-Phe. Therefore, a new compound is observed (Figure 41). The peak δ = 8.06 ppm is due to the NH_3^+ group (Figure 41), which is identical in all three spectra (Figure 39, 40, and 41) The integral of the NH_3^+ group (6) is the same as in the solution phase. The aromatic peak at δ = 7.30 ppm shows twice the number of hydrogen atoms, which indicates the absence of Leu-Phe. (Figure 41).

Like in the partial gel spectrum, the lack of NH group around δ = 6.80 ppm indicates the absence of Boc-Leu-Phe-O*t*Bu. In the self-supporting gel, the signal of *tert*-butyl alcohol is even more shifted at the upfield than in the solution and partial gel phases. The *tert*-BuOH signal (-OH) overlaps with the signal of the CH.

The peak at δ = 0.90 ppm showing the leucine CH_3 groups has an integral twice the number of hydrogen atoms, which refers to one Leu-Phe molecule and one Leu-Phe-O*t*Bu molecule. The peak δ = 1.30 ppm refers to the *tert*-butyl group, and the lack of peak δ = 1.36 ppm confirms that the full deprotection of the Boc group has been achieved. The ratio of the monoprotected Leu-Phe-O*t*Bu and fully deprotected Leu-Phe is approximately 1:1.

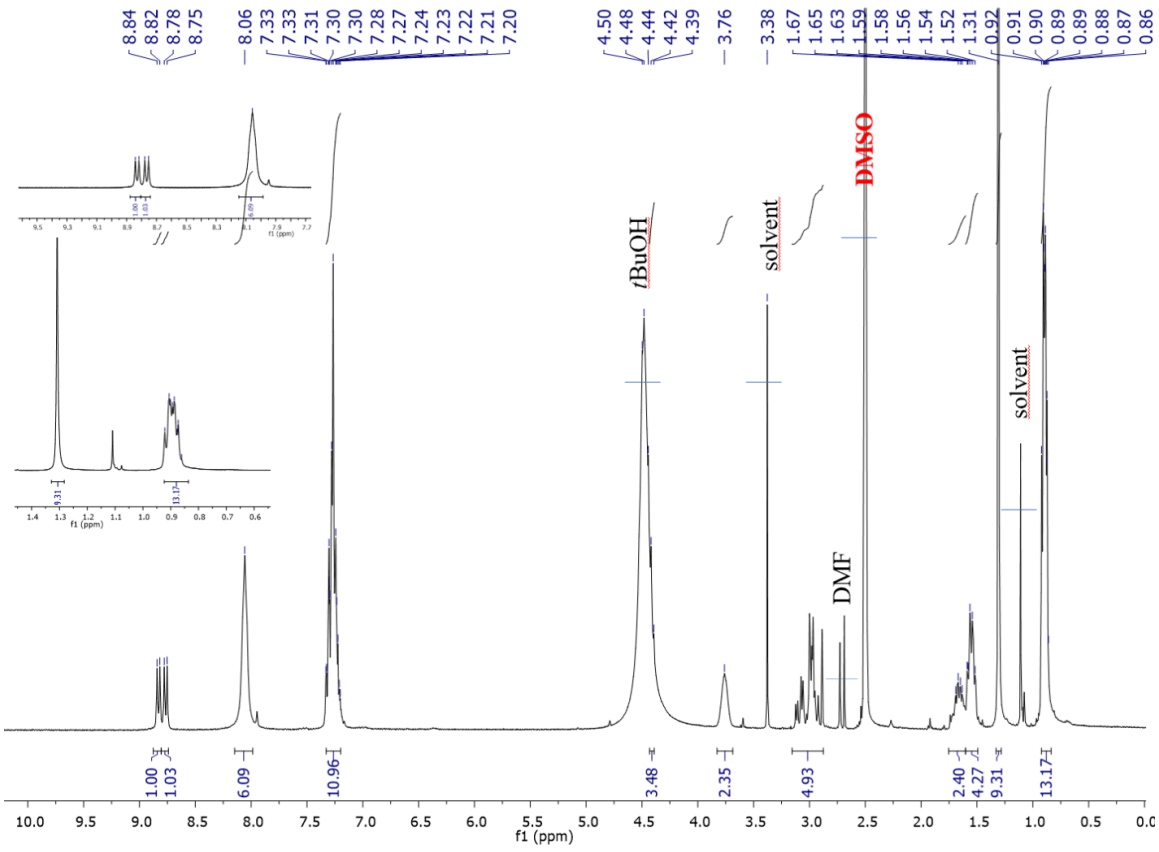

Figure 41. ^{1}H NMR (300 MHz d_6-DMSO) spectra of the Boc-Leu-Phe-O*t*Bu xerogel in *tert*-butyl methyl ether (1.0 eq) at day 13.

13.2.2 The effect of different solvents

Solvent effects were studied by comparing the ^{1}H NMR spectra of xerogels, prepared by drying two self-supporting gels in different solvents. Boc-Leu-Phe-O*t*Bu in *tert*-butyl chloroacetate (acid concentration 0.18 eq) and *tert*-butyl acetate (acid concentration 0.18 eq) were compared. The corresponding ^{1}H NMR spectra are shown in Appendix 3-4 and the ^{13}C NMR spectra in Appendix 5.

The ^{1}H NMR spectra are qualitatively similar except of the observed solvent impurities (Figure 42). The *t*BuOH peaks (-OH) are present in both spectra, but in *tert*-butyl chloroacetate the intensity is rather low. The two peaks at δ = 0.84 ppm and δ = 0.89 ppm correspond to the leucine CH_3 groups (negligible shift). Based on the spectra of the starting materials (neat powders), the Boc-Leu-Phe-O*t*Bu and Leu-Phe-O*t*Bu give identical shifts for the leucine CH_3 groups (Figure 43). The same phenomenon (negligible shift) is observed in the Boc-Leu-Phe-O*t*Bu sample in tert-butyl methyl ether which has not gelled (Figure 38). However, based on the peak intensities, the CH_3 group of Boc-Leu-Phe-O*t*Bu can be assumed to be located slightly up field although the CH_3 group signal should be located further downfield. The potential ratio of Boc-Leu-Phe-O*t*Bu and Leu-Phe-O*t*Bu is approximately 1:1 in both xerogels.

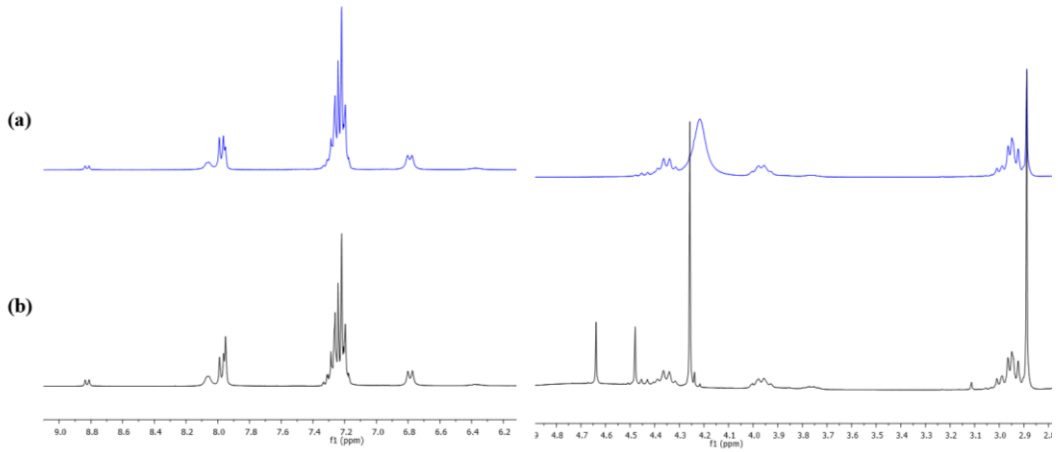

Figure 42. Comparison of two self-supporting gels in two different solvents. (a) Xerogel in *tert*-butyl acetate; (b) Xerogel in *tert*-butyl chloroacetate.

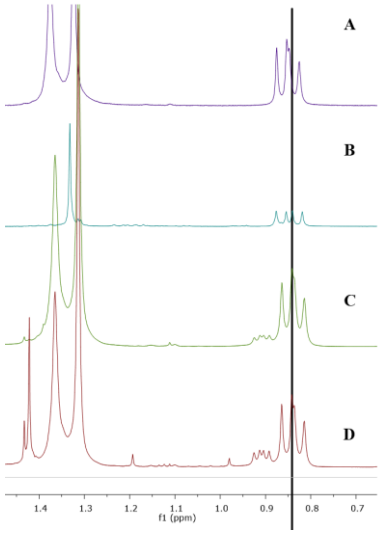

Figure 43. Shifting of leucine`s CH_3 group, (a) neat powder of Boc-Leu-Phe-O*t*Bu, (b) neat powder of Leu-Phe-O*t*Bu, (c) xerogel in *tert*-butyl acetate (0.18 eq) and (d) xerogel in *tert*-butyl chloroacetate (0.18 eq).

13.3 High-resolution mass spectrometry

High-resolution mass spectrometry was performed to confirm the presence of the different dipeptides (**25**, **26** and **27**) in the xerogels formed in *tert*-butyl acetate (0.18 eq of acid), *tert*-butyl chloroacetate (0.18 eq of acid) and *tert*-butyl methyl ether (1.0 eq of acid). The HR-MS results are given in Table 12.

Table 12. Molecular formulas, m/z values and mass accuracies of Boc-Leu-Phe-O*t*Bu (**25**), Leu-Phe-O*t*Bu (**26**) and Leu-Phe (**27**) in the xerogels prepared by precursor gelator Boc-Leu-Phe-O*t*Bu (**25**).

Sample	**Molecular formula**	**Ion**	**m/z (theor)**	**m/z (exp)**	**mass accuracy**
Boc-Leu-Phe-O*t*Bu	$C_{24}H_{38}N_2O_5$	[**25**+Na]$^+$	456.259	457.265	2.2 mDa
		[**25**+K]$^+$	472.233	473.239	2.12 mDa
Leu-Phe-O*t*Bu	$C_{19}H_{30}N_2O_3$	[**26**+H]$^+$	335.233	335.231	2.0 mDa
Xerogel in *tert*-butyl acetate	$C_{24}H_{35}N_2O_5$	[**25**+NH4]$^+$	453.235	453.284	0,0 mDa
	$C_{24}H_{38}N_2O_5$	[**25**+Na]$^+$	456.259	457.266	2.2 mDa
		[**25**+K]$^+$	472.233	273.239	2.4 mDa
	$C_{19}H_{30}N_2O_3$	[**26**+H]$^+$	335.233	335.231	1.8 mDa
	$C_{15}H_{22}N_2O_3$	[**27**+H]$^+$	279.170	279.168	2.2 mDa
Xerogel in *tert*-butyl chloroacetate	$C_{24}H_{38}N_2O_5$	[**25**+Na]$^+$	456.260	257.266	2.2 mDa
		[**25**+K]$^+$	472.233	473.240	2.1 mDa
	$C_{19}H_{30}N_2O_3$	[**26**+H]$^+$	335.233	335.231	2.4 mDa
	$C_{15}H_{22}N_2O_3$	[**27**+H]$^+$	279.170	279.169	1.8 mDa
Xerogel in *tert*-butyl methyl ether	$C_{19}H_{30}N_2O_3$	[**26**+H]$^+$	335.233	335.231	**5.9 mDa**
	$C_{15}H_{22}N_2O_3$	[**27**+H]$^+$	335.231	334.231	2.0 mDa
		[**27**+Na]$^+$	300.144	301.151	**3.3 mDa**
		[**27**+K]$^+$	316.118	317.121	**3.2 mDa**

The HR-MS results complement and are in accordance with the ^{1}H NMR findings for the Boc-Leu-Phe-O*t*Bu xerogels, obtained in *tert*-butyl acetate and *tert*-butyl chloroacetate solvents. However, the HR-MS analysis also verified the presence of Leu-Phe, which was difficult to assess by FT-IR or ^{1}H NMR spectroscopies. Interestingly, Leu-Phe-O*t*Bu and Leu-Phe appear to form a dimer (*m/z* 769.511) when *tert*-butyl acetate is used as a solvent.

The xerogel in *tert*-butyl methyl ether shows a strong Leu-Phe peak and a weaker of Leu-Phe-O*t*Bu. These observations support the ^{1}H NMR results. However, the ratio between Leu-Phe

and Leu-Phe-O*t*Bu seems different compared to NMR. Notably, ^{1}H NMR was measured on day 13 and HR-MS after 30 days, meaning that the ratio between these two components is still changing.

In addition, the acceptable mass accuracy is > 3mDa. Due to this limitation, the unacceptable accuracies are highlighted in Table 12. The HR-MS spectra are presented in Appendices 6-9.

13.4 Swelling tests

Three vials were prepared from each sample. The samples of Boc-Leu-Phe-O*t*Bu in *tert*-butyl chloroacetate (0.18 eq of acid) and *tert*-butyl acetate (0.18 eq of acid) were weighed at day one, and the corresponding solvents *tert*-butyl chloroacetate (200 µl) and *tert*-butyl acetate (1000 µl) were added on the surface of each gel, respectively. The gels were left to stand at R.T. overnight, after which the added solvents were gently removed by pipette, and the swollen gels were weighed.

The swelling degree (SD) was calculated according to equation (1), where w_t refers to the mass of the swollen gel and w_0 is the average mass of the dry gel. The behaviour of organogels in function of time is presented in Figure 44.

$$\mathrm{SD}\ (\%) = \left(\frac{w_t}{w_o}\right) * 100\% \qquad (1)$$

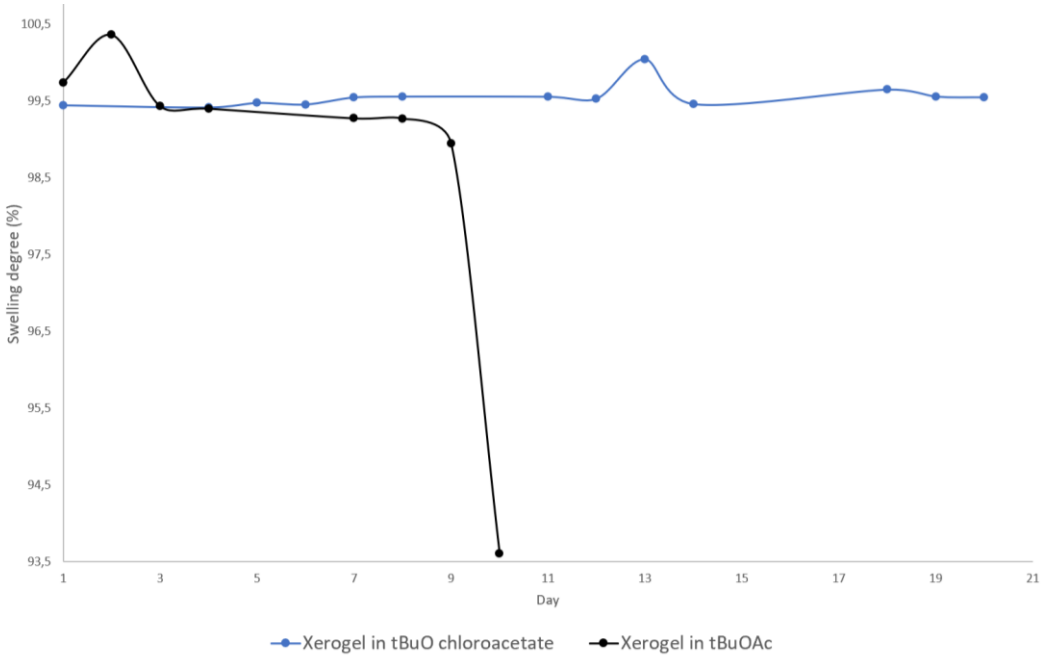

Figure 44. Swelling tests of Boc-Leu-Phe-O*t*Bu organogels in *tert*-butyl chloroacetate (0.18 eq of acid) and *tert*-butyl acetate (0.18 eq of acid) solvents.

The swelling results show that the swelling behaviour differs in each material, as the solvent has a considerable effect on controlling the equilibrium in the swelling dynamic process. The organogel in *tert*-butyl acetate breaks down on the tenth day of the study, whereas the organogel in *tert*-butyl chloroacetate seems to be stable and reaches an equilibrium. According to Chevigny *et al.*[6] *tert*-butyl acetate acts as a brake in the dynamic process of the Boc-Phe-Phe-O*t*Bu gelation (using 1.0 eq of acid), preventing the formation of *tert*-BuOH, which induces the gel to break down (Scheme 1). However, based on the swelling tests, the same conclusion cannot be made for the Boc-Leu-Phe-O*t*Bu gels (only 0.18 eq. were used). The ^{1}H NMR shows the presence of *t*BuOH in all studied xerogels. However, the formed *tert*-BuOH is now possibly insufficient to break the gel apparently due to its low concentration in the system.

13.5 Scanning electron microscopy

Scanning electron microscopy (SEM) was performed to visualise the three-dimensional network of the formed xerogels. The technique is based on electron emission, which in some parts destroyed the gel network, and therefore imaging appeared rather challenging.

Figure 46 shows the Boc-Leu-Phe-O*t*Bu xerogel obtained in *tert*-butyl acetate (1.0 eq) on day one. The formed gelators seem to form fibres, which can branch into several fibrils (Fig. 46; a-b). In addition, the fibres contain small circular structures. These could be due to the salts formed when the ester reacts with the base. The thickest fibres are ~5,9 µm. The images also show that the xerogel contains several layers of a fibrous three-dimensional network (Fig. 45; c).

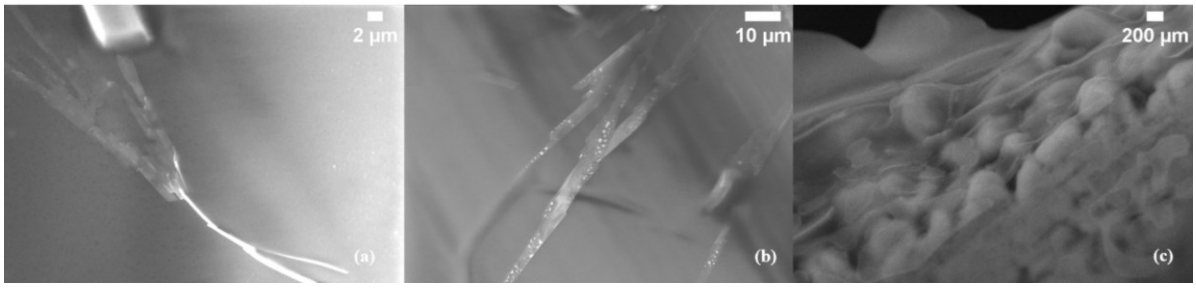

Figure 45. SEM imaging of the Boc-Leu-Phe-O*t*Bu xerogel in *tert*-butyl acetate (0.5 eq) after one day. Fibres (a and b) at several layers (c) are observed.

Figure 46 shows the Boc-Leu-Phe-O*t*Bu xerogel in *tert*-butyl chloroacetate (0.5 eq) at day four. The formed fibres appear quantitatively similar to the *tert*-butyl acetate sample, but these fibres are now strongly intertwined (Fig. 46; a-b). At their thickest formations, the clusters are closer to 200 µm. Unlike the *tert*-butyl acetate sample, circular structures (assumed to be salts) surround the fibres. In addition to the tightly interwoven fibres, SEM pictures clearly show smaller fibrils (Fig. 46; c-d), which can explain the two phases observed after gelation.

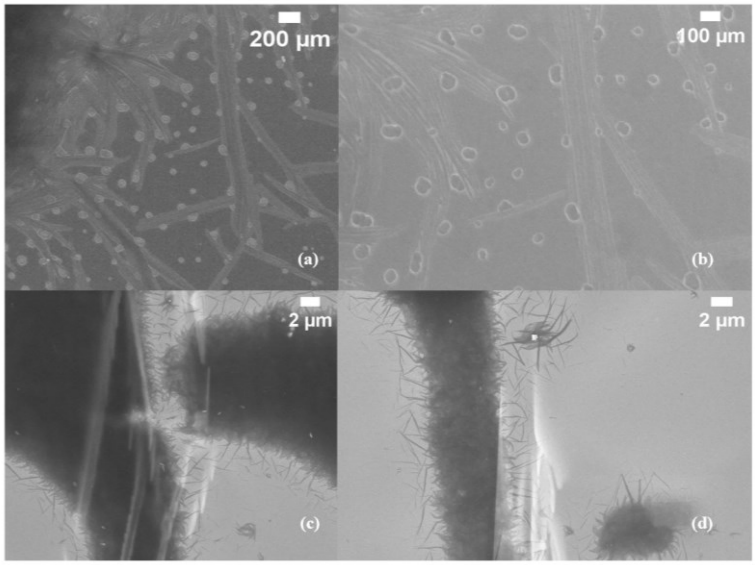

Figure 46. SEM imaging of the Boc-Leu-Phe-O*t*Bu xerogel in *tert*-butyl chloroacetate (0.5 eq) after 4 days. Tightly interwoven fibres (a-b) and independent fibrils (c-d) are observed.

14 Conclusion

The experimental part aimed to observe the transient (dynamic) self-assembly process towards the organogels of Boc-Leu-Phe-O*t*Bu in different solvents, capable of releasing the *tert*-butyl carbocations under acidic conditions. Indeed, five different solvents were used to form the gels. Gelation was achieved in *tert*-butyl acetate, *tert*-butyl chloroacetate and *tert*-butyl methyl ether. Thus, these solvents are proved to be chemically active and produce a *tert*-butyl group under acid conditions. No gels formed in *tert*-butyl acetoacetate and *tert*-butyl formate, which were excluded from this work. However, further research using these solvents, for example, exploring variations in the concentration of the dipeptide and that of the acid may be of interest.

The different solvents affected the gelation time and caused phase changes during the gelation process; thus, we focused on the transient self-assembly per se. Phase changes from colourless/transparent to pale opaque materials were observed with Boc-Leu-Phe-O*t*Bu gels in *tert*-butyl acetate, *tert*-butyl chloroacetate and *tert*-butyl methyl ether. The gelation in *tert*-butyl methyl ether took considerably more time than in esters. In general, esters are more polar than ethers and also more reactive. The *tert*-Butyl methyl ether has only one free electron pair, which can create non-covalent hydrogen bonds and form polar interactions, suggesting the difference in gelation times. The *tert*-Butyl methyl ether has the lowest molecular weight and small size, which can also affect its reactivity. Future studies could focus on solvent mixtures and explore variations in gelation time.

The FT-IR spectra of Boc-Leu-Phe-O*t*Bu xerogels in *tert*-butyl chloroacetate (0.18 eq) and *tert*-butyl acetate (0.18 eq) were compared. Based on the results, the solvent does not play an active role in changing the gelators' composition or the secondary structure of the gels. However, it must be considered that the behaviour of these gels was not studied over a longer period. The ^{1}H NMR studies of the xerogels in *tert*-butyl chloroacetate (0.18 eq) and *tert*-butyl acetate (0.18 eq) support the FT-IR observations.

The decomposition of Boc-Leu-Phe-O*t*Bu gels in different solvents was studied *via* the swelling test in samples prepared using *tert*-butyl acetate (0.18 eq of acid) and *tert*-butyl chloroacetate (0.18 eq of acid). The gels in *tert*-butyl acetate broke down on the tenth day, while those in *tert*-butyl chloroacetate were stable. Based on the ^{1}H NMR spectra, the Boc-Leu-Phe-O*t*Bu xerogels in *tert*-butyl chloroacetate contains only a minimum amount of *tert*-BuOH, which has been observed to be the reason for the gels' degradation. This can be the

reason of why the gels obtained in *tert*-butyl chloroacetate and in *tert*-butyl methyl ether were stable. Surprisingly, a transient degradation was not observed in the gel obtained in *tert*-butyl acetate.

SEM images showed that the type of solvent used affected the 3D network of the formed gels. Xerogels in *tert*-butyl acetate and *tert*-butyl chloroacetate formed fibres, but the their mode of assembly appears to be different. In addition, the *tert*-butyl chloroacetate sample seems to have two kinds of fibres. In future, the effect of time on the composition of the 3D network would be interesting to study.

The varied acid concentration was also reflected on the obtained IR spectra of the Boc-Leu-Phe-O*t*Bu xerogels in *tert*-butyl acetate. The composition of gelators and the secondary structures of the gels vary, as evidenced by changes in the NH, C=O and C-O absorption bands. Under less acidic conditions, the diprotected starting material did not reacted completely during the 12h gelation time. However, there is no indication of a completely deprotected Leu-Phe under more acidic conditions in both IR and NMR spectra; the ^{1}H NMR spectra of both acid concentrations still show unreacted Boc-Leu-Phe-O*t*Bu.

According to previous studies,[6] the ratio of the in-situ formed gelators in the gels changes during the lifetime of the gel (a potential dynamic interconversion between the formed gelators). ^{1}H NMR showed that gels had different gelator ratios when different assemblies (xerogels) were compared. The ratio between Boc-Leu-Phe-O*t*Bu and Leu-Phe-O*t*Bu was approximately 1:2 on day one in *tert*-butyl methyl ether. The partial gel in *tert*-butyl methyl ether includes Leu-Phe-O*t*Bu and not the precursor Boc-Leu-Phe-O*t*Bu, while the ratio for Leu-Phe-O*t*Bu and Leu-Phe is approximately 1:1. These observations combined with gelator tests indicate that Leu-Phe-O*t*Bu acts as an efficient LMWG in *tert*-butyl methyl ether. However, further studies are still needed. Based on the ^{1}H NMR spectra, also the formed Leu-Phe may affect formation of self-supporting gels as it is not observed in the partial gels. Also, the observed phase changes indicate internal changes in the gels' network.

In conclusion, three chemically active solvents were found to favour gelation, however no transient gels formed but rather the gelation itself was transient. The effect of different solvents on dynamic gelation, and the impact of acid concentration were studied by FT-IR, ^{1}H NMR, HR-MS, and SEM. The research was successful and supports further studies on the transient behaviour of gel systems in chemically active solvents.

Reference

1. Draper, E. R. ja Adams, D. J., Low-Molecular-Weight Gels: The State of the Art, *Chem*, **2017**, *3*, 390–410.
2. Colquhoun, C.; Draper, E. R.; Schweins, R.; Marcello, M.; Vadukul, D.; Serpell, L. C. ja Adams, D. J., Controlling the network type in self-assembled dipeptide hydrogels, *Soft Matter*, **2017**, *13*, 1914–1919.
3. Segarra-Maset, M. D.; Nebot, V. J.; Miravet, J. F. ja Escuder, B., Control of molecular gelation by chemical stimuli, *Chem. Soc. Rev.*, **2013**, *42*, 7086–7098.
4. Yu, G.; Yan, X.; Han, C. ja Huang, F., Characterization of supramolecular gels, *Chem. Soc. Rev.*, **2013**, *42*, 6697.
5. Zhao, C.; Wang, Y.; Shi, B.; Li, M.; Yan, W. ja Yang, H., Domination of H-Bond Interactions in the Solvent-Triggering Gelation Process, *Langmuir*, **2022**, *38*, 7965–7975.
6. Chevigny, R.; Schirmer, Johanna; Piras, C. C.; Johansson, A.; Kalenius, E.; Smith, D. K.; Pettersson, M.; Sitsanidis, E. D. ja Nissinen, M., Triggering a transient organo-gelation system in a chemically active solvent, *Chem. Commun.*, **2021**, 10375–10378.
7. Gupta, P.; Vermani, K. ja Garg, S., Hydrogels: from controlled release to pH-responsive drug delivery, *Drug Discovery Today*, **2002**, *7*, 569–579.
8. Wang, J.; Liu, K.; Xing, R. ja Yan, X., Peptide self-assembly: thermodynamics and kinetics, *Chem. Soc. Rev.*, **2016**, *45*, 5589–5604.
9. Adams, D. J. ja Topham, P. D., Peptide conjugate hydrogelators, *Soft Matter*, **2010**, *6*, 3707.
10. Ramos Sasselli, I.; Halling, P. J.; Ulijn, R. V. ja Tuttle, T., Supramolecular Fibers in Gels Can Be at Thermodynamic Equilibrium: A Simple Packing Model Reveals Preferential Fibril Formation *versus* Crystallization, *ACS Nano*, **2016**, *10*, 2661–2668.
11. B. Amabilino, D.; K. Smith, D. ja W. Steed, J., Supramolecular materials, *Chemical Society Reviews*, **2017**, *46*, 2404–2420.
12. Sanner, T., Formation of transient complexes in the glutamate dehydrogenase catalyzed reaction, *Biochemistry*, **1975**, *14*, 5094–5098.
13. Zhu, G. ja Dordick, J. S., Solvent Effect on Organogel Formation by Low Molecular Weight Molecules, *Chem. Mater.*, **2006**, *18*, 5988–5995.
14. Hirst, A. R. ja Smith, D. K., Two-Component Gel-Phase Materials—Highly Tunable Self-Assembling Systems, *Chem. Eur. J.*, **2005**, *11*, 5496–5508.

15. Jain, R. ja Roy, S., Tuning the gelation behavior of short laminin derived peptides via solvent mediated self-assembly, *Materials Science and Engineering: C*, **2020**, *108*, 110483.
16. Zhang, Y.; Li, S.; Ma, M.; Yang, M.; Wang, Y.; Hao, A. ja Xing, P., Tuning of gel morphology with supramolecular chirality amplification using a solvent strategy based on an Fmoc-amino acid building block, *New J. Chem.*, **2016**, *40*, 5568–5576.
17. Adams, D. J.; Butler, M. F.; Frith, W. J.; Kirkland, M.; Mullen, L. ja Sanderson, P., A new method for maintaining homogeneity during liquid–hydrogel transitions using low molecular weight hydrogelators, *Soft Matter*, **2009**, *5*, 1856.
18. Adams, D. J.; Mullen, L. M.; Berta, M.; Chen, L. ja Frith, W. J., Relationship between molecular structure, gelation behaviour and gel properties of Fmoc-dipeptides, *Soft Matter*, **2010**, *6*, 1971.
19. Fleming, S. ja Ulijn, R. V., Design of nanostructures based on aromatic peptide amphiphiles, *Chem. Soc. Rev.*, **2014**, *43*, 8150–8177.
20. Raeburn, J.; Mendoza-Cuenca, C.; Cattoz, B. N.; Little, M. A.; Terry, A. E.; Zamith Cardoso, A.; Griffiths, P. C. ja Adams, D. J., The effect of solvent choice on the gelation and final hydrogel properties of Fmoc–diphenylalanine, *Soft Matter*, **2015**, *11*, 927–935.
21. Radvar, E. ja Azevedo, H. S., Supramolecular Peptide/Polymer Hybrid Hydrogels for Biomedical Applications, *Macromol. Biosci.*, **2019**, *19*, 1800221.
22. Sodipo, J. O.; Lee, D. C. ja Morris, L. E., Cardiac output response to altered acid-base status during diethyl ether anaesthesia, *Can Anaesth Soc J*, **1975**, *22*, 673–679.
23. Zweep, N.; Hopkinson, A.; Meetsma, A.; Browne, W. R.; Feringa, B. L. ja van Esch, J. H., Balancing Hydrogen Bonding and van der Waals Interactions in Cyclohexane-Based Bisamide and Bisurea Organogelators, *Langmuir*, **2009**, *25*, 8802–8809.
24. Yang, Z.; Liang, G.; Ma, M.; Gao, Y. ja Xu, B., Conjugates of naphthalene and dipeptides produce molecular hydrogelators with high efficiency of hydrogelation and superhelical nanofibers, *J. Mater. Chem.*, **2007**, *17*, 850–854.
25. De Leon Rodriguez, L. M.; Hemar, Y.; Cornish, J. ja Brimble, M. A., Structure–mechanical property correlations of hydrogel forming β-sheet peptides, *Chem. Soc. Rev.*, **2016**, *45*, 4797–4824.
26. Wang, H.; Yang, Z. ja Adams, D., Controlling peptide based hydrogelation, *Materials Today*, **2012**, *15*.
27. Lan, Y.; Corradini, M. G.; Weiss, R. G.; Raghavan, S. R. ja Rogers, M. A., To gel or not to gel: correlating molecular gelation with solvent parameters, *Chem. Soc. Rev.*, **2015**, *44*, 6035–6058.

28. Safiullina, A. S.; Ziganshina, S. A.; Lyadov, N. M.; Klimovitskii, A. E.; Ziganshin, M. A. ja Gorbatchuk, V. V., Role of water in the formation of unusual organogels with *cyclo* (leucyl–leucyl), *Soft Matter*, **2019**, *15*, 3595–3606.

29. Wang, Y.; Xu, J.; Wang, Y. ja Chen, H., Emerging chirality in nanoscience, *Chem. Soc. Rev.*, **2013**, *42*, 2930–2962.

30. Lee, J. H.; Jung, S. H.; Lee, S. S.; Kwon, K.-Y.; Sakurai, K.; Jaworski, J. ja Jung, J. H., Ultraviolet Patterned Calixarene-Derived Supramolecular Gels and Films with Spatially Resolved Mechanical and Fluorescent Properties, *ACS Nano*, **2017**, *11*, 4155–4164.

31. Xing, P.; Chu, X.; Li, S.; Ma, M. ja Hao, A., Hybrid Gels Assembled from Fmoc-Amino Acid and Graphene Oxide with Controllable Properties, *ChemPhysChem*, **2014**, *15*, 2377–2385.

32. Liu, C.; Jin, Q.; Lv, K.; Zhang, L. ja Liu, M., Water tuned the helical nanostructures and supramolecular chirality in organogels, *Chem. Commun.*, **2014**, *50*, 3702.

33. Dudukovic, N. A. ja Zukoski, C. F., Evidence for equilibrium gels of valence-limited particles, *Soft Matter*, **2014**, *10*, 7849–7856.

34. Colquhoun, C.; Draper, E. R.; Eden, E. G. B.; Cattoz, B. N.; Morris, K. L.; Chen, L.; McDonald, T. O.; Terry, A. E.; Griffiths, P. C.; Serpell, L. C. ja Adams, D. J., The effect of self-sorting and co-assembly on the mechanical properties of low molecular weight hydrogels, *Nanoscale*, **2014**, *6*, 13719–13725.

35. Némethy, G. ja Scheraga, H. A., Structure of Water and Hydrophobic Bonding in Proteins. IV. The Thermodynamic Properties of Liquid Deuterium Oxide, *The Journal of Chemical Physics*, **1964**, *41*, 680–689.

36. McAulay, K.; Wang, H.; Fuentes-Caparrós, A. M.; Thomson, L.; Khunti, N.; Cowieson, N.; Cui, H.; Seddon, A. ja Adams, D. J., Isotopic Control over Self-Assembly in Supramolecular Gels, *Langmuir*, **2020**, *36*, 8626–8631.

37. Nishinari, K. ja Watase, M., Effects of sugars and polyols on the gel-sol transition of kappa-carrageenan gels, *Thermochimica Acta*, **1992**, *206*, 149–162.

38. Brenner, T.; Tuvikene, R.; Cao, Y.; Fang, Y.; Rikukawa, M.; Price, W. S. ja Matsukawa, S., Hydrogen isotope replacement changes hydration and large scale structure, but not small scale structure, of agarose hydrogel networks, *Eur. Phys. J. E*, **2019**, *42*, 53.

39. Canrinus, T. R.; Cerpentier, F. J. R.; Feringa, B. L. ja Browne, W. R., Remarkable solvent isotope dependence on gelation strength in low molecular weight hydro-gelators, *Chem. Commun.*, **2017**, *53*, 1719–1722.

40. Liao, J.; Huang, J.; Yang, S.; Wang, X.; Wang, T.; Sun, W. ja Tong, Z., Ultra-Strong and Fast Response Gel by Solvent Exchange and Its Shape Memory Applications, *ACS Appl. Polym. Mater.*, **2019**, *1*, 2703–2712.

41. Zhang, H. J.; Sun, T. L.; Zhang, A. K.; Ikura, Y.; Nakajima, T.; Nonoyama, T.; Kurokawa, T.; Ito, O.; Ishitobi, H. ja Gong, J. P., Tough Physical Double-Network Hydrogels Based on Amphiphilic Triblock Copolymers, *Adv. Mater.*, **2016**, *28*, 4884–4890.

42. Huang, J.; Liao, J.; Wang, T.; Sun, W. ja Tong, Z., Super strong dopamine hydrogels with shape memory and bioinspired actuating behaviours modulated by solvent exchange, *Soft Matter*, **2018**, *14*, 2500–2507.

43. Dai, H.; Chen, Q.; Qin, H.; Guan, Y.; Shen, D.; Hua, Y.; Tang, Y. ja Xu, J., A Temperature-Responsive Copolymer Hydrogel in Controlled Drug Delivery, *Macromolecules*, **2006**, *39*, 6584–6589.

44. Lin, L. S.; Lanza, T.; de Laszlo, S. E.; Truong, Q.; Kamenecka, T. ja Hagmann, W. K., Deprotection of N-tert-butoxycarbonyl (Boc) groups in the presence of tert-butyl esters, *Tetrahedron Letters*, **2000**, *41*, 7013–7016.

45. Yang, L.; Gan, S.; Guo, Q.; Zhang, H.; Chen, Q.; Li, H.; Shi, J. ja Sun, H., Stimuli-controlled peptide self-assembly with secondary structure transitions and its application in drug release, *Mater. Chem. Front.*, **2021**, *5*, 4664–4671.

46. Patel, P.; Ibrahim, N. M. ja Cheng, K., The Importance of Apparent pKa in the Development of Nanoparticles Encapsulating siRNA and mRNA, *Trends in Pharmacological Sciences*, **2021**, *42*, 448–460.

47. Paul, S.; Basu, K.; Das, K. S. ja Banerjee, A., Peptide-Based Hydrogels as a Scaffold for In Situ Synthesis of Metal Nanoparticles: Catalytic Activity of the Nanohybrid System, *ChemNanoMat*, **2018**, *4*, 882–887.

48. Yin, P.; Choi, H. M. T.; Calvert, C. R. ja Pierce, N. A., Programming biomolecular self-assembly pathways, *Nature*, **2008**, *451*, 318–322.

49. Kim, B. J. ja Xu, B., Enzyme-Instructed Self-Assembly for Cancer Therapy and Imaging, *Bioconjugate Chem.*, **2020**, *31*, 492–500.

50. Liao, L.; Jia, X.; Lou, H.; Zhong, J.; Liu, H.; Ding, S.; Chen, C.; Hong, S. ja Luo, X., Supramolecular gel formation regulated by water content in organic solvents: self-assembly mechanism and biomedical applications, *RSC Adv.*, **2021**, *11*, 11519–11528.

51. Liu, J.; Huang, Y.; Kumar, A.; Tan, A.; Jin, S.; Mozhi, A. ja Liang, X.-J., pH-Sensitive nano-systems for drug delivery in cancer therapy, *Biotechnology Advances*, **2014**, *32*, 693–710.

52. Li, J. ja Mooney, D. J., Designing hydrogels for controlled drug delivery, *Nat. Rev. Mater*, ***2016***, 16071.

53. Guyton, A. C. ja Hall, J. E., *Secretory functions of the alimentary tract. In Textbook of Medical Physiology (Guyton, A.C. and Hall, J.E., eds)*, W.B. Saunders Co., vol. **1998**, *14,* 1264

54. Brazel, C. S. ja Peppas, N. A., Pursatile local delivery of thrombolytic and antithrombotic agents using poly(N-isopropylacrylamide-co-methacrylic acid) hydrogels., *Journal of Controlled Release*, ***1996***, *39*, 57–64.

55. Kost, J. ja Lapidot, S. A., Drug Delivery Systems. Teoksessa: Schwartz, M. (toim.), *Encyclopedia of Smart Materials*, 1. painos, Wiley, **2002**, *2*, 1176.

56. Andrade, F.; Roca-Melendres, M. M.; Durán-Lara, E. F.; Rafael, D. ja Schwartz, S., Stimuli-Responsive Hydrogels for Cancer Treatment: The Role of pH, Light, Ionic Strength and Magnetic Field, *Cancers*, **2021**, *13*, 1164.

57. Silva, G. A.; Czeisler, C.; Niece, K. L.; Beniash, E.; Harrington, D. A.; Kessler, J. A. ja Stupp, S. I., Selective Differentiation of Neural Progenitor Cells by High-Epitope Density Nanofibers, *Science*, **2004**, *303*, 1352–1355.

58. Yeung, C. K.; Lauer, L.; Offenhäusser, A. ja Knoll, W., Modulation of the growth and guidance of rat brain stem neurons using patterned extracellular matrix proteins, *Neuroscience Letters*, **2001**, *301*, 147–150.

59. Thiébaud, P.; Lauer, L.; Knoll, W. ja Offenhäusser, A., PDMS device for patterned application of microfluids to neuronal cells arranged by microcontact printing, *Biosensors and Bioelectronics*, **2002**, *17*, 87–93.

60. Lauer, L.; Vogt, A.; Yeung, C. K.; Knoll, W. ja Offenhäusser, A., Electrophysiological recordings of patterned rat brain stem slice neurons, *Biomaterials*, **2002**, *23*, 3123–3130.

61. Wheeler, B. C.; Corey, J. M.; Brewer, G. J. ja Branch, D. W., Microcontact Printing for Precise Control of Nerve Cell Growth in Culture, *Journal of Biomechanical Engineering*, **1999**, *121*, 73–78.

62. Chang, J. C.; Brewer, G. J. ja Wheeler, B. C., Modulation of neural network activity by patterning, *Biosensors and Bioelectronics*, **2001**, *16*, 527–533.

63. Cornish, T.; Branch, D. W.; Wheeler, B. C. ja Campanelli, J. T., Microcontact Printing: A Versatile Technique for the Study of Synaptogenic Molecules, *Molecular and Cellular Neuroscience*, **2002**, *20*, 140–153.

64. Matsuzawa, M.; Weight, F. F.; Potember, R. S. ja Liesi, P., DIRECTIONAL NEURITE OUTGROWTH AND AXONAL DIFFERENTIATION OF EMBRYONIC

HIPPOCAMPAL NEURONS ARE PROMOTED BY A NEURITE OUTGROWTH DOMAIN OF THE B2-CHAIN OF LAMININ, *Int. j. dev. neurosci.*, **1996**, *14*, 283–295.

65. Kam, L., Axonal outgrowth of hippocampal neurons on micro-scale networks of polylysine-conjugated laminin, *Biomaterials*, **2001**, *22*, 1049–1054.
66. Pincus, D. W.; Goodman, R. R.; Fraser, R. A. R.; Nedergaard, M. ja Goldman, S. A., Neural Stem and Progenitor Cells: A Strategy for Gene Therapy and Brain Repair, *Neurosurgery*, **1998**, *42*, 858–867.
67. Mehler, M. F. ja Kessler, J. A., Progenitor Cell Biology: Implications for Neural Regeneration, *Arch Neurol*, **1999**, *56*, 780.
68. Okano, H., Stem cell biology of the central nervous system, *J. Neurosci. Res.*, **2002**, *69*, 698–707.
69. O'Reilly, K. T.; Moir, M. E.; Taylor, C. D.; Smith, C. A. ja Hyman, M. R., Hydrolysis of *tert* -Butyl Methyl Ether (MTBE) in Dilute Aqueous Acid, *Environ. Sci. Technol.*, **2001**, *35*, 3954–3961.
70. Barth, A., Infrared spectroscopy of proteins, *Biochimica et Biophysica Acta (BBA) - Bioenergetics*, **2007**, *1767*, 1073–1101.
71. Goormaghtigh, E.; Ruysschaert, J.-M. ja Raussens, V., Evaluation of the Information Content in Infrared Spectra for Protein Secondary Structure Determination, *Biophysical Journal*, **2006**, *90*, 2946–2957.

Appendices

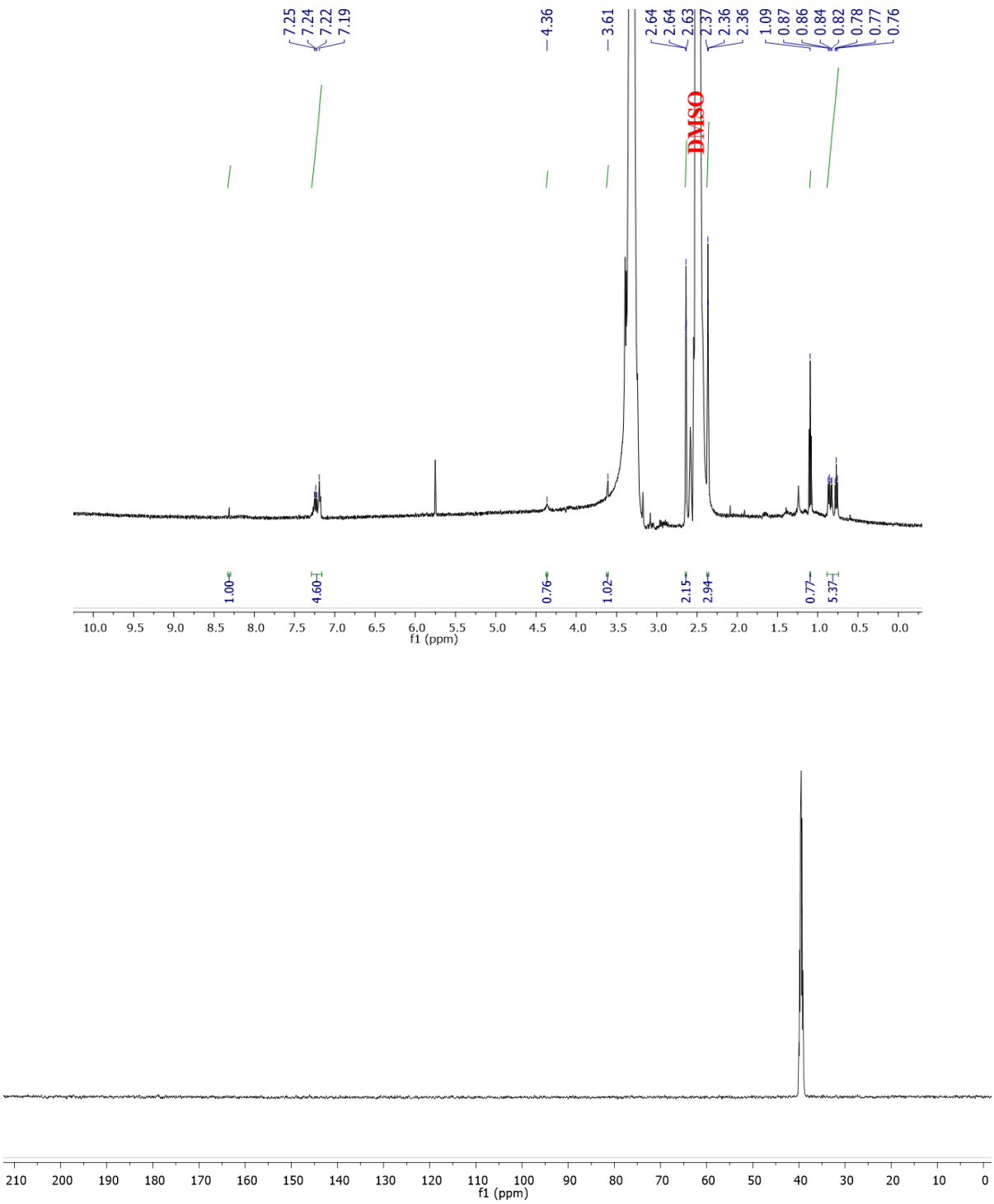

Figure 3A. ^{1}H and ^{13}C NMR result of Leu-Phe.**^{1}H NMR** (500 MHz, DMSO) δ 8.31 (s, 1H), 7.22 (dd, *J* = 19.2, 11.2 Hz, 2H), 4.36 (s, 2H), 3.60 (s, 1H), 2.66 – 2.58 (m, 1H), 2.39 – 2.35 (m, 1H), 1.09 (s, 1H), 0.87 – 0.75 (m, 1H). The sample was too dilute for ^{13}C NMR. The sample was measured overnight.

(A)

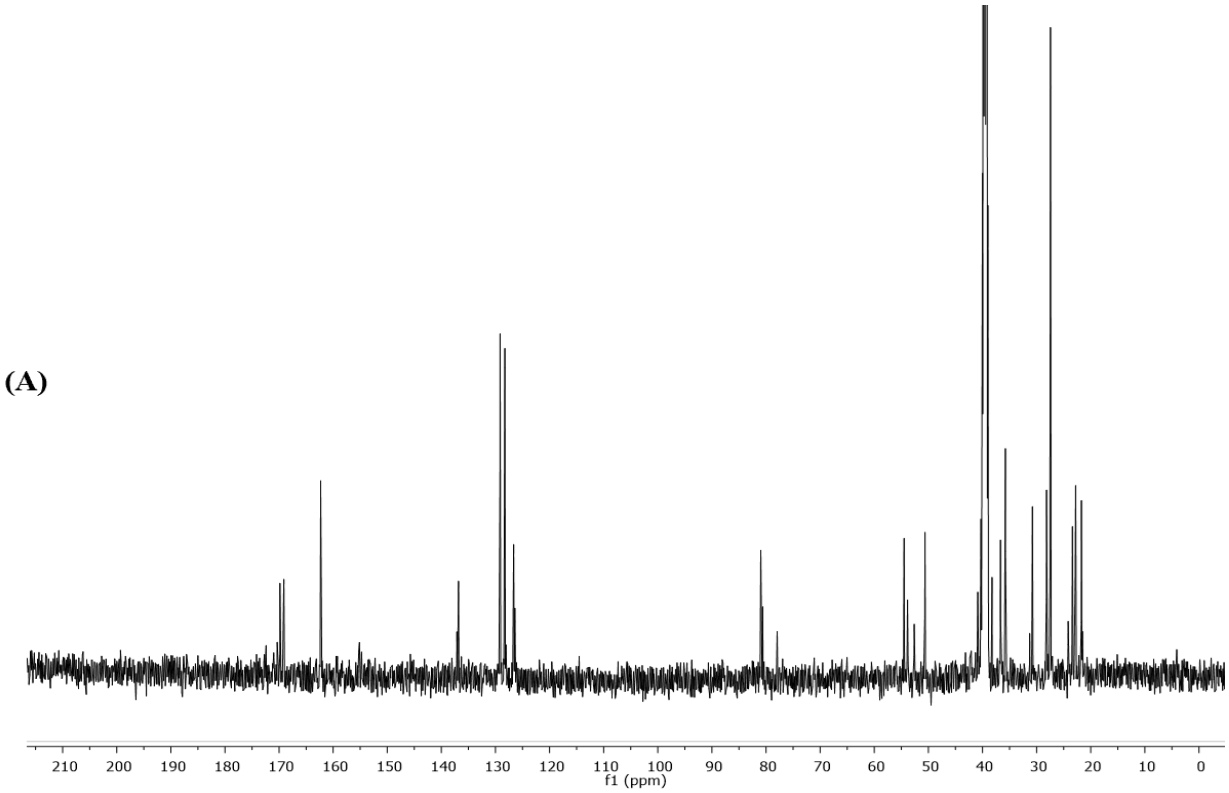
210 200 190 180 170 160 150 140 130 120 110 100 90 80 70 60 50 40 30 20 10 0
f1 (ppm)

(B)

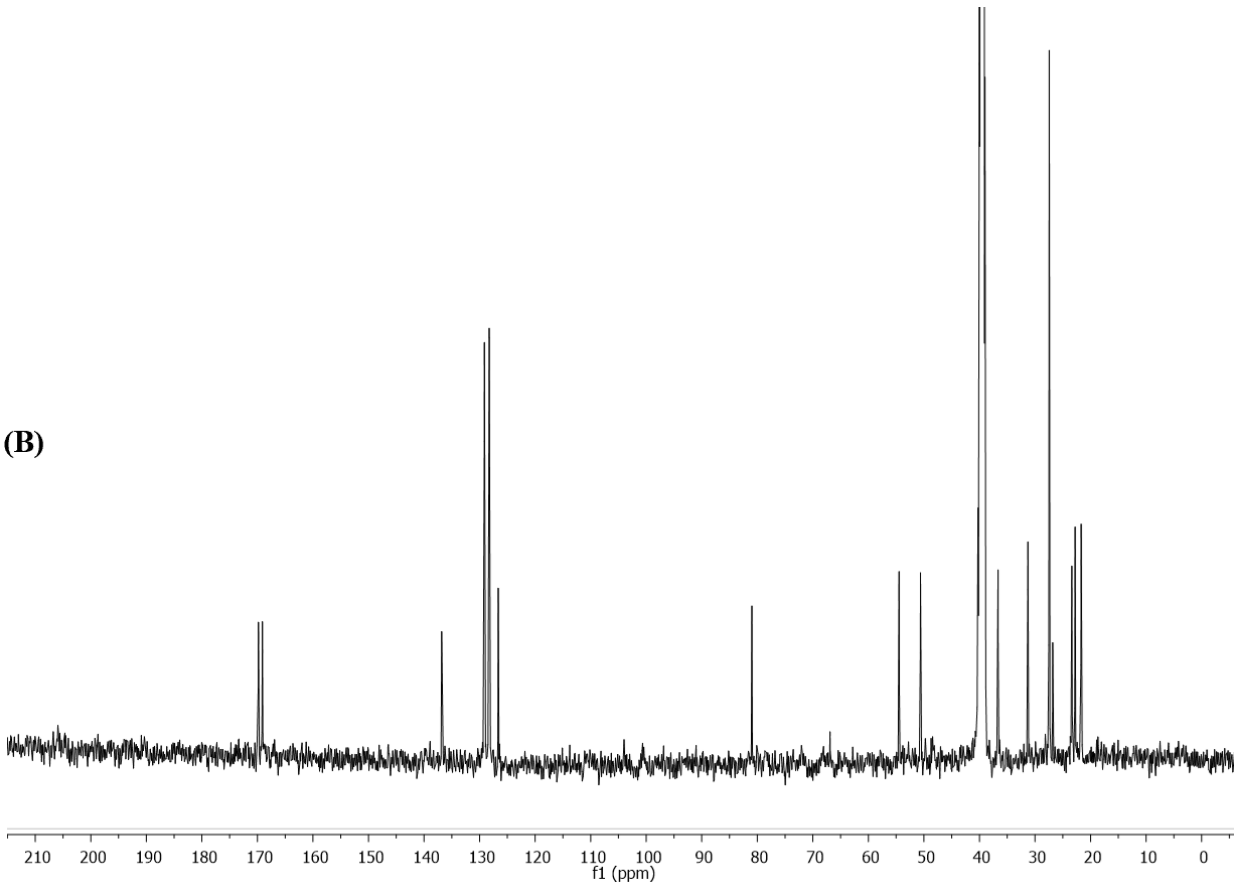
210 200 190 180 170 160 150 140 130 120 110 100 90 80 70 60 50 40 30 20 10 0
f1 (ppm)

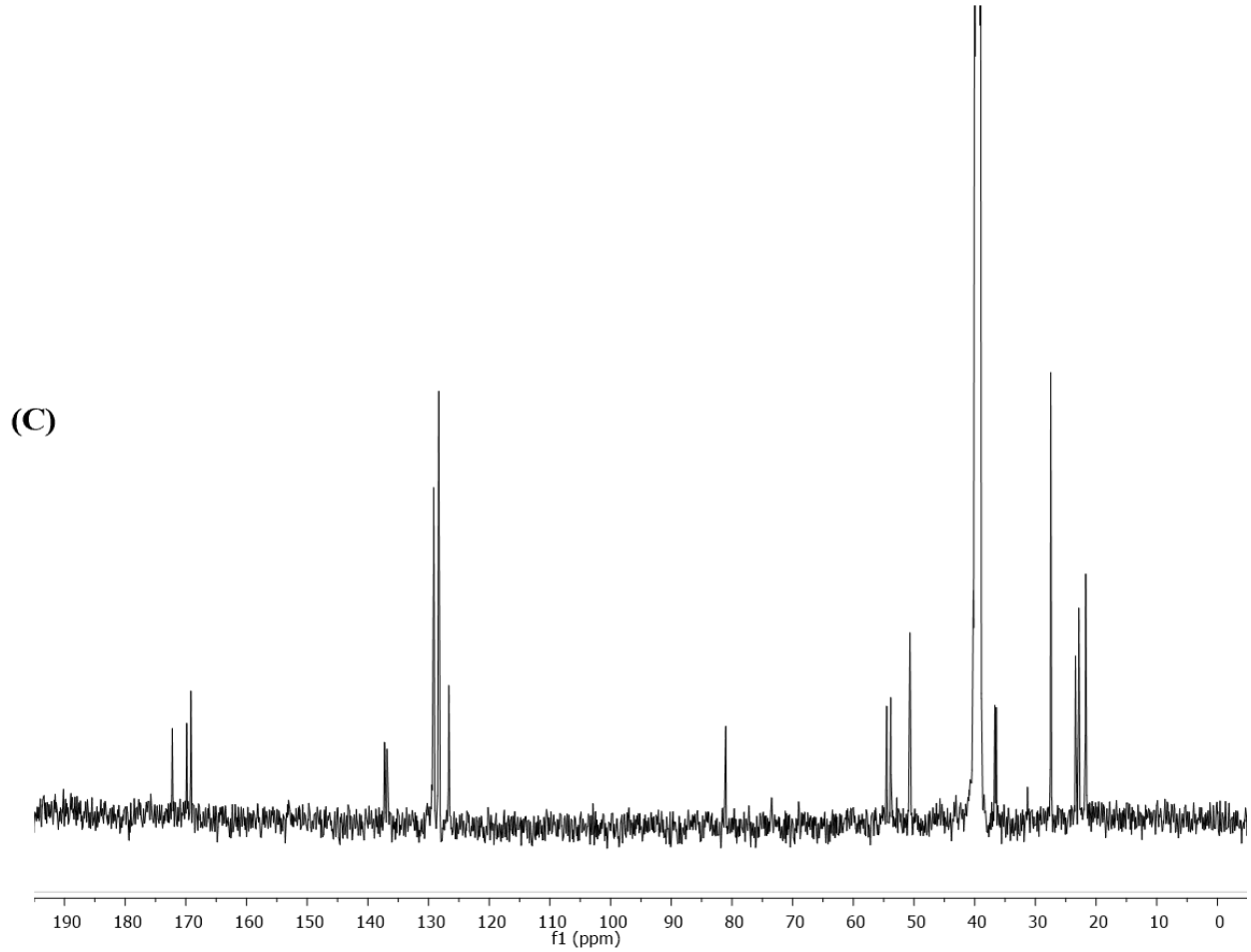

Figure 2A. **^{13} C NMR** (500 MHz, DMSO) of xerogel in *tert*-butyl methyl ether (A) sol, (B) partial gel, and (C) self-supporting gel.

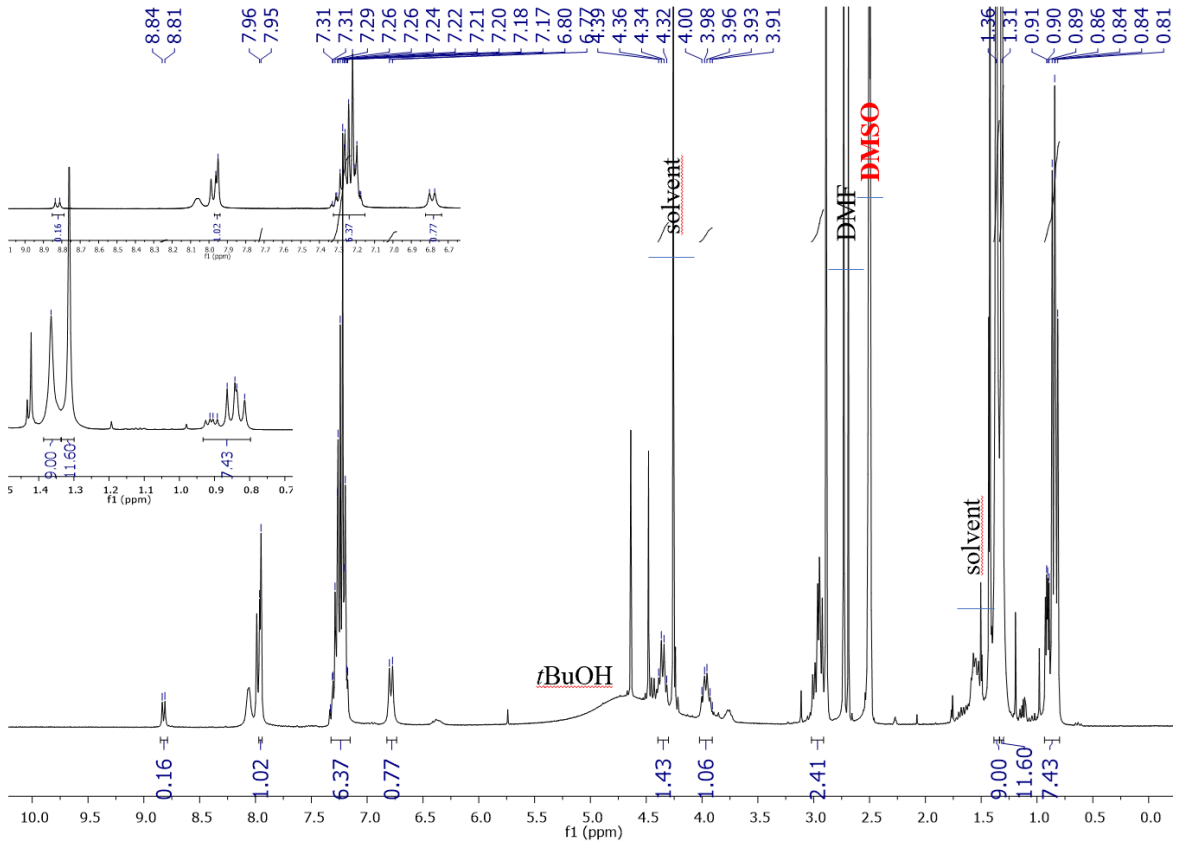

Figure A3. ^{1}H NMR (300 MHz d_6-DMSO) spectra of Boc-Leu-Phe-O*t*Bu xerogel in *tert*-butyl acetate (0.18 eq).

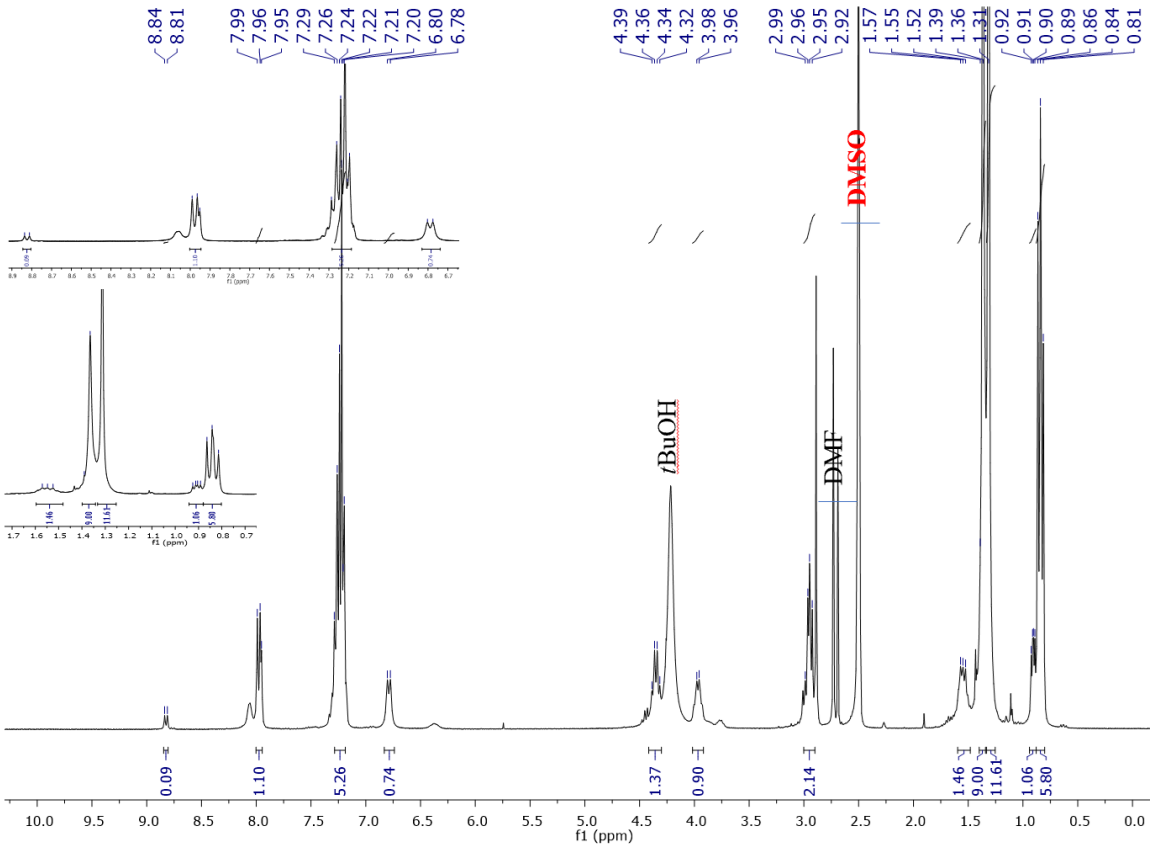

Figure A4. ^{1}H NMR (300 MHz d_6-DMSO) spectra of Boc-Leu-Phe-O*t*Bu xerogel in *tert*-butyl chloroacetate (0.18 eq).

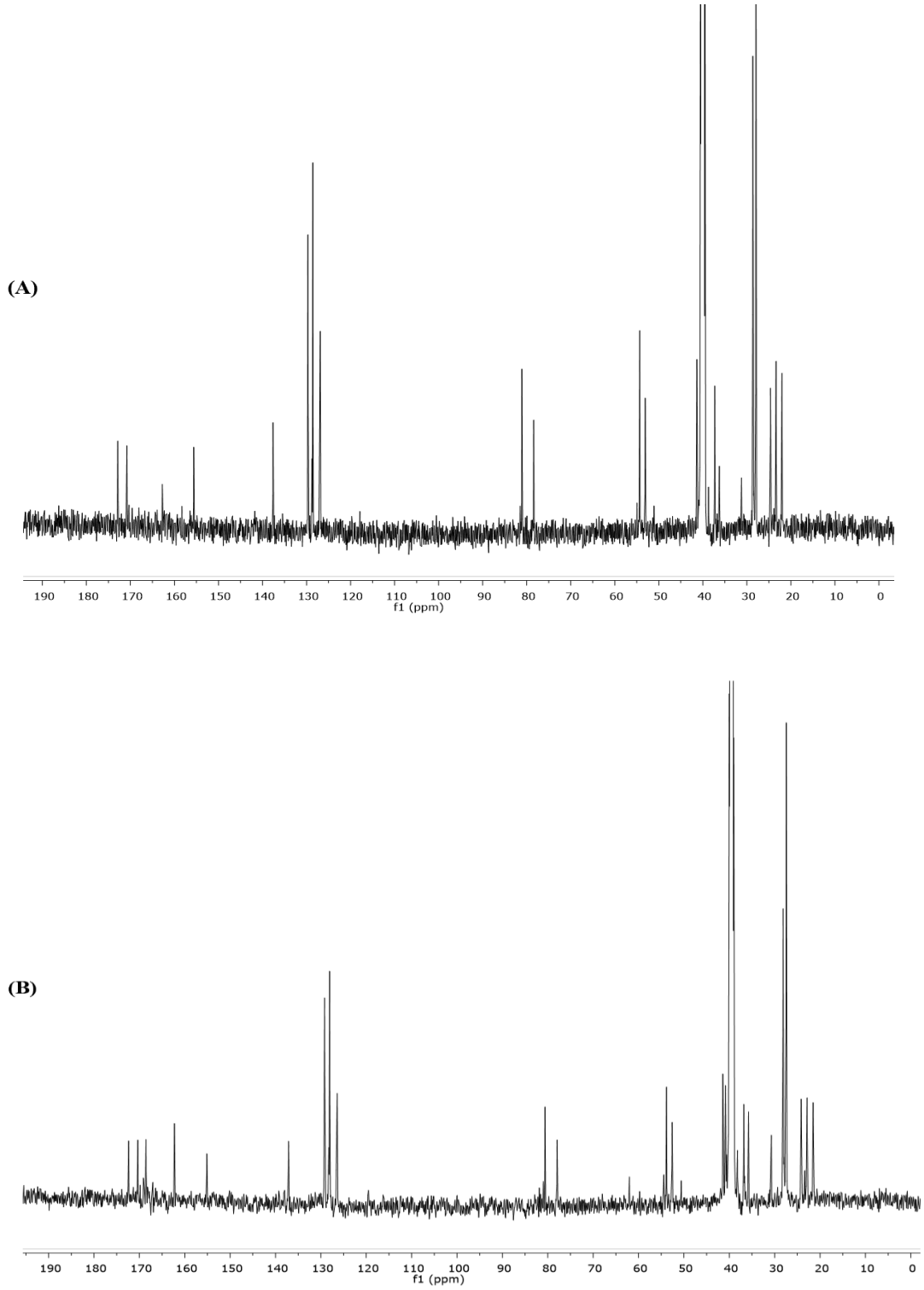

Figure A5. **^{13} C NMR** (500 MHz, DMSO) of xerogel in (A) *tert*-butyl methyl ether and (B) *tert*-butyl chloroacetate.

1

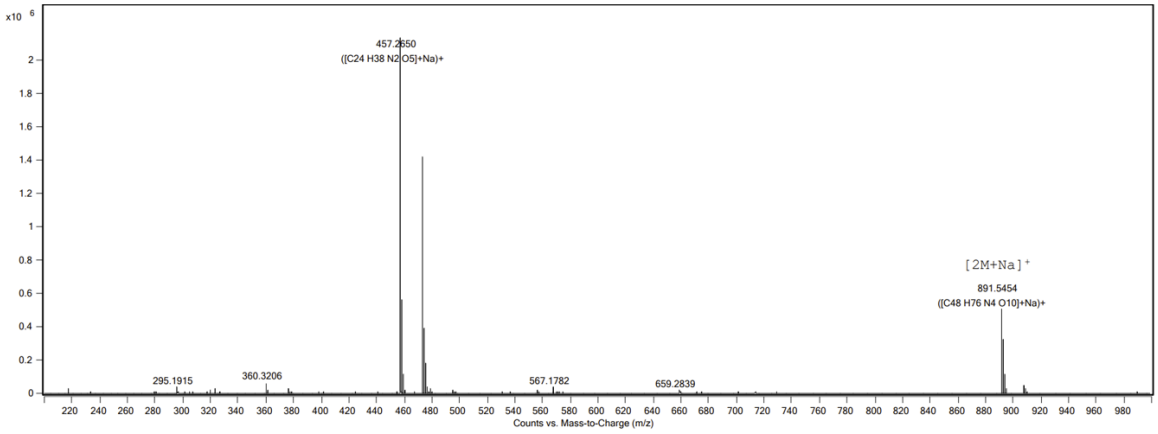

Peak List

m/z	z	Abund	Formula	Ion
360.3206	1	61671.98		
457.265	1	2145563.01	C24 H38 N2 O5	(M+Na)+
458.2692	1	563373.65	C24 H38 N2 O5	(M+Na)+
459.2705	1	114122.76	C24 H38 N2 O5	(M+Na)+
473.2388	1	1436149.57	C24 H38 N2 O5	(M+K)+
474.2428	1	389835.23	C24 H38 N2 O5	(M+K)+
475.2404	1	180333.19	C24 H38 N2 O5	(M+K)+
891.5454	1	509636.48	C48 H76 N4 O10	(M+Na)+
892.5469	1	322496.35	C48 H76 N4 O10	(M+Na)+
893.5473	1	112597.39	C48 H76 N4 O10	(M+Na)+

2

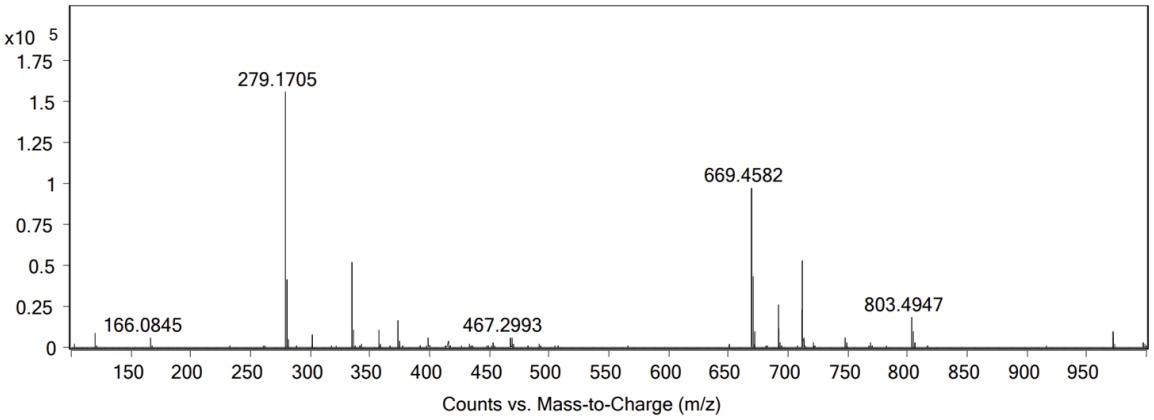

Peak List

m/z	z	Abund	Formula	Ion
86.095	1	19058.58		
279.1705	1	156948.28		
280.1716	1	42002.73		
335.2308	1	52525.05	C19 H30 N2 O3	(M+H)+
669.4582	1	97387.22		
670.4607	1	44616.01		
691.4391	1	26236.29		
711.4685	1	52789.9		
712.4715	1	23583.6		
803.4947	1	18612.61		

Figure A6. HR-MS of (1) Boc-Leu-Phe-O*t*Bu and (2) Leu-Phe-O*t*Bu.

1

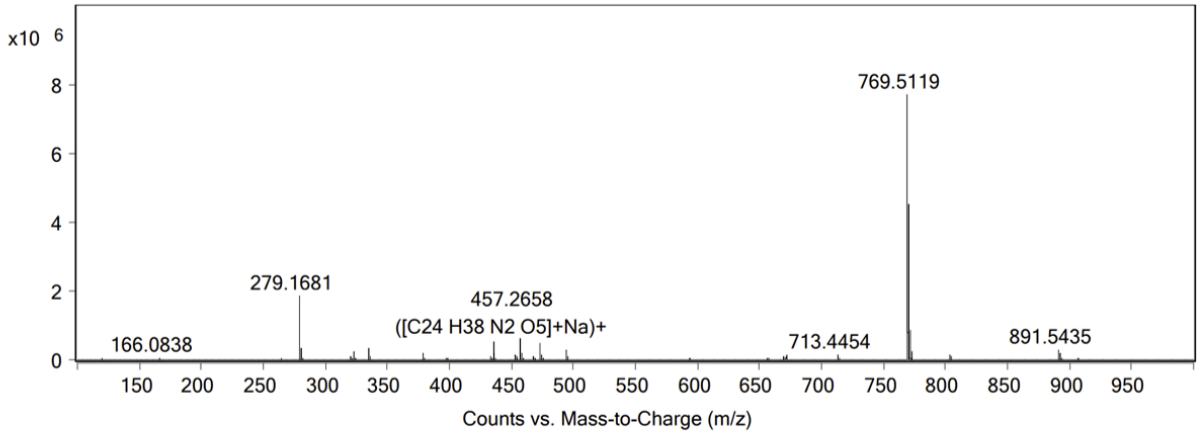

Peak List

m/z	z	Abund	Formula	Ion
279.1681	1	1873654.95		
280.1714	1	359981.04		
335.2307	1	332316.47		
435.2842	1	524576.43	C24 H35 N O5	(M+NH4)+
457.2658	1	603959.51	C24 H38 N2 O5	(M+Na)+
473.2393	1	491065.87	C24 H38 N2 O5	(M+K)+
769.5119	1	7721482.61		
770.5129	1	4527452.2		
771.52	1	876237.67		
891.5435	1	315819.6		

2

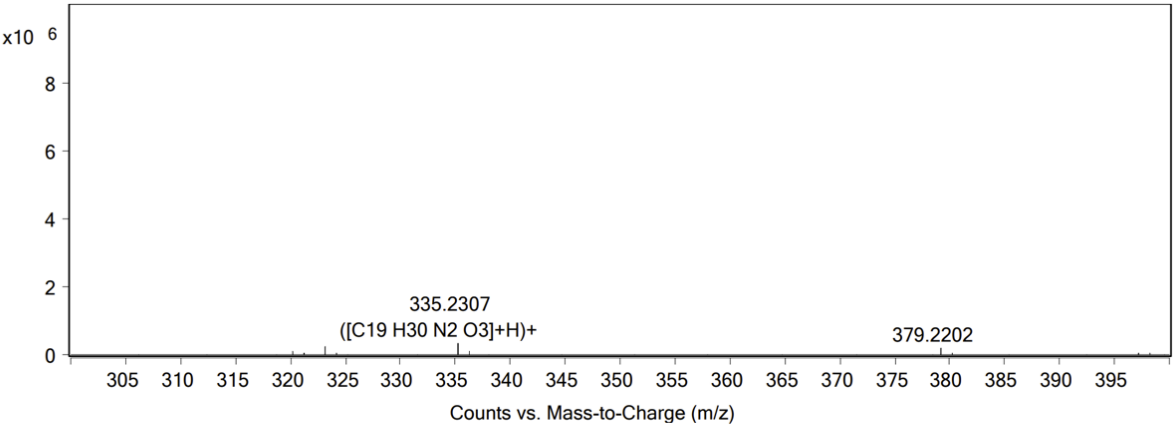

Peak List

m/z	z	Abund	Formula	Ion
279.1681	1	1873654.95		
280.1714	1	359981.04		
335.2307	1	332316.47	C19 H30 N2 O3	(M+H)+
435.2842	1	524576.43		
457.2658	1	603959.51		
473.2393	1	491065.87		
769.5119	1	7721482.61		
770.5129	1	4527452.2		
771.52	1	876237.67		
891.5435	1	315819.6		

3

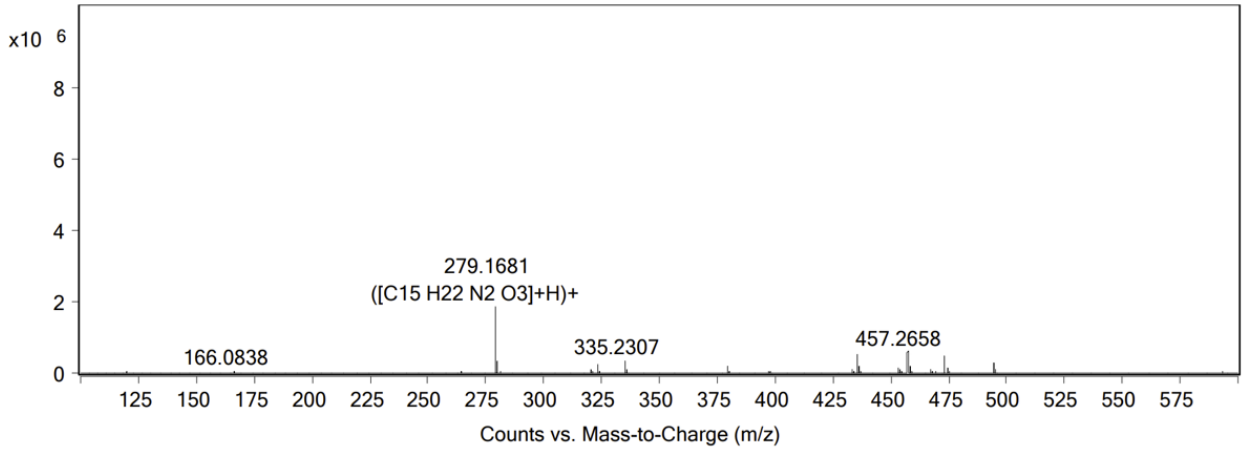

Peak List

m/z	z	Abund	Formula	Ion
279.1681	1	1873654.95	C15 H22 N2 O3	(M+H)+
280.1714	1	359981.04	C15 H22 N2 O3	(M+H)+
335.2307	1	332316.47		
435.2842	1	524576.43		
457.2658	1	603959.51		
473.2393	1	491065.87		
769.5119	1	7721482.61		
770.5129	1	4527452.2		
771.52	1	876237.67		
891.5435	1	315819.6		

Figure A7. HR-MS results of xerogel in *tert*-butyl acetate (0.18 eq). (1) Boc-Leu-Phe-OtBu, (2) Leu-Phe-OtBu, and (3) Leu-Phe.

1

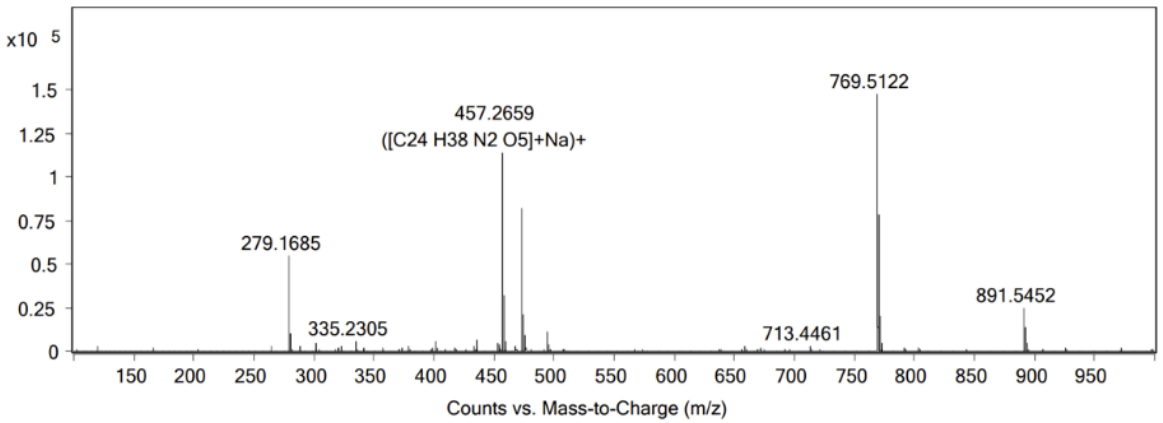

Peak List

m/z	z	Abund	Formula	Ion
279.1685	1	55683.48		
457.2659	1	114312.72	C24 H38 N2 O5	(M+Na)+
458.2682	1	32168.62	C24 H38 N2 O5	(M+Na)+
473.2396	1	81777.37	C24 H38 N2 O5	(M+K)+
474.2422	1	22408.07	C24 H38 N2 O5	(M+K)+
769.5122	1	147398.21		
770.5141	1	77900.07		
771.517	1	20097.72		
891.5452	1	25105.99		
892.5487	1	13612		

2

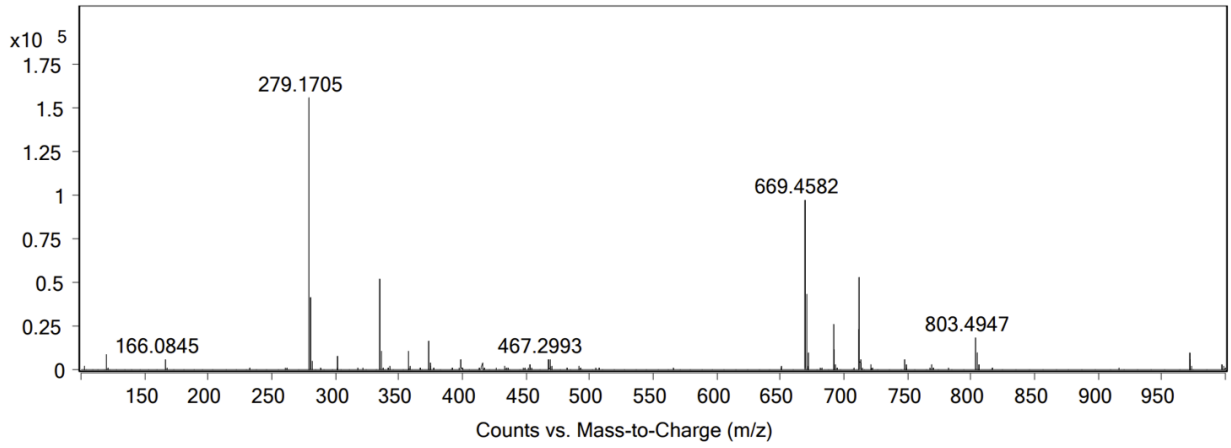

Peak List

m/z	z	Abund	Formula	Ion
86.095	1	19058.58		
279.1705	1	156948.28		
280.1716	1	42002.73		
335.2308	1	52525.05	C19 H30 N2 O3	(M+H)+
669.4582	1	97387.22		
670.4607	1	44616.01		
691.4391	1	26236.29		
711.4685	1	52789.9		
712.4715	1	23583.6		
803.4947	1	18612.61		

3

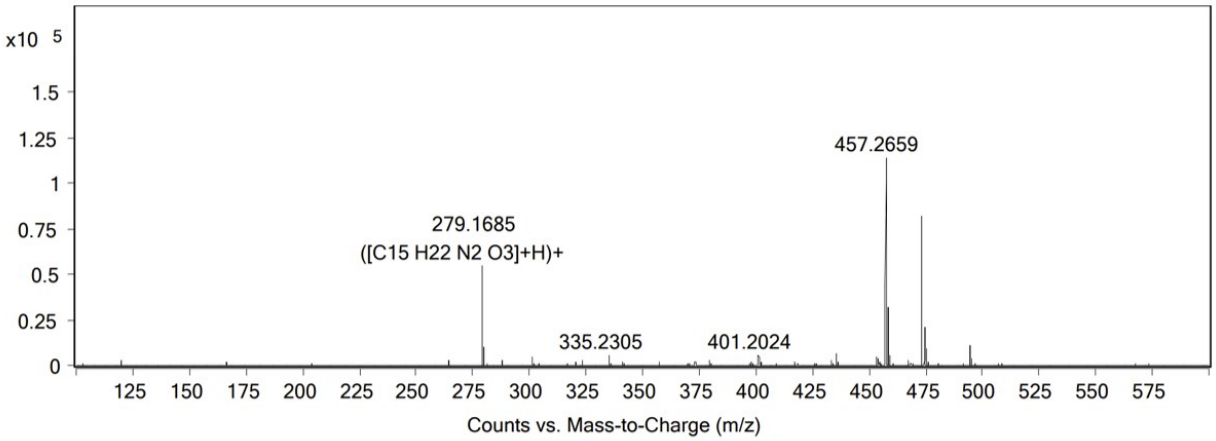

Peak List

m/z	z	Abund	Formula	Ion
279.1685	1	55683.48	C15 H22 N2 O3	(M+H)+
457.2659	1	114312.72		
458.2682	1	32168.62		
473.2396	1	81777.37		
474.2422	1	22408.07		
769.5122	1	147398.21		
770.5141	1	77900.07		
771.517	1	20097.72		
891.5452	1	25105.99		
892.5487	1	13612		

Figure A8. HR-MS results of xerogel in *tert*-butyl chloroacetate (0.18 eq). (1) Boc-Leu-Phe-OtBu, (2) Leu-Phe-OtBu, and (3) Leu-Phe.

1

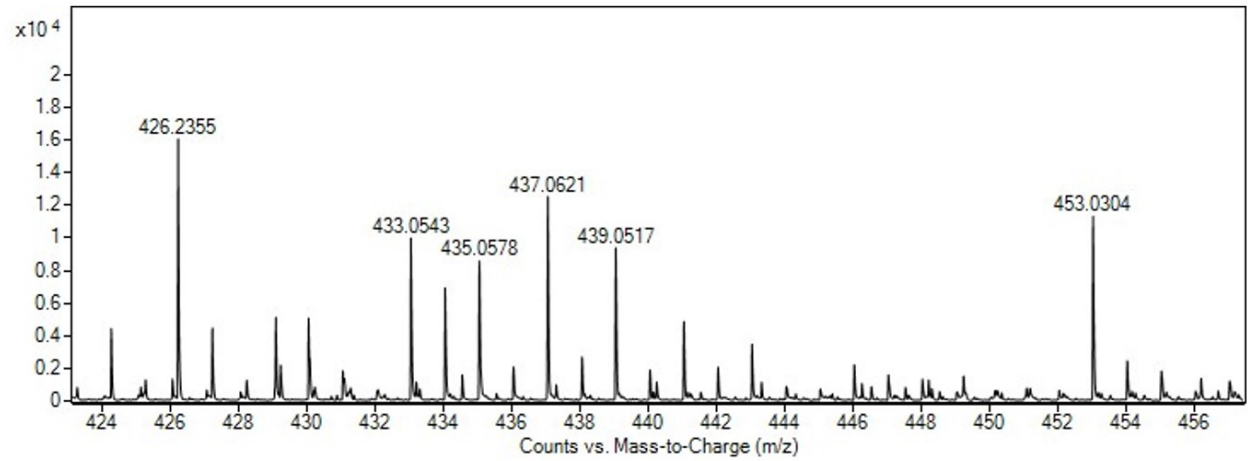

2

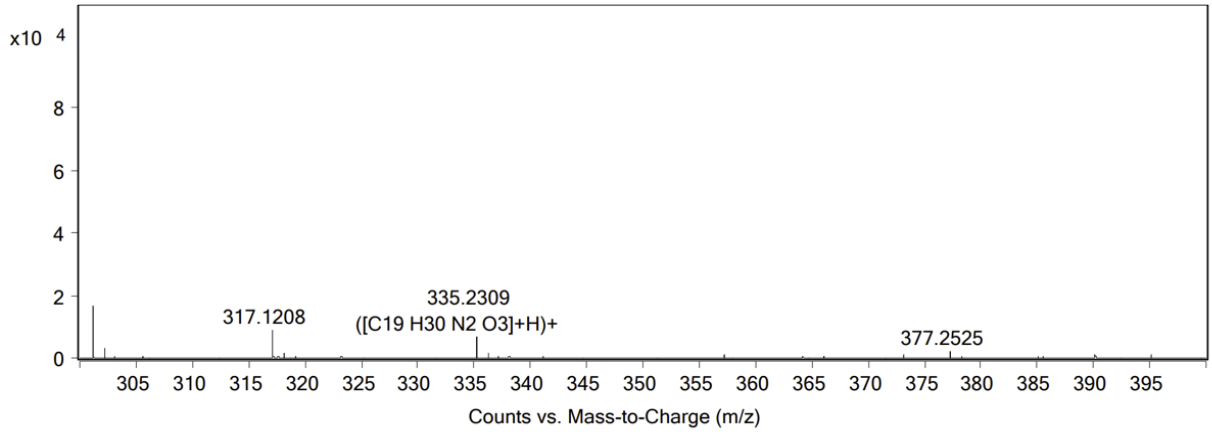

Peak List

m/z	z	Abund	Formula	Ion
86.0959	1	5754.15		
279.1693	1	84989.97		
280.172	1	16154.44		
298.1425	2	8050.82		
301.1505	1	16460.81		
317.1208	1	9132.23		
335.2309	1	6856.82	C19 H30 N2 O3	(M+H)+
557.331	1	10272.82		
595.2795	1	12011.57		
873.4428	1	6212.69		

3

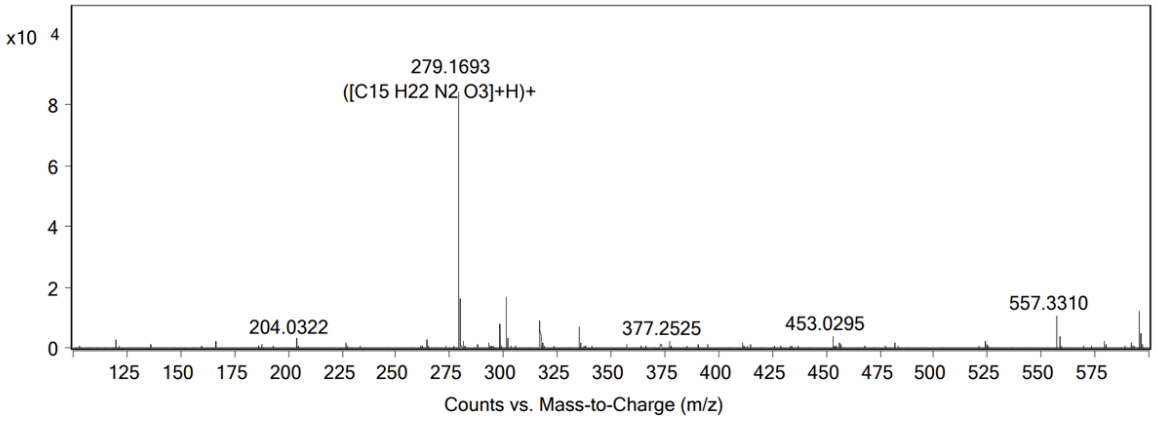

Peak List

m/z	z	Abund	Formula	Ion
86.0959	1	5754.15		
279.1693	1	84989.97	C15 H22 N2 O3	(M+H)+
280.172	1	16154.44	C15 H22 N2 O3	(M+H)+
298.1425	2	8050.82		
301.1505	1	16460.81	C15 H22 N2 O3	(M+Na)+
317.1208	1	9132.23	C15 H22 N2 O3	(M+K)+
335.2309	1	6856.82		
557.331	1	10272.82		
595.2795	1	12011.57		
873.4428	1	6212.69		

Figure A9. HR-MS results of xerogel in *tert*-butyl methyl ether (1.0 eq). (1) No Boc-Leu-Phe-OtBu was observerved**,** (2) Leu-Phe-OtBu, and (3) Leu-Phe.